CIPM MRA
Comparison reports

APMP.PR-S8

Optical fibre length

SUPPLEMENTARY COMPARISON

Any further distribution of this Report must be cited as:
Sun Do Lim *et al* 2026 *CIPM MRA Comparison reports* **02001**
https://doi.org/10.59161/DIHH8181

APMP Supplementary Comparison on Optical Fiber Length

APMP.PR-S8

Final Report

Sun Do Lim[1,*], Seung Kwan Kim[1,*], Ki-Suk Hong[1], Jing Zhang[2], Kuniaki Amemiya[3], Jacques Morel[4], Jimmy Dubard[5], Vladimir Kravtsov[6], Mariesa Nel[7], Pritesh Jivan[7], Osama Terra[8], Zeus Ruiz[9]

[1]*Division of Physical Metrology, Korea Research Institute of Standards and Science, KRISS,* [2]*Optical Radiation Laboratory, NMC, A*STAR,* [3]*Applied Optical Measurement Group, NMIJ, AIST,* [4]*Photonics, Time and Frequency Laboratory, Swiss Federal Institute of Metrology, METAS,* [5]*Laboratoire National de métrologie et d'Essais, LNE,* [6]*Laboratory, All Russian Research Institute for Optical and Physical Measurements (VNIIOFI),* [7]*National Metrology Institute of South Africa (NMISA),* [8]*Length and Precision Engineering Division, National Institute for standards (NIS),* [9]*Optics and Radiometry Division, National Metrology Center of México (CENAM)*

*Correspondence to: sdlim@kriss.re.kr, skkfiber@kriss.re.kr

APMP Supplementary Comparison on Optical Fiber Length

Sun Do Lim[1,*], Seung Kwan Kim[1,*], Ki-Suk Hong[1], Jing Zhang[2], Kuniaki Amemiya[3], Jacques Morel[4], Jimmy Durbard[5], Vladimir Kravtsov[6], Mariesa Nel[7], Pritesh Jivan[7], Osama Terra[8], Zeus Ruiz[9]

[1]*Division of Physical Metrology, Korea Research Institute of Standards and Science, KRISS,* [2]*Optical Radiation Laboratory, NMC, A*STAR,* [3]*Applied Optical Measurement Group, NMIJ, AIST,* [4]*Photonics, Time and Frequency Laboratory, Swiss Federal Institute of Metrology, METAS,* [5]*Métrologie Scientfique et Industrielle, LNE, Fiber Optical Systems Metrology,* [6]*Laboratory, All Russian Research Institute for Optical and Physical Measurements (VNIIOFI),* [7]*National Metrology Institute of South Africa (NMISA),* [8]*Length and Precision Engineering Division, National Institute for standards (NIS),* [9]*Optics and Radiometry Division, National Metrology Center of México (CENAM)*

*sdlim@kriss.re.kr, *skkfiber@kriss.re.kr

Abstract

KRISS, NMC, NMIJ, LNE, NMISA, METAS, VNIIOFI, NIS, and CENAM conducted a supplementary comparison on optical fiber length at 1310 nm, 1550 nm, and 1625 nm. The aim of this comparison is to examine the equivalence of the optical fiber length among participating laboratories and to provide supporting evidence for associated CMC claims in BIPM KCDB.

Table of Contents

1. Introduction

Under the Mutual Recognition Arrangement (MRA) the metrological equivalence of national measurement standards will be determined by a set of key comparisons chosen and organized by the Consultative Committees of the CIPM working closely with the Regional Metrology Organizations (RMOs).

At the meeting of Technical Committee for Photometry and Radiometry (TCPR) of the Asia Pacific Metrology Programme (APMP) in Kuala Lumpur, Malaysia in 2009, the APMP international supplementary comparison on optical fiber length (APMP.PR-S8) was agreed to be conducted and KRISS agreed to act as a pilot lab. The aim of this comparison is to assess the equivalence of the optical fiber length scales among the participants and to underpin the relevant claim of the Calibration and Measurement Capability in BIPM KCDB.

NIM (China), NMC (Singapore), NMIJ (Japan), and NMISA (South Africa) confirmed their intention to be participants during the period of call for participants to APMP in February, 2014. In addition, LNE (France), METAS (Switzerland), and VNIIOFI (Russia) confirmed their intention to join this comparison during the period of call for participants to other RMO's in February, 2014. Later, NIS (Egypt) and CENAM (Mexico) submitted their intention to become participants and were accepted by all the participants unanimously in September and October, 2014, respectively.

The technical protocol was prepared by KRISS and agreed by all the other participants. The comparison was carried out through the calibration of optical fiber length artifacts and organized in three rounds; the first round with NIM (China), NMC (Singapore), NMIJ (Japan), the second round with LNE (France), METAS (Switzerland), and VNIIOFI (Russia), and the third with NMISA (South Africa), NIS (Egypt) and CENAM (Mexico). The comparison began in January, 2015 with ten participants and ended up a little delayed with nine participants in November 2017. NIM informed of withdrawal from the comparison due to equipment failure.

For more details, the Technical Protocol of the APMP.PR-S8 can be referred.

2. Organization of Comparison

2.1. Participants

The participants of this supplementary comparison were: KRISS (Republic of Korea), NMC (Singapore), NMIJ (Japan), LNE (France), NMISA (South Africa), METAS (Switzerland), VNIIOFI (Russia), NIS (Egypt), CENAM (México). KRISS acted as a pilot laboratory among the participants in this comparison.

All the participants were able to demonstrate traceability to an independent realization of the quantity.

2.2. Participants' details

Table 2-2-1. Contact list of participants.

NMI Name (Country)	Personnel	Contact information
KRISS (Republic of Korea)	Sun Do Lim	Division of Physical Metrology, KRISS 267 Gajeong-Ro, Yuseong-Gu, Daejeon 34113, Republic of Korea Tel: +82 42 868-5181 Fax: E-mail: sdlim@kriss.re.kr
NMC (Singapore)	Jing Zhang	Optical Radiation Laboratory, NMC, A*STAR 8 CleanTech Loop #01-20, Singapore 637145 Tel: +65 6714 9274 Fax: E-mail: zhang_jing@nmc.a-star.edu.sg
NMIJ (Japan)	Kuniaki Amemiya	Applied Optical Measurement Group, NMIJ, AIST 1-1-1 Umezono, Tsukuba, Ibaraki 305-8563, Japan Tel: +81 29 861 4191 Fax: +81 29 861 1434 E-mail: k.amemiya@aist.go.jp
METAS (Switzerland)	Jacques Morel	Federal Institute of Metrology, METAS Photonics, Time and Frequency Laboratory Lindenweg 50, CH-3003 Bern-Wabern, Switzerland Tel: +41 58 38 70 350 Fax: +41 58 38 70 210 E-mail: jacques.morel@metas.ch
LNE (France)	Jimmy Dubard	Laboratoire National de métrologie et d'Essais, LNE 29, avenue Roger Hennequin - 78197 Trappes cedex, France Tel: +33 130691237 Fax: +33 140433737 E-mail: jimmy.dubard@lne.fr

VNIIOFI (Russia)	Aleksei Mitiurev	Fiber Optical Systems Metrology Laboratory, All Russian Research Institute for Optical and Physical Measurements (VNIIOFI) Ozernaya st.46, Moscow, 119361, Russia Tel: +7 (495) 781 4583 Fax: E-mail: mak@vniiofi.ru
NMISA (South Africa)	Mariesa Nel / Pritesh Jivan	National Metrology Institute of South Africa (NMISA) Bldg 5, CSIR campus Pretoria, Meiring Naude road, Brummeria, Pretoria, Gauteng, South Africa, 0001 Tel: +27 12 947 2800 Fax: E-mail: mnel@nmisa.org / pjivan@nmisa.org
NIS (Egypt)	Osama Terra	Primary Length Standard and Laser Technology lab., National Institute of standards (NIS) Tersa street,Haram, 12211 Giza; P.O.Box: 136 Giza, Egypt Tel: +201141172900 Fax: E-mail: osama.terra@nis.sci.eg
CENAM (México)	Zeus Ruiz	Optics and Radiometry Division, National Metrology Center of México (CENAM) km 4.5 Carretera a Los Cués, Municipio El Marqués, Qro. C.P. 76246 México Tel: +52 442 2110500 Fax: E-mail: zruiz@cenam.mx

2.3. Form of the comparison

The comparison was carried out through calibrations of a group of optical fiber length artifacts that had been prepared by KRISS and METAS. Each artifact contained an optical fiber spool with predetermined length of single mode fiber above 1300 nm manufactured by an optical fiber cable company in a package designed by KRISS or METAS. The artifact had an input and output lead fiber cable with an FC/PC type connector for both ends. The full description of the artifacts is given in Section 3.

The comparison consisted of three rounds: the first round measurements were planned to be taken by KRISS, NMC, NIM, and NMIJ in sequence using KRISS artifacts and finalized by the 2nd measurements of KRISS to check the stability of the artifacts. The second round used METAS artifacts and the measurements were taken by METAS, LNE, VNIIOFI, and KRISS in sequence to be finalized by METAS to check the stability of the artifacts. The third round used KRISS artifacts again, and they were measured by KRISS, NMISA, NIS, and CENAM in sequence and finalized by KRISS after checking the stability of the artifacts. During the first round, NIM informed of withdrawal, and NMC requested a re-measurement after the third round, which was accepted by all participants.

Each participant had two month period for measurements and then sent the artifacts to the next participant right away so that the artifacts can be delivered to the next participant within one month after finish of measurements. The participants were asked to immediately report to the pilot lab when they found any problem that might delay the predetermined schedule.

2.4. Timetable

Timetable of the original plan of the comparison as given in the technical protocol is shown in Table 2-4-1 to 2-4-3.

Table 2-4-1 to 2-4-3. Scheduled timetable of the comparison in the beginning.

2-4-1 First Round (using KRISS artifacts)

Activity	Start Date	End Date
First Calibration at KRISS (Korea)	**1 January, 2015**	**28 February, 2015**
Delivery to NMC	1 March, 2015	31 March, 2015
Calibration at NMC (Singapore)	**1 April, 2015**	**31 May, 2015**
Delivery to NIM	1 June, 2015	30 June, 2015
Calibration at NIM (China)	**1 July, 2015**	**31 August, 2015**
Delivery to NMIJ	1 September, 2015	30 September, 2015
Calibration at NMIJ (Japan)	**1 October, 2015**	**30 November, 2015**
Delivery to KRISS	1 December, 2015	31 December, 2015
Second Calibration at KRISS (Korea)	**1 January, 2016**	**29 February, 2016**

2-4-2 Second Round (using METAS artifacts)

Activity	Start Date	End Date
First Calibration at METAS (Switzerland)	**1 April, 2015**	**31 May, 2015**
Delivery to LNE	1 June, 2015	30 June, 2015
Calibration at LNE (France)	**1 July, 2015**	**31 August, 2015**
Delivery to VNIIOFI	1 September, 2015	30 September, 2015

Calibration at VNIIOFI (Russia)	**1 October, 2015**	**30 November, 2015**
Delivery to KRISS	1 December, 2015	31 December, 2015
Calibration at KRISS (Korea)	**1 January, 2016**	**29 February, 2016**
Delivery to METAS	1 March, 2016	31 March, 2016
Second Calibration at METAS (Switzerland)	**1 April, 2016**	**30 May, 2016**

2-4-3 Third Round (using KRISS artifacts)

Activity	Start Date	End Date
First Calibration at KRISS (Korea) = Second Calibration in the 1st round	**1 January, 2016**	**29 February, 2016**
Delivery to NMISA	1 March, 2016	31 March, 2016
Calibration at NMISA (South Africa)	**1 April, 2016**	**31 May, 2016**
Delivery to NIS	1 June, 2016	30 June, 2016
Calibration at NIS (Egypt)	**1 July, 2016**	**31 August, 2016**
Delivery to CENAM	1 September, 2016	30 September, 2016
Calibration at CENAM (Mexico)	**1 October, 2016**	**30 November, 2016**
Delivery to KRISS	1 December, 2016	31 December, 2016
Second Calibration at KRISS (Korea)	**1 January, 2017**	**28 February, 2017**

However, the actual measurements were delayed due to each of the laboratory's specific circumstances, such as customs clearance, re-measurements, etc. Table 2-4-4 to 2-4-7 list the actual time sequence.

Table 2-4-4 to 2-4-7. History of the comparison measurements.

2-4-4 First Round (using KRISS artifacts)

Activity	Start Date	End Date
First Calibration at KRISS (Korea)	**1 January, 2015**	**11 March, 2015**
Delivery to NMC	11 March, 2015	27 March, 2015
Calibration at NMC (Singapore)	**1 April, 2015**	**29 May, 2015**
Delivery to NIM	3 July, 2015	25 Aug, 2015
Calibration at NIM (China)	**1 September, 2015**	**20 October, 2015**
Delivery to NMIJ	11 December, 2015	1 January, 2016
Calibration at NMIJ (Japan)	**1 January, 2016**	**28 January, 2016**
Delivery to KRISS	28 January, 2016	5 February, 2016
Second Calibration at KRISS (Korea)	**5 February, 2016**	**25 March, 2016**

2-4-5 Second Round (using METAS artifacts)

Activity	Start Date	End Date
First Calibration at METAS (Switzerland)	**1 April, 2015**	**31 May, 2015**
Delivery to LNE	1 June, 2015	5 June, 2015
Calibration at LNE (France)	**6 July, 2015**	**21 September, 2015**
Delivery to VNIIOFI	22 September, 2015	30 September, 2015

Calibration at VNIIOFI (Russia)	**1 October, 2015**	**15 December, 2015**
Delivery to KRISS	16 December, 2015	4 January, 2016
Calibration at KRISS (Korea)	**5 January, 2016**	**7 April, 2016**
Delivery to METAS	8 April, 2016	13 May, 2016
Second Calibration at METAS (Switzerland)	**14 May, 2016**	**11 July, 2016**

2-4-6 Third Round (using KRISS artifacts)

Activity	Start Date	End Date
First Calibration at KRISS (Korea) = Second Calibration in the 1st round	**8 February, 2016**	**24 March, 2016**
Delivery to NMISA	25 March, 2016	30 May, 2016
Calibration at NMISA (South Africa)	**1 June, 2016**	**26 June, 2016**
Delivery to NIS	27 June, 2016	3 July, 2016
Calibration at NIS (Egypt)	**4 July, 2016**	**1 September, 2016**
Delivery to CENAM	1 September, 2016	11 Octorber, 2016
Calibration at CENAM (Mexico)	**12 October, 2016**	**9 December, 2016**
Delivery to KRISS	10 December, 2016	19 December, 2016
Second Calibration at KRISS (Korea)	**20 December, 2016**	**2 March, 2017**

2-4-7 First Round 2 for NMC and NIM (using KRISS artifacts)

Activity	Start Date	End Date
NIM (China) withdraw	**3 March, 2017**	
Delivery to NMC from KRISS	11 April, 2017	14 May, 2017
Calibration at NMC (Singapore)	**14 May, 2017**	**22 June, 2017**

Delivery to KRSS	22 June, 2017	21 July, 2017
Calibration at KRISS (Korea)	**31 July, 2016**	**22 November, 2017**

Timeline at a glance (Plan and Action)

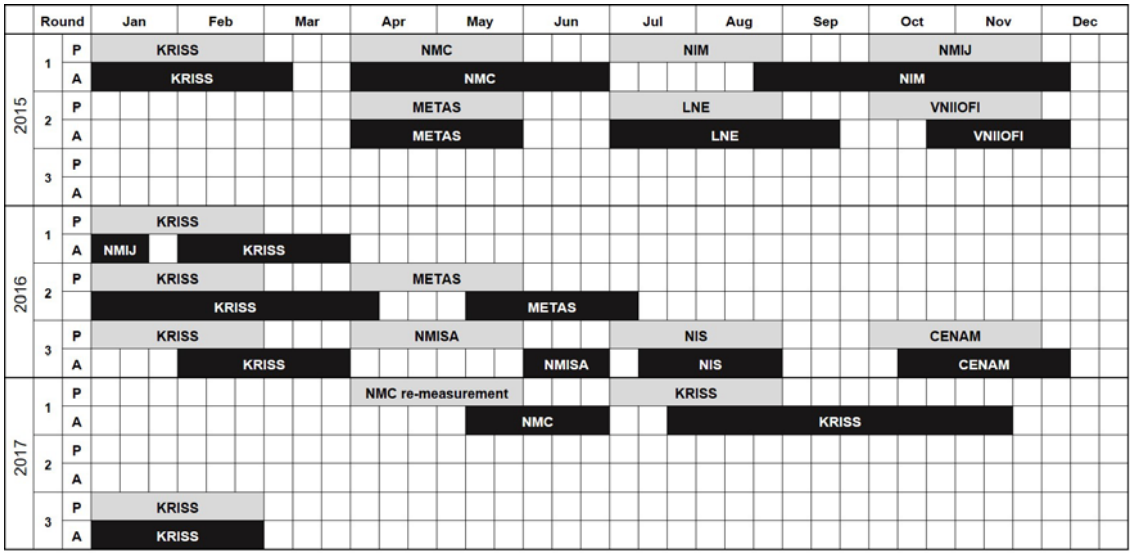

※ P: Plan, A: Action

2.5 Comparison artifact

2.5.1 KRISS artifacts

The KRISS artifacts are two spools of step-index single mode optical fiber (SMF) with approximately 3 km and 13 km, respectively. Each SMF spool is packaged in a plastic case designed to fit its shape as shown in Fig.2-5-1. Both ends of SMF in the artifact are spliced to about 1.5 m-long standard FC/PC connector cables with 2 mm or 3 mm diameter, which are placed outside of the case so that one can connect his own fibers with FC/PC connectors to the artifact using standard FC/PC adaptors. The two FC/PC connector ends of the artifact are protected with caps from dust inside the transportation package.

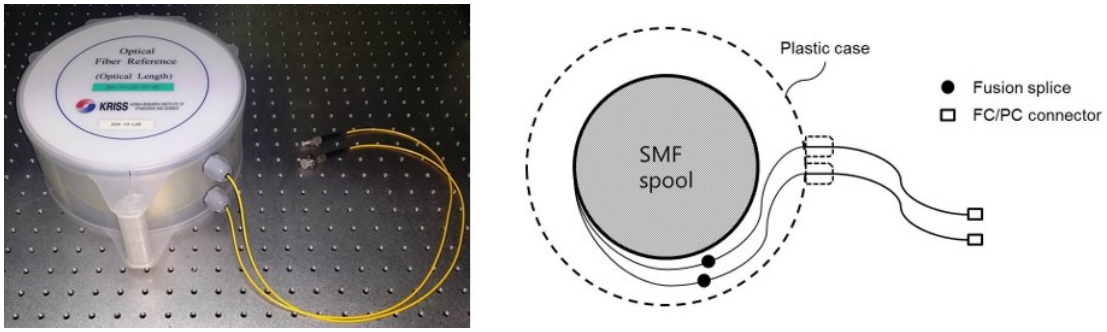

Fig. 2-5-1 Photograph of the KRISS artifact and internal structure of the KRISS artifact

2.5.2 METAS artifacts

The METAS artifacts are also two spools of step-index SMF with approximately 2 km and 12 km, respectively. Each SMF spool is packaged in a metal case designed to contain the spool securely and safely as shown in Fig. 2-5-2. Each METAS Length Reference Fibres (LRF) consists of a G.652 fibre spool. Two patch cables, each with a length of approximately 2 m, are fitted with FC/PC connectors. The internal structure of the LRF is shown in Fig. 2-5-3.

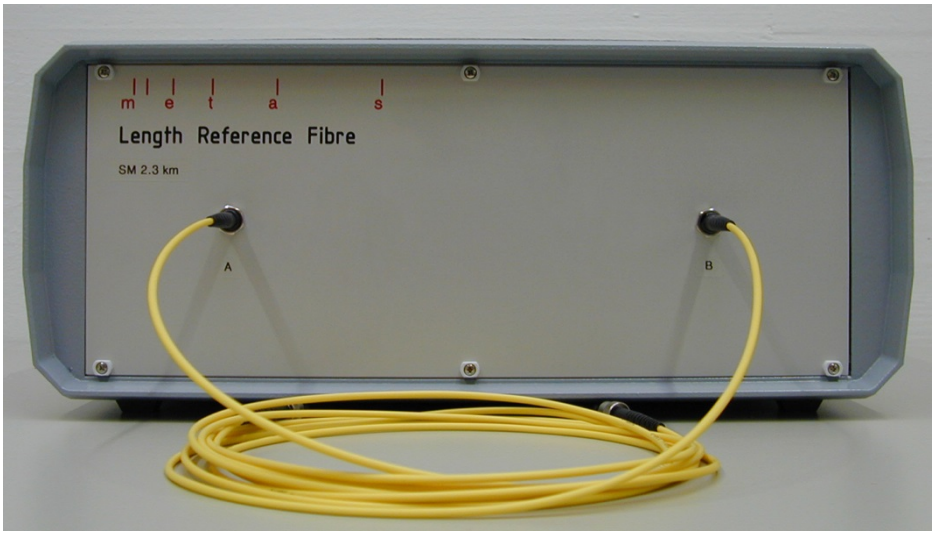

Fig. 2-5-2 Photograph of the METAS artifact.

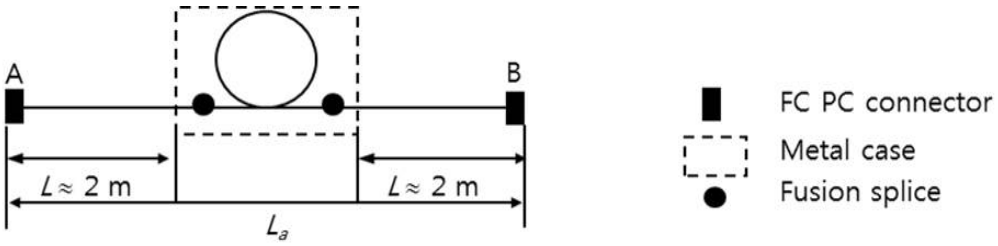

Fig. 2-5-3. Internal structure of the METAS artifact.

2.6 Handling of Artifacts

All participants were asked to immediately examine the optical fiber length artifacts upon receipt. However, care should be taken to ensure that the artifacts have sufficient time to acclimatize to the room environment thus preventing any condensation, etc. The condition of the artifacts and the associated package should be noted and communicated to the coordinator of the pilot lab if there is anything abnormal found. Before comparison measurements, the participant should check the artifact state, especially the FC/PC connector ends, by visual inspection and the photographs should be taken for record. Microscope inspection of the connector ends can be carried out if the participating lab has the equipment. Simple attenuation measurements can be optionally carried out without uncertainty analysis where the attenuation includes connector loss. The same check should be made before the artifacts are packaged for delivery. Care must be taken to maintain the FC/PC connector ends clean at all times. Cleaning can be done using standard fiber optic connector cleaning method if necessary. If there is any damage or problem found to potentially affect the comparison measurements, the participant should immediately report it to the pilot lab by e-mail. If the pilot lab finally decides to repair it after sufficient communication, the participant should deliver the artifact to KRISS for KRISS artifact or METAS for METAS artifact for repair. The repaired artifact only affects the round where the problem occurs and that round should go again with the repaired artifacts. When the comparison measurements are completed, the artifacts should be repackaged in their original container. Please ensure that the content of the package is complete by checking the packing list that was delivered together with the artifacts. The original packaging container should be used unless it is significantly damaged. Please inform the coordinator if the participant decides to make a new container. The participant should inform the contact person of the next participant and the coordinator of the pilot lab of the delivery schedule when the artifact package is ready to be sent.

2.7 Transportation of Artifacts

It is important that the artifact should be transported in a manner such that they will not be lost, damaged or handled by un-authorized persons. The artifacts should be packaged in a container that is suitably robust to protect the artifacts from being deformed or damaged during transportation. Fig. 2-7-1 and Fig. 2-7-2 are artifact packages provided by KRISS and METAS, respectively.

Transportation is at each participating lab's responsibility and cost. Each participating lab should cover the cost for its own measurements, one-way transportation including insurance, customs clearance, and any expense to be occurred in its own country. Choice of transportation method is up to each participating lab. Use of ATA Carnet is recommended if the local transport company of the country is fully aware of the process of ATA Carnet. Otherwise, it may cause potential delay until the requirement of appropriate documentation is fulfilled. If ATA Carnet is not used, an invoice or an equivalent document should accompany the package, which specifies that the packaged goods (artifacts) are of no commercial value and will be exported after about two months of comparison measurements from imported date.

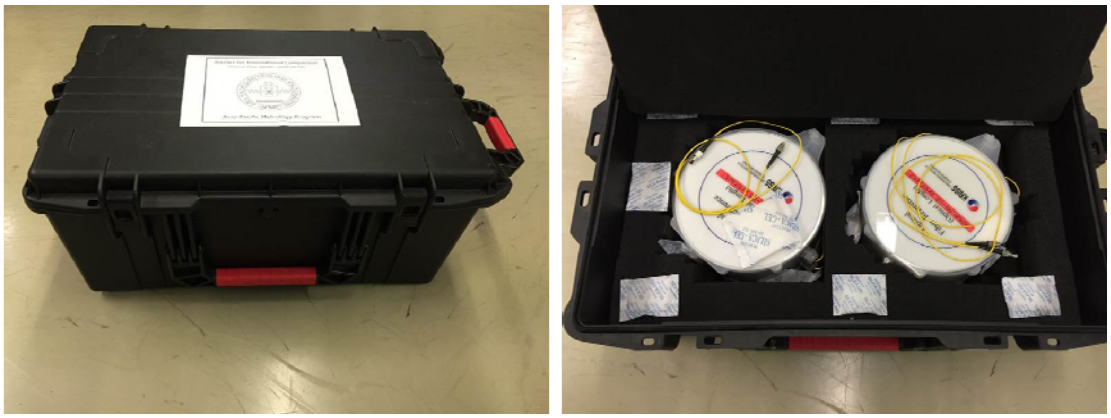

Fig. 2-7-1 Photograph of the KRISS artifacts in a delivery package.

Fig. 2-7-2 Photograph of the METAS artifact in a delivery package.

3. Measurement Capability and Results of Pilot Laboratory

3.1. Traceability

The KRISS reference standard of the optical fiber length is a modified time-of-flight (TOF) measurement setup. Time-of-flight (TOF) method is known to be a reference method for optical fiber length measurement. In TOF method, a variable frequency pulse generator is used to adjust the pulse repetition rate so that the delay time of the pulse in a fiber under test (FUT) can be equal to the period of the pulse [1]. Since the repetition rate can be measured by a frequency counter, the delay time can be measured very accurately. The frequency counter is calibrated using a KRISS frequency standard at 10 MHz that is traceable to the SI unit, second, through the Cs atomic clock in KRISS. The traceability chart is shown in Fig. 3-1-1.

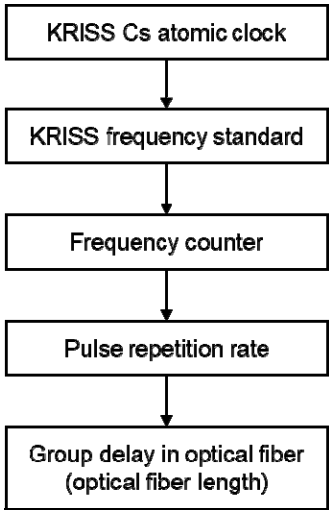

Fig. 3-1-1. Traceability of optical fiber length measurements at KRISS.

3.2. Description of measurement facility

Fig. 3-2-1 shows a schematic of KRISS TOF measurement setup for optical fiber length. We used a tunable laser source (TLS, New Focus Velocity 6300) for 1310 nm band and another TLS (Agilent 81624A) for 1550 nm band. The laser output power was made to modulate in the form of periodic pulse using the pulse generating mode in an arbitrary waveform generator (Agilent, 33250A). The driving electrical pulse had a maximum repetition rate of 50 MHz, a width of 8 ns, and a rising and falling time of 5 ns. In order to measure the repetition rate of the pulse accurately, we used a frequency counter (Agilent, 53132A). A variable optical attenuator (VOA) was inserted between the TLS and a directional coupler (DC) to adjust the input signal power not to excite any nonlinear effect in FUT such as stimulated Brillouin scattering [2]. The laser beam was divided into two paths using the DC. One was directly led to the photo detector (PD) 1 and the other to the PD 2 after the dummy optical fiber and the FUT. Another VOA was inserted between the DC and the PD 1 to adjust the final signal levels of the two PDs to be equal. The two output pulses were compared using a dual channel oscilloscope (Tektronix, TDS5052B). We verified that there was no additional time delay other than optical fiber in the setup.

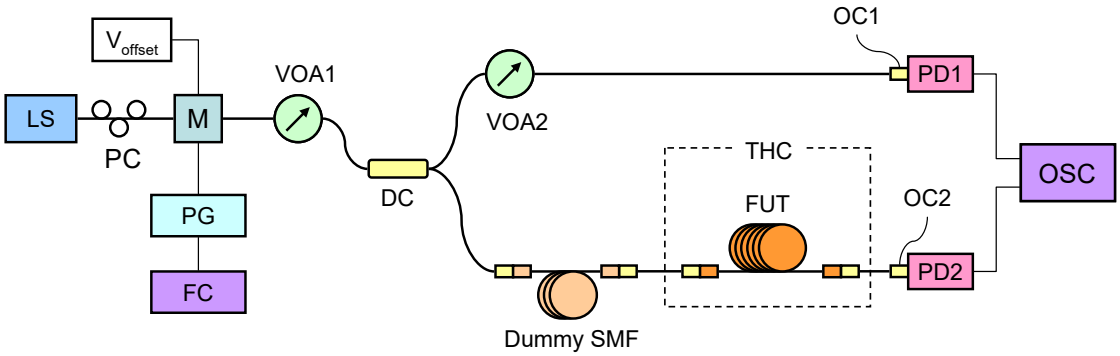

Fig. 3-2-1. A schematic of a standard setup for optical fiber length measurement. DC, directional coupler; FC, frequency counter; FUT, fiber under test; LS, laser source; M, modulator; OC, output coupler; OSC, oscilloscope; PD, photo detector; PG, pulse generator; SMF, single mode fiber; THC, temperature chamber; VOA, variable optical attenuator.

In an ordinary TOF method, the pulse repetition rate is measured when it becomes exactly the same as inverse of a group delay by FUT. However, our pulse generator had an effective

number digit limitation of 5 in repetition rate and so its minimum relative resolution varied from almost 10^{-5} at 99999 to 10^{-4} at 10000. Therefore, we modified the TOF method such that we inserted many pulses in a fiber delay to minimize the resolution as long as we determine the number of pulse without any uncertainty.

If the physical length of the fiber is L, the pulse repetition rate f_1 in an ordinary TOF is shown in Eq. 3-2-1

$$f_1 = \frac{1}{\tau} = \frac{c}{L_{op}} = \frac{c}{n_g L} \tag{3-2-1}$$

, where c, τ, L_{op}, and n_g are speed of light in vacuum, group delay of the optical pulse, optical length of the fiber, and the group index of the FUT, respectively. Now that the measurement accuracy of the optical length is determined by the accuracy of pulse repetition rate, the relative accuracy depends on the resolution of the pulse generator as shown in Eq. 3-2-2.

$$\frac{\Delta L}{L} = \frac{\Delta f_1}{f_1} \tag{3-2-2}$$

If we first measure the delay time as in an ordinary TOF method, the following relationship must be satisfied in order to uniquely determine the number of pulse, N in a delay, τ as shown in Eq 3-2-3 and 3-2-4.

$$\tau_1 = \frac{1}{f_1} = \frac{N}{f_2} \tag{3-2-3}$$

$$N < \frac{\tau}{2\Delta\tau} = \frac{f_1}{2\Delta f_1} \tag{3-2-4}$$

, where f_2 is the repetition rate of the pulse when the delay time of N pulses becomes equal to the delay time of the optical fiber. In the worst case, the last term in Eq. (3-2-4) becomes 5000. Therefore, as long as the number of pulses is less than 5000 in a delay time, we can obtain almost 10^{-5} resolution regardless of the fiber length. It means that we can apply our modified TOF method to optical fiber length of up to 100 km. We placed a comparison artifact in a temperature chamber to maintain the temperature at 23 °C. We first measured the delay time of the total length, τ_{tot} including the dummy single mode fiber (SMF) and the FUT. Then we

measured the delay time of the length, τ_{dum} without the FUT, which was almost equal to the delay time of the dummy SMF. Then the delay time and the optical length of the FUT were determined by subtracting the latter value from the former value as shown in Eq. (3-2-5) and (3-2-6), respectively.

$$\tau_{FUT} = \tau_{tot} - \tau_{dum} = \left(\frac{N}{f_2}\right)_{tot} - \left(\frac{N}{f_2}\right)_{dum} \tag{3-2-5}$$

$$L_{op,FUT} = L_{op,tot} - L_{op,dum} = c\left(\frac{N}{f_2}\right)_{tot} - c\left(\frac{N}{f_2}\right)_{dum} \tag{3-2-6}$$

3.3. Laboratory condition

The laboratory temperature was maintained at (23 ± 2) °C and the humidity at (45 ± 15) % throughout the calibration and measurements. The FUT was placed inside the temperature chamber of which the temperature was maintained at 23 °C.

3.4. Measurement procedure

Before measurements, all equipment was turned on and they were left to get stabilized at least for one hour. The detailed procedure for the calibration of the optical fiber length is as follows:

(1) Configure the calibration setup as shown in Fig. 3-2-1 to operate at the wavelength of interest.

(2) Apply the signal from the pulse generator to the EO modulator, and adjust the polarization controller to obtain maximum output power. Then, adjust the driving voltage and the bias voltage of the EO modulator so that the detected pulse shape can be optimized.

(3) Adjust VOA1 so that any unwanted nonlinear effect cannot be observed and VOA2 so that the two detected pulses can have the same level.

(4) Roughly calculate the delay time and the repetition rate. Adjusting the pulse repetition rate around the calculated value, find the frequency, f_1 so that the two detected pulses can be overlapped in time.

(5) Set the pulse repetition rate to be 9.9999 MHz. Decreasing the rate, find the frequency, f_2 so that the two detected pulses can be overlapped in time. Then the number of pulses, N in the delay time can be determined by dividing f_2 by f_1.

(6) Detach the FUT from the setup and connect the output of the dummy fiber to the input fiber

to detector, PD2.

(7) Repeat the step (4) and (5).

(8) Configure the calibration setup to operate at another wavelength.

(9) Conduct the step from (2) to (7).

3.5. Measurement results

Table 3-5-1 summarizes the measurement results.

Table 3-5-1 Optical fiber length of the comparison artifact measured at KRISS.

Round	Artifact	Wavelength (nm)	Optical fiber length (m)	Uncertainty (m) (k=2)
1	KRISS-1	1310	3250.1216	0.0282
		1550	3251.5312	0.0282
		1625	3252.4821	0.0282
	KRISS-2	1310	13305.9489	0.1097
		1550	13311.8170	0.1098
		1625	13315.6851	0.1098
2	METAS-1	1310	2346.5950	0.0241
		1550	2347.5400	0.0211
		1625	2348.1750	0.0212
	METAS-2	1310	12104.4590	0.1172
		1550	12109.0890	0.1169
		1625	12112.3560	0.1002
3	KRISS-1	1310	3250.1389	0.0446
		1550	3251.5419	0.0365
		1625	3252.4807	0.0282
	KRISS-2	1310	13305.9500	0.1097
		1550	13311.8124	0.1098
		1625	13315.6859	0.1098

3.6. Uncertainty

For convenience, we evaluated the uncertainty of the optical length of FUT instead of the group delay. From Eq. (3-2-6), we can derive the uncertainty propagation equation as shown in Eq. (3-2-7) because $f_{2,\mathrm{tot}}$ and $f_{2,\mathrm{dum}}$ measurements are uncorrelated.

$$u^2\left(L_{op}\right)=u^2\left(L_{op,tot}\right)+\ u^2\left(L_{op,dum}\right)=\left(\frac{cN_{tot}}{f_{2,tot}}\right)u^2\left(f_{2,tot}\right)+\ \left(\frac{cN_{dum}}{f_{2,dum}}\right)u^2\left(f_{2,dum}\right) \quad (3\text{-}2\text{-}7)$$

$$u(L) = u(L_{op}) / n_g \tag{3-2-8}$$

Frequency measurements of pulse repetition rate in Eq. (3-2-7) had uncertainty components originated from the resolution of pulse generator, frequency adjustment to make two pulses overlapped, repeatability, room temperature drift, and temperature uncertainty of the chamber. Calibration uncertainty of frequency counter is negligible.

The uncertainty budgets of KRISS are summarized in the following tables from Table 3-6-1 and Table 3-6-2 according to the comparison round and artifact.

Table 3-6-1 Uncertainty budget (Round 1 with KRISS artifact 1).

Wavelength: 1310 nm (Round 1, KRISS-1)

Component	Description	PDF	Standard uncertainty $u(x_i)$	Sensitivity coefficient $C_i = \delta f/\delta x_i$	Contribution $\|C_i\|u(x_i)$	DOF
$u(L_{Dd})$			40.1 ns	0.00051	0.020 m	1.8×10^{12}
$u(L_{Dd})_{res}$	Resolution of pulse generator	rect	28.9 ns	0.00051 m/ns	0.015 m	∞
$u(L_{Dd})_{set}$	Pulse timing synchronization	t	0 ns	0.00051 m/ns	0.000 m	9
$u(L_{Dd})_{rep}$	Repeatability	t	0.1 ns	0.00051 m/ns	0.000 m	9
$u(L_{Dd})_{tmp}$	Ambient temperature	rect	6.5 ns	0.00051 m/ns	0.003 m	∞
$u(L_{Dd})_{chm}$	Chamber temperature	rect	27.1 ns	0.00051 m/ns	0.014 m	∞
$u(L_d)$			113.0 ns	0.0000302	0.003 m	1.13×10^{14}
$u(L_d)_{res}$	Resolution of pulse generator	rect	28.9 ns	0.0000302 m/ns	0.001 m	∞
$u(L_d)_{set}$	Pulse timing synchronization	t	0 ns	0.0000302 m/ns	0.000 m	9
$u(L_d)_{rep}$	Repeatability	t	0.1 ns	0.0000302 m/ns	0.000 m	9
$u(L_d)_{tmp}$	Ambient temperature	rect	109.2 ns	0.0000302 m/ns	0.003 m	∞
$u(L_d)_{chm}$	Chamber temperature	rect	0 ns	0.0000302 m/ns	0.000 m	∞
	Combined standard uncertainty of optical length				**0.021 m**	1.90×10^{12}
	Expanded uncertainty of optical length (k = 2)				**0.041 m**	
	Expanded uncertainty (k = 2) (Exp. Unc. Optical length / 1.46)				**0.028 m**	

Wavelength: 1550 nm (Round 1, KRISS-1)

Component	Description	PDF	Standard uncertainty $u(x_i)$	Sensitivity coefficient $C_i = \delta f/\delta x_i$	Contribution $\|C_i\|u(x_i)$	DOF
$u(L_{Dd})$			40.1 ns	0.00051	0.020 m	1.8×10^{12}
$u(L_{Dd})_{res}$	Resolution of pulse generator	rect	28.9 ns	0.00051 m/ns	0.015 m	∞
$u(L_{Dd})_{set}$	Pulse timing synchronization	t	0 ns	0.00051 m/ns	0.000 m	9
$u(L_{Dd})_{rep}$	Repeatability	t	0.1 ns	0.00051 m/ns	0.000 m	9
$u(L_{Dd})_{tmp}$	Ambient temperature	rect	6.5 ns	0.00051 m/ns	0.003 m	∞
$u(L_{Dd})_{chm}$	Chamber temperature	rect	27.1 ns	0.00051 m/ns	0.014 m	∞
$u(L_d)$			115.6 ns	0.0000302	0.003 m	4460
$u(L_d)_{res}$	Resolution of pulse generator	rect	28.9 ns	0.0000302 m/ns	0.001 m	∞
$u(L_d)_{set}$	Pulse timing synchronization	t	24.5 ns	0.0000302 m/ns	0.001 m	9
$u(L_d)_{rep}$	Repeatability	t	0.1 ns	0.0000302 m/ns	0.000 m	9
$u(L_d)_{tmp}$	Ambient temperature	rect	109.2 ns	0.0000302 m/ns	0.003 m	∞
$u(L_d)_{chm}$	Chamber temperature	rect	0 ns	0.0000302 m/ns	0.000 m	∞
	Combined standard uncertainty of optical length				**0.021 m**	5.42×10^{6}
	Expanded uncertainty of optical length (k = 2)				**0.041 m**	
	Expanded uncertainty (k = 2) (Exp. Unc. Optical length / 1.46)				**0.028 m**	

Wavelength: 1625 nm (Round 1, KRISS-1)

Component	Description	PDF	Standard uncertainty $u(x_i)$	Sensitivity coefficient $C_i = \delta f/\delta x_i$	Contribution $\|C_i\|u(x_i)$	DOF
$u(L_{Dd})$			40.1 ns	0.00051	0.020 m	1.8×10^{12}
$u(L_{Dd})_{res}$	Resolution of pulse generator	rect	28.9 ns	0.00051 m/ns	0.015 m	∞
$u(L_{Dd})_{set}$	Pulse timing synchronization	t	0 ns	0.00051 m/ns	0.000 m	9
$u(L_{Dd})_{rep}$	Repeatability	t	0.1 ns	0.00051 m/ns	0.000 m	9
$u(L_{Dd})_{tmp}$	Ambient temperature	rect	6.5 ns	0.00051 m/ns	0.003 m	∞
$u(L_{Dd})_{chm}$	Chamber temperature	rect	27.1 ns	0.00051 m/ns	0.014 m	∞
$u(L_d)$			114.7 ns	0.0000302	0.003 m	972
$u(L_d)_{res}$	Resolution of pulse generator	rect	28.9 ns	0.0000302 m/ns	0.001 m	∞
$u(L_d)_{set}$	Pulse timing synchronization	t	20.0 ns	0.0000302 m/ns	0.001 m	9
$u(L_d)_{rep}$	Repeatability	t	0.1 ns	0.0000302 m/ns	0.000 m	9
$u(L_d)_{tmp}$	Ambient temperature	rect	109.1 ns	0.0000302 m/ns	0.003 m	∞
$u(L_d)_{chm}$	Chamber temperature	rect	0 ns	0.0000302 m/ns	0.000 m	∞
	Combined standard uncertainty of optical length				**0.021 m**	1.22×10^{7}
	Expanded uncertainty of optical length (k = 2)				**0.041 m**	
	Expanded uncertainty (k = 2) (Exp. Unc. / 1.46)				**0.028 m**	

Table 3-6-2 Uncertainty budget (Round 1 with KRISS artifact 2).

Wavelength: 1310 nm (Round 1, KRISS-2)

Component	Description	PDF	Standard uncertainty $u(x_i)$	Sensitivity coefficient $C_i = \delta f/\delta x_i$	Contribution $\|C_i\|u(x_i)$	DOF
$u(L_{Dd})$			40.5 ns	0.00197	0.080 m	1.88×10^{12}
$u(L_{Dd})_{res}$	Resolution of pulse generator	rect	28.9 ns	0.00197 m/ns	0.057 m	∞
$u(L_{Dd})_{set}$	Pulse timing synchronization	t	0 ns	0.00197 m/ns	0.000 m	9
$u(L_{Dd})_{rep}$	Repeatability	t	0.1 ns	0.00197 m/ns	0.000 m	9
$u(L_{Dd})_{tmp}$	Ambient temperature	rect	1.7 ns	0.00197 m/ns	0.003 m	∞
$u(L_{Dd})_{chm}$	Chamber temperature	rect	28.4 ns	0.00197 m/ns	0.056 m	∞
$u(L_d)$			114.7 ns	0.0000302	0.003 m	9745
$u(L_d)_{res}$	Resolution of pulse generator	rect	28.9 ns	0.0000302 m/ns	0.001 m	∞
$u(L_d)_{set}$	Pulse timing synchronization	t	20.0 ns	0.0000302 m/ns	0.001 m	9
$u(L_d)_{rep}$	Repeatability	t	0.1 ns	0.0000302 m/ns	0.000 m	9
$u(L_d)_{tmp}$	Ambient temperature	rect	109.2 ns	0.0000302 m/ns	0.003 m	∞
$u(L_d)_{chm}$	Chamber temperature	rect	0 ns	0.0000302 m/ns	0.000 m	∞
	Combined standard uncertainty of optical length				**0.080 m**	2.79×10^{9}
	Expanded uncertainty of optical length (k = 2)				**0.160 m**	
	Expanded uncertainty (k = 2) (Exp. Unc. / 1.46)				**0.110 m**	

Wavelength: 1550 nm (Round 1, KRISS-2)

Component	Description	PDF	Standard uncertainty $u(x_i)$	Sensitivity coefficient $C_i = \delta f/\delta x_i$	Contribution $\|C_i\|u(x_i)$	DOF
$u(L_{Dd})$			40.5 ns	0.00197	0.080 m	1.88×10^{12}
$u(L_{Dd})_{res}$	Resolution of pulse generator	rect	28.9 ns	0.00197 m/ns	0.057 m	∞
$u(L_{Dd})_{set}$	Pulse timing synchronization	t	0.0 ns	0.00197 m/ns	0.000 m	9
$u(L_{Dd})_{rep}$	Repeatability	t	0.1 ns	0.00197 m/ns	0.000 m	9
$u(L_{Dd})_{tmp}$	Ambient temperature	rect	1.7 ns	0.00197 m/ns	0.003 m	∞
$u(L_{Dd})_{chm}$	Chamber temperature	rect	28.4 ns	0.00197 m/ns	0.056 m	∞
$u(L_d)$			114.7 ns	0.0000302	0.003 m	9730
$u(L_d)_{res}$	Resolution of pulse generator	rect	28.9 ns	0.0000302 m/ns	0.001 m	∞
$u(L_d)_{set}$	Pulse timing synchronization	t	20.0 ns	0.0000302 m/ns	0.001 m	9
$u(L_d)_{rep}$	Repeatability	t	0.1 ns	0.0000302 m/ns	0.000 m	9
$u(L_d)_{tmp}$	Ambient temperature	rect	109.2 ns	0.0000302 m/ns	0.003 m	∞
$u(L_d)_{chm}$	Chamber temperature	rect	0 ns	0.0000302 m/ns	0.000 m	∞
	Combined standard uncertainty of optical length				**0.080 m**	2.79×10^{9}
	Expanded uncertainty of optical length (k = 2)				**0.160 m**	
	Expanded uncertainty (k = 2) (Exp. Unc. / 1.46)				**0.110 m**	

Wavelength: 1625 nm (Round 1, KRISS-2)

Component	Description	PDF	Standard uncertainty $u(x_i)$	Sensitivity coefficient $C_i = \delta f/\delta x_i$	Contribution $\|C_i\|u(x_i)$	DOF
$u(L_{Dd})$			40.5 ns	0.00198	0.080 m	1.87×10^{12}
$u(L_{Dd})_{res}$	Resolution of pulse generator	rect	28.9 ns	0.00198 m/ns	0.057 m	∞
$u(L_{Dd})_{set}$	Pulse timing synchronization	t	0.0 ns	0.00198 m/ns	0.000 m	9
$u(L_{Dd})_{rep}$	Repeatability	t	0.1 ns	0.00198 m/ns	0.000 m	9
$u(L_{Dd})_{tmp}$	Ambient temperature	rect	1.7 ns	0.00198 m/ns	0.003 m	∞
$u(L_{Dd})_{chm}$	Chamber temperature	rect	28.4 ns	0.00198 m/ns	0.056 m	∞
$u(L_d)$			115.5 ns	0.0000302	0.003 m	4450
$u(L_d)_{res}$	Resolution of pulse generator	rect	28.9 ns	0.0000302 m/ns	0.001 m	∞
$u(L_d)_{set}$	Pulse timing synchronization	t	24.5 ns	0.0000302 m/ns	0.001 m	9
$u(L_d)_{rep}$	Repeatability	t	0.1 ns	0.0000302 m/ns	0.000 m	9
$u(L_d)_{tmp}$	Ambient temperature	rect	109.1 ns	0.0000302 m/ns	0.003 m	∞
$u(L_d)_{chm}$	Chamber temperature	rect	0 ns	0.0000302 m/ns	0.000 m	∞
	Combined standard uncertainty of optical length				**0.080 m**	1.24×10^{9}
	Expanded uncertainty of optical length (k = 2)				**0.160 m**	
	Expanded uncertainty (k = 2) (Exp. Unc. / 1.46)				**0.110 m**	

Table 3-6-3 Uncertainty budget (Round 2 with METAS artifact 1).

Wavelength: 1310 nm (Round 2, METAS-1)

Component	Description	PDF	Standard uncertainty $u(x_i)$	Sensitivity coefficient $C_i = \delta f/\delta x_i$	Contribution $\|C_i\|u(x_i)$	DOF
$u(L_{Dd})$			46.2 ns	0.00037	0.017 m	3.17×10^{12}
$u(L_{Dd})_{res}$	Resolution of pulse generator	rect	28.9 ns	0.00037 m/ns	0.011 m	∞
$u(L_{Dd})_{set}$	Pulse timing synchronization	t	0 ns	0.00037 m/ns	0.000 m	9
$u(L_{Dd})_{rep}$	Repeatability	t	0.1 ns	0.00037 m/ns	0.000 m	9
$u(L_{Dd})_{tmp}$	Ambient temperature	rect	8.8 ns	0.00037 m/ns	0.003 m	∞
$u(L_{Dd})_{chm}$	Chamber temperature	rect	35.0 ns	0.00037 m/ns	0.013 m	∞
$u(L_d)$			115.1 ns	0.0000302	0.003 m	6321
$u(L_d)_{res}$	Resolution of pulse generator	rect	28.9 ns	0.0000302 m/ns	0.001 m	∞
$u(L_d)_{set}$	Pulse timing synchronization	t	22.4 ns	0.0000302 m/ns	0.001 m	9
$u(L_d)_{rep}$	Repeatability	t	0.1 ns	0.0000302 m/ns	0.000 m	9
$u(L_d)_{tmp}$	Ambient temperature	rect	109.2 ns	0.0000302 m/ns	0.003 m	∞
$u(L_d)_{chm}$	Chamber temperature	rect	0 ns	0.0000302 m/ns	0.000 m	∞
	Combined standard uncertainty of optical length				**0.0018 m**	4.18×10^{5}
	Expanded uncertainty of optical length (k = 2)				**0.035 m**	
	Expanded uncertainty (k = 2) (Exp. Unc. Optical length / 1.46)				**0.024 m**	

Wavelength: 1550 nm (Round 2, METAS-1)

Component	Description	PDF	Standard uncertainty $u(x_i)$	Sensitivity coefficient $C_i = \delta f/\delta x_i$	Contribution $\|C_i\|u(x_i)$	DOF
$u(L_{Dd})$			40.1 ns	0.00037	0.015 m	1.8×10^{12}
$u(L_{Dd})_{res}$	Resolution of pulse generator	rect	28.9 ns	0.00037 m/ns	0.011 m	∞
$u(L_{Dd})_{set}$	Pulse timing synchronization	t	0 ns	0.00037 m/ns	0.000 m	9
$u(L_{Dd})_{rep}$	Repeatability	t	0.1 ns	0.00037 m/ns	0.000 m	9
$u(L_{Dd})_{tmp}$	Ambient temperature	rect	8.8 ns	0.00037 m/ns	0.003 m	∞
$u(L_{Dd})_{chm}$	Chamber temperature	rect	26.5 ns	0.00037 m/ns	0.010 m	∞
$u(L_d)$			117.0 ns	0.0000302	0.004 m	1890
$u(L_d)_{res}$	Resolution of pulse generator	rect	28.9 ns	0.0000302 m/ns	0.001 m	∞
$u(L_d)_{set}$	Pulse timing synchronization	t	30.7 ns	0.0000302 m/ns	0.001 m	9
$u(L_d)_{rep}$	Repeatability	t	0.1 ns	0.0000302 m/ns	0.000 m	9
$u(L_d)_{tmp}$	Ambient temperature	rect	109.1 ns	0.0000302 m/ns	0.003 m	∞
$u(L_d)_{chm}$	Chamber temperature	rect	0 ns	0.0000302 m/ns	0.000 m	∞
	Combined standard uncertainty of optical length				**0.015 m**	6.84×10^{5}
	Expanded uncertainty of optical length (k = 2)				**0.031 m**	
	Expanded uncertainty (k = 2) (Exp. Unc. Optical length / 1.46)				**0.021 m**	

Wavelength: 1625 nm (Round 2, METAS-1)

Component	Description	PDF	Standard uncertainty $u(x_i)$	Sensitivity coefficient $C_i = \delta f/\delta x_i$	Contribution $\|C_i\|u(x_i)$	DOF
$u(L_{Dd})$			40.1 ns	0.00037	0.015 m	1.8×10^{12}
$u(L_{Dd})_{res}$	Resolution of pulse generator	rect	28.9 ns	0.00037 m/ns	0.011 m	∞
$u(L_{Dd})_{set}$	Pulse timing synchronization	t	0 ns	0.00037 m/ns	0.000 m	9
$u(L_{Dd})_{rep}$	Repeatability	t	0.1 ns	0.00037 m/ns	0.000 m	9
$u(L_{Dd})_{tmp}$	Ambient temperature	rect	8.8 ns	0.00037 m/ns	0.003 m	∞
$u(L_{Dd})_{chm}$	Chamber temperature	rect	26.5 ns	0.00037 m/ns	0.010 m	∞
$u(L_d)$			118.9 ns	0.0000302	0.004 m	971
$u(L_d)_{res}$	Resolution of pulse generator	rect	28.9 ns	0.0000302 m/ns	0.001 m	∞
$u(L_d)_{set}$	Pulse timing synchronization	t	37.4 ns	0.0000302 m/ns	0.001 m	9
$u(L_d)_{rep}$	Repeatability	t	0.1 ns	0.0000302 m/ns	0.000 m	9
$u(L_d)_{tmp}$	Ambient temperature	rect	109.1 ns	0.0000302 m/ns	0.003 m	∞
$u(L_d)_{chm}$	Chamber temperature	rect	0 ns	0.0000302 m/ns	0.000 m	∞
	Combined standard uncertainty of optical length				**0.015 m**	1.22×10^{7}
	Expanded uncertainty of optical length (k = 2)				**0.031 m**	
	Expanded uncertainty (k = 2) (Exp. Unc. / 1.46)				**0.021 m**	

Table 3-6-4 Uncertainty budget (Round 2 with METAS artifact 2).

Wavelength: 1310 nm (Round 2, METAS-2)

Component	Description	PDF	Standard uncertainty $u(x_i)$	Sensitivity coefficient $C_i = \delta f/\delta x_i$	Contribution $\|C_i\|u(x_i)$	DOF
$u(L_{Dd})$			47.5 ns	0.00180	0.085 m	2.58×10^{5}
$u(L_{Dd})_{res}$	Resolution of pulse generator	rect	28.9 ns	0.00180 m/ns	0.052 m	∞
$u(L_{Dd})_{set}$	Pulse timing synchronization	t	3.7 ns	0.00180 m/ns	0.007 m	9
$u(L_{Dd})_{rep}$	Repeatability	t	0.1 ns	0.00180 m/ns	0.000 m	9
$u(L_{Dd})_{tmp}$	Ambient temperature	rect	1.8 ns	0.00180 m/ns	0.003 m	∞
$u(L_{Dd})_{chm}$	Chamber temperature	rect	37.5 ns	0.00180 m/ns	0.067 m	∞
$u(L_d)$			117.1 ns	0.0000302	0.004 m	1896
$u(L_d)_{res}$	Resolution of pulse generator	rect	28.9 ns	0.0000302 m/ns	0.001 m	∞
$u(L_d)_{set}$	Pulse timing synchronization	t	30.7 ns	0.0000302 m/ns	0.001 m	9
$u(L_d)_{rep}$	Repeatability	t	0.1 ns	0.0000302 m/ns	0.000 m	9
$u(L_d)_{tmp}$	Ambient temperature	rect	109.2 ns	0.0000302 m/ns	0.003 m	∞
$u(L_d)_{chm}$	Chamber temperature	rect	0 ns	0.0000302 m/ns	0.000 m	∞
	Combined standard uncertainty of optical length				**0.086 m**	3.68×10^{7}
	Expanded uncertainty of optical length (k = 2)				**0.171 m**	
	Expanded uncertainty (k = 2) (Exp. Unc. / 1.46)				**0.117 m**	

Wavelength: 1550 nm (Round 2, METAS-2)

Component	Description	PDF	Standard uncertainty $u(x_i)$	Sensitivity coefficient $C_i = \delta f/\delta x_i$	Contribution $\|C_i\|u(x_i)$	DOF
$u(L_{Dd})$			47.5 ns	0.00180	0.085 m	2.31×10^{6}
$u(L_{Dd})_{res}$	Resolution of pulse generator	rect	28.9 ns	0.00180 m/ns	0.052 m	∞
$u(L_{Dd})_{set}$	Pulse timing synchronization	t	2.1 ns	0.00180 m/ns	0.004 m	9
$u(L_{Dd})_{rep}$	Repeatability	t	0.1 ns	0.00180 m/ns	0.000 m	9
$u(L_{Dd})_{tmp}$	Ambient temperature	rect	1.8 ns	0.00180 m/ns	0.003 m	∞
$u(L_{Dd})_{chm}$	Chamber temperature	rect	37.6 ns	0.00180 m/ns	0.068 m	∞
$u(L_d)$			115.6 ns	0.0000302	0.003 m	4460
$u(L_d)_{res}$	Resolution of pulse generator	rect	28.9 ns	0.0000302 m/ns	0.001 m	∞
$u(L_d)_{set}$	Pulse timing synchronization	t	24.5 ns	0.0000302 m/ns	0.001 m	9
$u(L_d)_{rep}$	Repeatability	t	0.1 ns	0.0000302 m/ns	0.000 m	9
$u(L_d)_{tmp}$	Ambient temperature	rect	109.2 ns	0.0000302 m/ns	0.003 m	∞
$u(L_d)_{chm}$	Chamber temperature	rect	0 ns	0.0000302 m/ns	0.000 m	∞
	Combined standard uncertainty of optical length				**0.085 m**	2.32×10^{6}
	Expanded uncertainty of optical length (k = 2)				**0.171 m**	
	Expanded uncertainty (k = 2) (Exp. Unc. / 1.46)				**0.117**	

Wavelength: 1625 nm (Round 2, METAS-2)

Component	Description	PDF	Standard uncertainty $u(x_i)$	Sensitivity coefficient $C_i = \delta f/\delta x_i$	Contribution $\|C_i\|u(x_i)$	DOF
$u(L_{Dd})$			40.6 ns	0.00180	0.073 m	5.51×10^{5}
$u(L_{Dd})_{res}$	Resolution of pulse generator	rect	28.9 ns	0.00180 m/ns	0.052 m	∞
$u(L_{Dd})_{set}$	Pulse timing synchronization	t	2.6 ns	0.00180 m/ns	0.005 m	9
$u(L_{Dd})_{rep}$	Repeatability	t	0.1 ns	0.00180 m/ns	0.000 m	9
$u(L_{Dd})_{tmp}$	Ambient temperature	rect	1.8 ns	0.00180 m/ns	0.003 m	∞
$u(L_{Dd})_{chm}$	Chamber temperature	rect	28.4 ns	0.00180 m/ns	0.051 m	∞
$u(L_d)$			115.5 ns	0.0000302	0.003 m	4450
$u(L_d)_{res}$	Resolution of pulse generator	rect	28.9 ns	0.0000302 m/ns	0.001 m	∞
$u(L_d)_{set}$	Pulse timing synchronization	t	24.5 ns	0.0000302 m/ns	0.001 m	9
$u(L_d)_{rep}$	Repeatability	t	0.1 ns	0.0000302 m/ns	0.000 m	9
$u(L_d)_{tmp}$	Ambient temperature	rect	109.1 ns	0.0000302 m/ns	0.003 m	∞
$u(L_d)_{chm}$	Chamber temperature	rect	0 ns	0.0000302 m/ns	0.000 m	∞
	Combined standard uncertainty of optical length				**0.073 m**	5.53×10^{5}
	Expanded uncertainty of optical length (k = 2)				**0.146 m**	
	Expanded uncertainty (k = 2) (Exp. Unc. / 1.46)				**0.100 m**	

Table 3-6-5 Uncertainty budget (Round 3 with KRISS artifact 1).

Wavelength: 1310 nm (Round 3, KRISS-1)

Component	Description	PDF	Standard uncertainty $u(x_i)$	Sensitivity coefficient $C_i = \delta f/\delta x_i$	Contribution $\|C_i\|u(x_i)$	DOF
$u(L_{Dd})$			64.1 ns	0.00051	0.032 m	2.43×10^{1}
$u(L_{Dd})_{res}$	Resolution of pulse generator	rect	28.9 ns	0.00051 m/ns	0.015 m	∞
$u(L_{Dd})_{set}$	Pulse timing synchronization	t	50.0 ns	0.00051 m/ns	0.025 m	9
$u(L_{Dd})_{rep}$	Repeatability	t	0.1 ns	0.00051 m/ns	0.000 m	9
$u(L_{Dd})_{tmp}$	Ambient temperature	rect	6.5 ns	0.00051 m/ns	0.003 m	∞
$u(L_{Dd})_{chm}$	Chamber temperature	rect	27.1 ns	0.00051 m/ns	0.014 m	∞
$u(L_d)$			113.0 ns	0.0000302	0.003 m	1.13×10^{14}
$u(L_d)_{res}$	Resolution of pulse generator	rect	28.9 ns	0.0000302 m/ns	0.001 m	∞
$u(L_d)_{set}$	Pulse timing synchronization	t	0 ns	0.0000302 m/ns	0.000 m	9
$u(L_d)_{rep}$	Repeatability	t	0.1 ns	0.0000302 m/ns	0.000 m	9
$u(L_d)_{tmp}$	Ambient temperature	rect	109.2 ns	0.0000302 m/ns	0.003 m	∞
$u(L_d)_{chm}$	Chamber temperature	rect	0 ns	0.0000302 m/ns	0.000 m	∞
	Combined standard uncertainty of optical length				**0.033 m**	2.49×10^{1}
	Expanded uncertainty of optical length (k = 2)				**0.065 m**	
	Expanded uncertainty (k = 2) (Exp. Unc. Optical length / 1.46)				**0.045 m**	

Wavelength: 1550 nm (Round 3, KRISS-1)

Component	Description	PDF	Standard uncertainty $u(x_i)$	Sensitivity coefficient $C_i = \delta f/\delta x_i$	Contribution $\|C_i\|u(x_i)$	DOF
$u(L_{Dd})$			52.2 ns	0.00051	0.026 m	5.40×10^{1}
$u(L_{Dd})_{res}$	Resolution of pulse generator	rect	28.9 ns	0.00051 m/ns	0.015 m	∞
$u(L_{Dd})_{set}$	Pulse timing synchronization	t	33.3 ns	0.00051 m/ns	0.017 m	9
$u(L_{Dd})_{rep}$	Repeatability	t	0.1 ns	0.00051 m/ns	0.000 m	9
$u(L_{Dd})_{tmp}$	Ambient temperature	rect	6.5 ns	0.00051 m/ns	0.003 m	∞
$u(L_{Dd})_{chm}$	Chamber temperature	rect	27.1 ns	0.00051 m/ns	0.014 m	∞
$u(L_d)$			112.9 ns	0.0000302	0.003 m	1.13×10^{14}
$u(L_d)_{res}$	Resolution of pulse generator	rect	28.9 ns	0.0000302 m/ns	0.001 m	∞
$u(L_d)_{set}$	Pulse timing synchronization	t	0.0 ns	0.0000302 m/ns	0.000 m	9
$u(L_d)_{rep}$	Repeatability	t	0.1 ns	0.0000302 m/ns	0.000 m	9
$u(L_d)_{tmp}$	Ambient temperature	rect	109.2 ns	0.0000302 m/ns	0.003 m	∞
$u(L_d)_{chm}$	Chamber temperature	rect	0.0 ns	0.0000302 m/ns	0.000 m	∞
	Combined standard uncertainty of optical length				**0.027 m**	5.58×10^{1}
	Expanded uncertainty of optical length (k = 2)				**0.053 m**	
	Expanded uncertainty (k = 2) (Exp. Unc. Optical length / 1.46)				**0.036 m**	

Wavelength: 1625 nm (Round 3, KRISS-1)

Component	Description	PDF	Standard uncertainty $u(x_i)$	Sensitivity coefficient $C_i = \delta f/\delta x_i$	Contribution $\|C_i\|u(x_i)$	DOF
$u(L_{Dd})$			40.1 ns	0.00051	0.020 m	1.8×10^{12}
$u(L_{Dd})_{res}$	Resolution of pulse generator	rect	28.9 ns	0.00051 m/ns	0.015 m	∞
$u(L_{Dd})_{set}$	Pulse timing synchronization	t	0.0 ns	0.00051 m/ns	0.000 m	9
$u(L_{Dd})_{rep}$	Repeatability	t	0.1 ns	0.00051 m/ns	0.000 m	9
$u(L_{Dd})_{tmp}$	Ambient temperature	rect	6.5 ns	0.00051 m/ns	0.003 m	∞
$u(L_{Dd})_{chm}$	Chamber temperature	rect	27.1 ns	0.00051 m/ns	0.014 m	∞
$u(L_d)$			116.5 ns	0.0000302	0.004 m	2390
$u(L_d)_{res}$	Resolution of pulse generator	rect	28.9 ns	0.0000302 m/ns	0.001 m	∞
$u(L_d)_{set}$	Pulse timing synchronization	t	28.9 ns	0.0000302 m/ns	0.001 m	9
$u(L_d)_{rep}$	Repeatability	t	0.1 ns	0.0000302 m/ns	0.000 m	9
$u(L_d)_{tmp}$	Ambient temperature	rect	109.1 ns	0.0000302 m/ns	0.003 m	∞
$u(L_d)_{chm}$	Chamber temperature	rect	0 ns	0.0000302 m/ns	0.000 m	∞
	Combined standard uncertainty of optical length				**0.021 m**	2.81×10^{6}
	Expanded uncertainty of optical length (k = 2)				**0.041 m**	
	Expanded uncertainty (k = 2) (Exp. Unc. / 1.46)				**0.028 m**	

Table 3-6-6 Uncertainty budget (Round 3 with KRISS artifact 2).

Wavelength: 1310 nm (Round 3, KRISS-2)

Component	Description	PDF	Standard uncertainty $u(x_i)$	Sensitivity coefficient $C_i = \delta f/\delta x_i$	Contribution $\|C_i\|u(x_i)$	DOF
$u(L_{Dd})$			40.5 ns	0.00197	0.080 m	1.88×10^{12}
$u(L_{Dd})_{res}$	Resolution of pulse generator	rect	28.9 ns	0.00197 m/ns	0.057 m	∞
$u(L_{Dd})_{set}$	Pulse timing synchronization	t	0.0 ns	0.00197 m/ns	0.000 m	9
$u(L_{Dd})_{rep}$	Repeatability	t	0.1 ns	0.00197 m/ns	0.000 m	9
$u(L_{Dd})_{tmp}$	Ambient temperature	rect	1.7 ns	0.00197 m/ns	0.003 m	∞
$u(L_{Dd})_{chm}$	Chamber temperature	rect	28.4 ns	0.00197 m/ns	0.056 m	∞
$u(L_d)$			117.8 ns	0.0000302	0.004 m	1403
$u(L_d)_{res}$	Resolution of pulse generator	rect	28.9 ns	0.0000302 m/ns	0.001 m	∞
$u(L_d)_{set}$	Pulse timing synchronization	t	33.3 ns	0.0000302 m/ns	0.001 m	9
$u(L_d)_{rep}$	Repeatability	t	0.1 ns	0.0000302 m/ns	0.000 m	9
$u(L_d)_{tmp}$	Ambient temperature	rect	109.2 ns	0.0000302 m/ns	0.003 m	∞
$u(L_d)_{chm}$	Chamber temperature	rect	0.0 ns	0.0000302 m/ns	0.000 m	∞
	Combined standard uncertainty of optical length				**0.080 m**	3.62×10^{8}
	Expanded uncertainty of optical length (k = 2)				**0.160 m**	
	Expanded uncertainty (k = 2) (Exp. Unc. / 1.46)				**0.110 m**	

Wavelength: 1550 nm (Round 3, KRISS-2)

Component	Description	PDF	Standard uncertainty $u(x_i)$	Sensitivity coefficient $C_i = \delta f/\delta x_i$	Contribution $\|C_i\|u(x_i)$	DOF
$u(L_{Dd})$			40.5 ns	0.00197	0.080 m	1.88×10^{12}
$u(L_{Dd})_{res}$	Resolution of pulse generator	rect	28.9 ns	0.00197 m/ns	0.057 m	∞
$u(L_{Dd})_{set}$	Pulse timing synchronization	t	0.0 ns	0.00197 m/ns	0.000 m	9
$u(L_{Dd})_{rep}$	Repeatability	t	0.1 ns	0.00197 m/ns	0.000 m	9
$u(L_{Dd})_{tmp}$	Ambient temperature	rect	1.7 ns	0.00197 m/ns	0.003 m	∞
$u(L_{Dd})_{chm}$	Chamber temperature	rect	28.4 ns	0.00197 m/ns	0.056 m	∞
$u(L_d)$			112.9 ns	0.0000302	0.003 m	1.13×10^{14}
$u(L_d)_{res}$	Resolution of pulse generator	rect	28.9 ns	0.0000302 m/ns	0.001 m	∞
$u(L_d)_{set}$	Pulse timing synchronization	t	0.0 ns	0.0000302 m/ns	0.000 m	9
$u(L_d)_{rep}$	Repeatability	t	0.1 ns	0.0000302 m/ns	0.000 m	9
$u(L_d)_{tmp}$	Ambient temperature	rect	109.2 ns	0.0000302 m/ns	0.003 m	∞
$u(L_d)_{chm}$	Chamber temperature	rect	0.0 ns	0.0000302 m/ns	0.000 m	∞
	Combined standard uncertainty of optical length				**0.080 m**	1.88×10^{12}
	Expanded uncertainty of optical length (k = 2)				**0.160 m**	
	Expanded uncertainty (k = 2) (Exp. Unc. / 1.46)				**0.110 m**	

Wavelength: 1625 nm (Round 3, KRISS-2)

Component	Description	PDF	Standard uncertainty $u(x_i)$	Sensitivity coefficient $C_i = \delta f/\delta x_i$	Contribution $\|C_i\|u(x_i)$	DOF
$u(L_{Dd})$			40.5 ns	0.00198	0.080 m	1.87×10^{12}
$u(L_{Dd})_{res}$	Resolution of pulse generator	rect	28.9 ns	0.00198 m/ns	0.057 m	∞
$u(L_{Dd})_{set}$	Pulse timing synchronization	t	0.0 ns	0.00198 m/ns	0.000 m	9
$u(L_{Dd})_{rep}$	Repeatability	t	0.1 ns	0.00198 m/ns	0.000 m	9
$u(L_{Dd})_{tmp}$	Ambient temperature	rect	1.7 ns	0.00198 m/ns	0.003 m	∞
$u(L_{Dd})_{chm}$	Chamber temperature	rect	28.4 ns	0.00198 m/ns	0.056 m	∞
$u(L_d)$			126.8 ns	0.0000302	0.004 m	209
$u(L_d)_{res}$	Resolution of pulse generator	rect	28.9 ns	0.0000302 m/ns	0.001 m	∞
$u(L_d)_{set}$	Pulse timing synchronization	t	57.7 ns	0.0000302 m/ns	0.002 m	9
$u(L_d)_{rep}$	Repeatability	t	0.1 ns	0.0000302 m/ns	0.000 m	9
$u(L_d)_{tmp}$	Ambient temperature	rect	109.1 ns	0.0000302 m/ns	0.003 m	∞
$u(L_d)_{chm}$	Chamber temperature	rect	0.0 ns	0.0000302 m/ns	0.000 m	∞
	Combined standard uncertainty of optical length				**0.080 m**	4.02×10^{7}
	Expanded uncertainty of optical length (k = 2)				**0.160 m**	
	Expanded uncertainty (k = 2) (Exp. Unc. / 1.46)				**0.110 m**	

References

[1] http://www.npl.co.uk/photonics/services/length_cert.html, Certificate of calibration of optical length, NPL, UK.

[2] G.P. Agrawal, *Nonlinear Fiber Optics*, 3rd ed. (Academic Press, 2001), chapter 9.

4. Measurement Capabilities and Results of Participants

4.1. NMC

Comparison APMP.PR-S8 Optical Fiber Length

Description of the measurement facility in NMC A*STAR Singapore

1. Measurement facility

The measurement was carried out by using following reference standard, intensity stabilized tunable laser sources, variable attenuator and other equipment in NMC

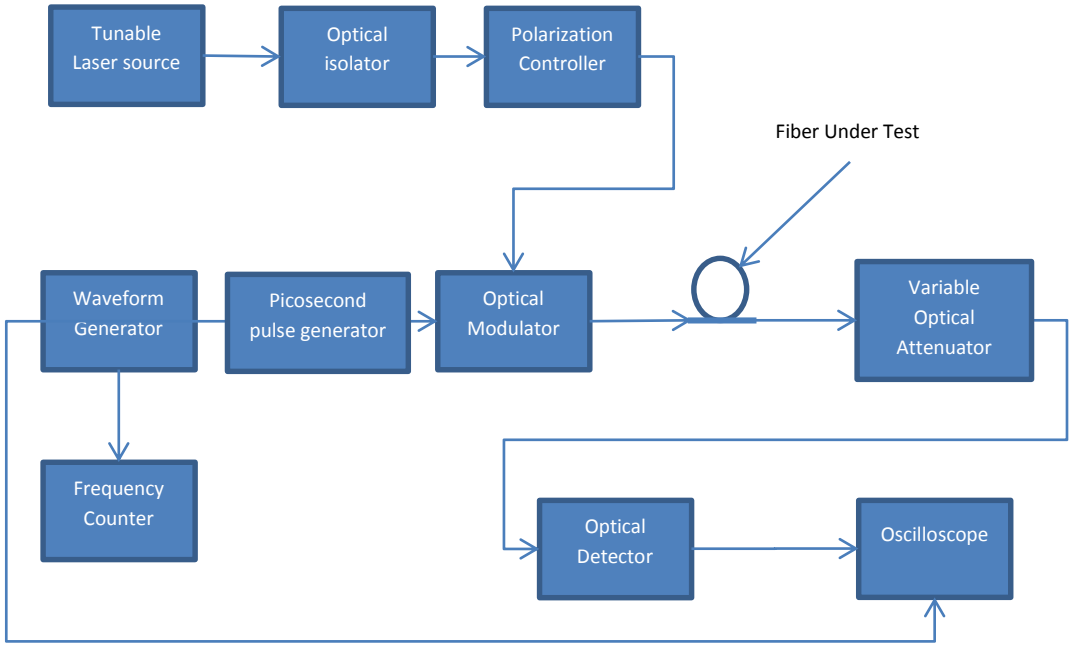

Fig. 1 Schematic diagram of the measurement facility

Equipment list:

1) ANDO AQ4321D – 1550 nm tunable laser source
2) Santec TSL-510 – 1310 nm tunable laser source
3) A reference standard (RS) wavelength meter (Burleigh, model: WA-1500)
4) An adjustable optical attenuator (EXFO, model: IQ-3100-BEI, s/n: 121725-36) is used to change single mode optical output power level
5) A working standard (WS) - fibre optic power meter (EXFO, model: IQ-1103, s/n: 118320-35) or (ILX Lightwave, model: FPM-8210, s/n: 82104281)
6) Universal counter HP53131A
7) Newport Multifunction polarization controller 2580P
8) Tektronix arbitrary waveform generator AFG 3251

9) Picosecond pulse generator

10) Tektronix Digital Phosphor Oscilloscope DPO 720004

11) Lutron HT-3003 Digital Thermometer

12) ESPEC PU-2KT temperature chamber

13) Agilent E3620A DC power supply

14) High speed InGaAs photodetector SIR5

15) JDSU OC-192y optical modulator

16) A single mode fiber optic isolator with FC/PC connectors (COPENETI, part number: IS-D-13/15-P-L-10-FC dual stage isolator) used to connect tunable laser source and other equipment so as to eliminate the inter-reflectance effect between fiber connectors.

17) Single mode fiber patchcords

2. Measurement procedure:

1) The artefacts were put in the temperature chamber and the temperature chamber was set to be 23 °C. Use the digital thermometer to monitor the temperature and ensure the temperature is as close as possible to 23 °C. Wait for 12 hours for the temperature in the chamber to be stable. Record the temperature in the chamber.

2) The tunable laser was adjusted to the nominal wavelength (1550 nm or 1310 nm) and checked by using the wavelength standard to ensure the wavelength is as close as possible to the desired wavelength. Record the wavelength.

3) The waveform generator was set to drive picosecond pulse generator and the picosecond pulse generator drove the optical modulator. The fast speed photo detector was used to detect the optical pulses. The electrical signal from the photo detector was displayed in the oscilloscope.

4) The optical attenuator was adjusted so that the optical power reaching the photodetector was the same level.

5) The period of the pulses generated by the waveform generator was adjusted so that the optical pulses with and without the fiber artefact overlap in time. Under this condition, the time delay caused by the fiber artefact is the same as the period of the pulses. The period of pulses was measured by the universal counter. The optical fiber length is $L = T * c / 1.46$, where T is the total delay caused by the artifact, c is the speed of light.

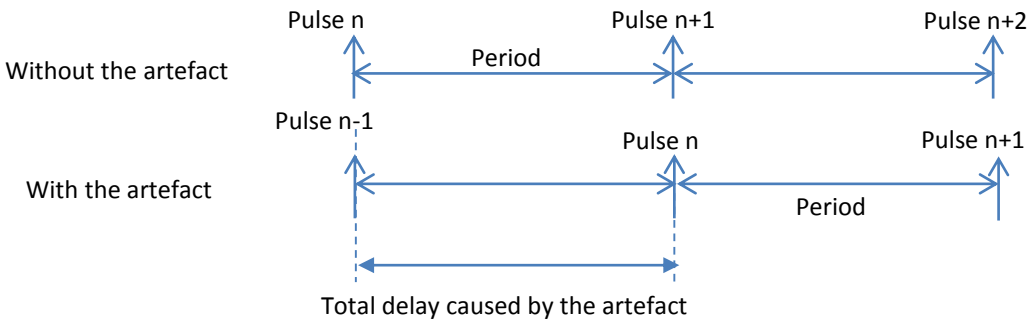

Fig. 2 Artefact time delay measurement

3. Traceability and uncertainty budget

The traceability of NMC's fibre length measurement is based on our time & frequency scale as shown in Figure 3. The laser wavelength measurement is traceable to the primary standard of laser wavelength maintained in NMC, A*STAR, Singapore. The breakdown uncertainty budget of measurement was estimated and its results are shown in the attached file.

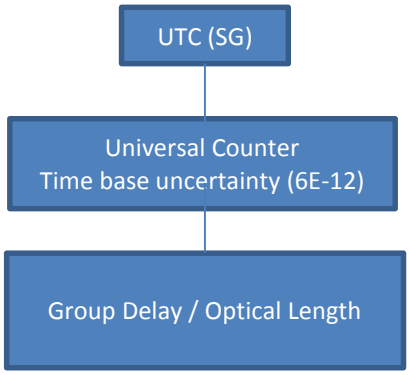

(All uncertainty values in the chart refer to combined standard uncertainty, $k = 2$)

Fig. 3 Traceability chart for fiber length measurement

4. Laboratory conditions

Temperature: 23 ± 2 ◦C and Relative Humidity: 60 ± 10 % rh

Laboratory: NMC A*STAR Singapore Officer in Charge: Zhang Jing

Date: 20 Jul 2017 Signature:

Result of APMP Supplementary Comparison on Optical Fiber Length – NMC, A*STAR, Singapore

The measurement was done under environment temperature of 23 ± 2 °C and humidity of 60 ± 10 % rh. Each fiber artifact was measured for five runs. The final measurement results and uncertainties are listed in the below tables at a level of confidence of approximately 95% with a covering factor $k = 2$.

Table 1. Result and uncertainty at 1550 nm.

Wavelength	1550 nm			
	Group Delay (ns)	Uncertainty (ns) @ $k = 2$	Fiber Length (m)	Uncertainty (m) @ $k = 2$
Fiber Artefact 1	15835.069	0.061	3251.530	0.013
Fiber Artefact 2	64828.759	0.15	13311.762	0.031

Table 2. Result and uncertainty at 1310 nm.

Wavelength	1310 nm			
	Group Delay (ns)	Uncertainty (ns) @ $k = 2$	Fiber Length (m)	Uncertainty (m) @ $k = 2$
Fiber Artefact 1	15828.227	0.061	3250.125	0.013
Fiber Artefact 2	64800.005	0.15	13305.858	0.031

Laboratory: NMC A*STAR Singapore Officer in Charge: Zhang Jing

Date: 20 Jul 2017 Signature: 

Uncertainty Budget of APMP Supplementary Comparison on Optical Fiber Length – NMC, A*STAR, Singapore

Table 1. Uncertainty table of one measurement for Artefact 1 at 1550 nm

1550nm Fiber 1	Uncertainty	Ci	*k*	u_x(i) (ns)	DOF	Probability Distribution
Uncertainty of Universal Counter Time Base	6.00E-12	15835	2.00E+00	4.75E-08	∞	Normal
jitter of t1 peak (ns)	1.00E-02	1	1.73E+00	5.78E-03	∞	Rectangular
jitter of t2 peak (ns)	1.00E-02	1	1.73E+00	5.78E-03	∞	Rectangular
Resolution of Universal Counter Reading Take (ns)	1.00E-03	1	1.73E+00	5.78E-04	∞	Rectangular
Repeatability of Universal Counter measurement (ns)	1.60E-03	1	1.00E+00	1.60E-03	4	Normal
Error caused by wavelength @1550nm (nm)	0.01	0.06ns/nm	1.73E+00	3.47E-04	∞	Rectangular
Error caused by temperature (C°)	0.25	0.2ns/C°	1.73E+00	2.89E-02	∞	Rectangular
Combined uncertainty (ns)				3.01-02	∞	
Expanded Uncertainty (ns)				6.02E-02		
Expanded Uncertainty (m)				1.24E-02		

Table 2. Uncertainty table of one measurement for Artefact 2 at 1550 nm

1550nm Fiber 2	Uncertainty	Ci	*k*	u_x(i) (ns)	DOF	Probability Distribution
Uncertainty of Universal Counter Time Base	6.00E-12	64828	2.00E+00	1.94E-07	∞	Normal
jitter of t1 peak (ns)	2.00E-02	1	1.73E+00	1.16E-02	∞	Rectangular
jitter of t2 peak (ns)	2.00E-02	1	1.73E+00	1.16E-02	∞	Rectangular
Resolution of Universal Counter Reading Take (ns)	1.00E-03	1	1.73E+00	5.78E-04	∞	Rectangular
Repeatability of Universal Counter measurement (ns)	1.00E-02	1	1.00E+00	1.00E-02	4	Normal
Error caused by wavelength @1550nm (nm)	0.01	0.23ns/nm	1.73E+00	1.33E-03	∞	Rectangular
Error caused by temperature (C°)	0.25	0.5ns/C°	1.73E+00	7.23E-02	∞	Rectangular
Combined uncertainty (ns)				7.48E-02	∞	
Expanded Uncertainty (ns)				1.50E-01		
Expanded Uncertainty (m)				3.07E-02		

Table 3. Uncertainty table of one measurement for Artefact 1 at 1310 nm

1310nm Fiber 1	Uncertainty	Ci	*k*	u_x(i) (ns)	DOF	Probability Distribution
Uncertainty of Universal Counter Time Base	6.00E-12	15828	2.00E+00	4.75E-08	∞	Normal
jitter of t1 peak (ns)	1.00E-02	1	1.73E+00	5.78E-03	∞	Rectangular
jitter of t2 peak (ns)	1.00E-02	1	1.73E+00	5.78E-03	∞	Rectangular
Resolution of Universal Counter Reading Take (ns)	1.00E-03	1	1.73E+00	5.78E-04	∞	Normal
Repeatability of Universal Counter measurement (fiber delay) (ns)	1.60E-03	1	1.00E+00	1.60E-03	4	Normal
Error cause by wavelength @1310nm (nm)	0.03	0.003ns/nm	1.73E+00	5.20E-05	∞	Rectangular
Error cause by temperature (C°)	0.25	0.2ns/C°	1.73E+00	2.89E-02	∞	Normal
Combined uncertainty (ns)				3.01E-02	∞	
Expanded Uncertainty (ns)				6.02E-02		
Expanded Uncertainty (m)				1.24E-02		

Table 4. Uncertainty table of one measurement for Artefact 2 at 1310 nm

1310nm Fiber 2	Uncertainty	Ci	*k*	u_x(i) (ns)	DOF	Probability Distribution
Uncertainty of Universal Counter Time Base	6.00E-12	64800	2.00E+00	1.94E-07	∞	Normal
jitter of t1 peak (ns)	2.00E-02	1	1.73E+00	1.16E-02	∞	Rectangular
jitter of t2 peak (ns)	2.00E-02	1	1.73E+00	1.16E-02	∞	Rectangular
Resolution of Universal Counter Reading Take (ns)	1.00E-03	1	1.73E+00	5.78E-04	∞	Normal
Repeatability of Universal Counter measurement (ns)	1.00E-02	1	1.00E+00	1.00E-02	4	Normal
Error caused by wavelength @1310nm (nm)	0.03	0.02ns/nm	1.73E+00	3.47E-04	∞	Rectangular
Error caused by temperature (C°)	0.25	0.5ns/C°	1.73E+00	7.23E-02	∞	Normal
Combined uncertainty (ns)				7.48E-02	∞	
Expanded Uncertainty (ns)				1.50E-01		
Expanded Uncertainty (m)				3.07E-02		

Laboratory: NMC A*STAR Singapore Officer in Charge: Zhang Jing

Date: 20 Jul 2017 Signature: 

4.2. NMIJ

Report of the calibration performed by NMIJ on the optical fibre artifacts of the APMP-PR.S8 intercomparison

Scope

The aim of this project is to perform a comparison and to assess the equivalence of the optical fiber length (group delay) scale among the participants. The participants were recommended to measure the group delay of each artifact at wavelength of 1310 nm, 1550 nm and 1625 nm at 23 °C.

Artefact

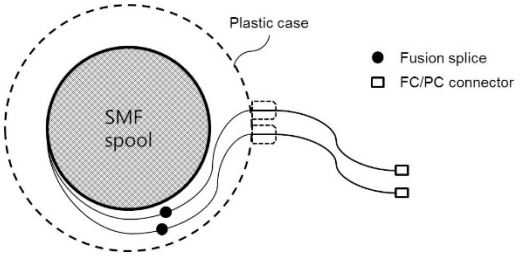

Fig. 1 The measurement artifact.

The measurement artefacts were two spools of single mode optical fiber of 3 km and 13 km approximately, having FC/PC connectors on each end.

Calibration facility of NMIJ

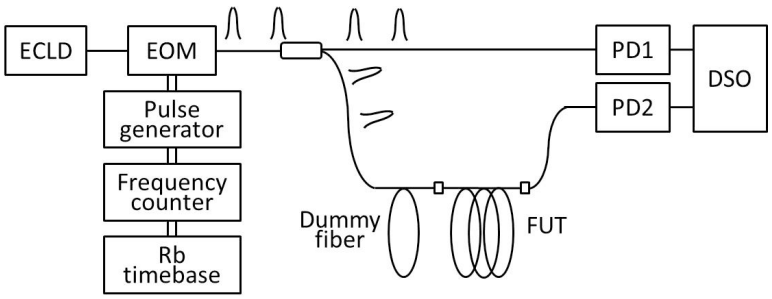

Fig. 2 Setup of optical fiber group delay calibration facility of NMIJ.
ECLD, external cavity laser diode; EOM, electro-optic modulator;
FUT, fiber under test; PD, InGaAs photodiode; DSO, digital storage oscilloscope.

The optical fiber group delay calibration facility of NMIJ is schematically presented in Fig. 2. Optical pulse generated by EOM is split with 50:50 coupler into two optical paths and each optical pulses are detected with high-speed InGaAs photodiodes. The PD signals are monitored on a DSO. The one of the paths always has long dummy fiber (typically 1 km). The optical pulse via dummy-fiber path delayed against another path. If the pulse repetition frequency is appropriately adjusted, a single pulse signal via dummy-fiber path and neighboring optical pulse via another path can be detected at the same time on the DSO. By recording the repetition frequencies for coincident detection of those optical pulses with and without FUT in the dummy fiber path, ν_1, ν_2, respectively, we can determine the group delay τ of the FUT as follows:

$$\tau = \left(\frac{1}{\upsilon_1} - \frac{1}{\upsilon_2} \right) \cdot \left(1 + \delta_{\text{temp}} + \delta_{\text{wav}} + \delta_{\text{rep}} \right).$$

Therein, δ_{temp}, δ_{wav}, δ_{rep} respectively represent the corrections for temperature dependence, wavelength dependence and reproducibility of the measurement, which are considered to be zero and discussed only in uncertainty analyses. The optical length L of the FUT is determined as $L = c\tau / N$, by assuming group index $N \equiv 1.460000$, where c is the speed of light. The frequency counter is calibrated by the Rb time base, which is annually calibrated traceably to Japanese national standard of time and frequency.

Calibration measurements were conducted for temperatures within 23.0 °C +/− 1 °C. The relative humidity was 50 % +/− 20 %. Temperature and relative humidity were monitored by calibrated temperature/humidity meter throughout the calibration operation. Center wavelength of the laser source was determined with an optical spectrum analyzer (OSA) whose wavelength scale is calibrated with an acetylene gas cell absorption lines.

Results

Artefact No. 1

Wavelength (nm)	Group delay (μs)	Optical length (m)	Relative expanded uncertainty (k=2)
1310.01	15.82833	3250.147	0.0015%
1549.990	15.83514	3251.544	0.0015%
1625.00	15.83972	3252.485	0.0015%

Artefact No. 2

Wavelength (nm)	Group delay (μs)	Optical length (m)	Relative expanded uncertainty (k=2)
1310.01	64.80054	13305.97	0.0015%
1549.990	64.82919	13311.85	0.0015%
1625.00	64.84815	13315.74	0.0015%

Uncertainty analyses

As described above, group delay τ and optical length L of the FUT can be determined by the following equations:

$$\tau = \left(\frac{1}{\upsilon_1} - \frac{1}{\upsilon_2} \right) \cdot \left(1 + \delta_{\text{temp}} + \delta_{\text{wav}} + \delta_{\text{rep}} \right) \tag{1}$$

$$L = c\tau / N$$

The value of c is exactly defined, and N is considered here as a constant with zero uncertainty. Therefore, the relative uncertainty of the group delay is same with that of the optical length.

The relative standard uncertainty for the group delay measurement of FUT is derived from the following equations:

$$\frac{u_c(\tau)}{\tau_0} = \sqrt{\left[\frac{u(\tau_0)}{\tau_0} \right]^2 + u^2(\delta_{\text{temp}}) + u^2(\delta_{\text{wav}}) + u^2(\delta_{\text{rep}}) + u^2{}_{\text{repeat}}} \tag{2}$$

where

$$\tau_0 = \left(\frac{1}{\upsilon_1} - \frac{1}{\upsilon_2} \right) \tag{3}$$

$$\frac{u(\tau_0)}{\tau_0} = \frac{1}{\tau_0} \sqrt{\frac{1}{\upsilon_1^2} \left[\frac{u(\upsilon_1)}{\upsilon_1} \right]^2 + \frac{1}{\upsilon_2^2} \left[\frac{u(\upsilon_2)}{\upsilon_2} \right]^2} \tag{4}$$

The estimations of each uncertainty factors are as follows:

(1) Uncertainty from pulse repetition frequency measurement $u(\tau_0)/\tau_0$

The relative standard uncertainty from pulse repetition frequency measurement can be described as:

$$\frac{u(\upsilon)}{\upsilon} = \sqrt{\left[\frac{u(\upsilon_{\text{std\_cal}})}{\upsilon_{\text{std}}} \right]^2 + \left[\frac{u(\upsilon_{\text{std\_stab}})}{\upsilon_{\text{std}}} \right]^2 + \left[\frac{\upsilon_{\text{res}}}{2\sqrt{3}\upsilon} \right]^2} \tag{5}$$

The relative uncertainty of Rb time base calibration $u(v_{\text{std\_cal}})/v_{\text{std}}$ is 2.6E-12, and that of the temporal stability (for 1 year) $u(v_{\text{std\_stab}})/v_{\text{std}}$ is 2.9E-10. The frequency counter resolution is 0.000 001 Hz.

When the dummy fiber length is approx. 1 km, v_2 is approx. 200 kHz. When the FUT is approx. 3 km/ 13 km, v_1 is respectively approx. 50 kHz/ 15 kHz. By substituting these values into Eq. (4), the relative standard uncertainty from pulse repetition frequency measurement were estimated as 4.0E-10 for 3 km, 3.1E-10 for 13 km FUT, respectively.

(2) Temperature dependence of FUT $u(\delta_{\text{temp}})$

Temperature dependence of the typical FUT group delay was investigated and determined to be 13.0 ppm/K as the worst case. The calibration room temperature fluctuates within 23.0 °C +/− 1 °C. Therefore, the relative standard uncertainty from the temperature dependence was estimated as:

13.0 ppm/K × 1 K /√3 = 7.53 ppm.

(3) Wavelength dependence of FUT $u(\delta_{\text{wav}})$

The chromatic dispersion of the typical FUT was measured as 0.18 ps/nm/km at 1310 nm wavelength, 16.96 ps/nm/km at 1550 nm, and 20.94 ps/nm/km at 1625 nm, respectively. The accuracy of wavelength determination with an OSA was 0.2 nm for 1310 nm and 1625 nm, and 0.02 nm for 1550 nm, respectively.

Therefore, the relative standard uncertainty from the wavelength dependence was

estimated as:

- For 1310 nm (actual wavelength: 1310.01 nm)

0.18 ps/nm/km × √((1310.01-1310.00)² + (0.2 nm)²) / √3 × 299792458 m/s / 1.460000
= 4.28E-9

- For 1550 nm (actual wavelength: 1549.990 nm)

16.96 ps/nm/km ×√((1549.990-1550.000)² + (0.02 nm)²) /√3 × 299792458 m/s / 1.460000
= 5.32E-8

- For 1625 nm (actual wavelength: 1625.00 nm)

20.94 ps/nm/km ×√((1625.00-1625.00)² + (0.2 nm)²) /√3 × 299792458 m/s / 1.460000
= 4.96E-7

(4) Measurement repeatability u_{repeat}

Measurement repeatability was 0.286 ppm for 3 km FUT, 0.113 ppm for 13 km FUT, respectively, at 5 times measurement. Therefore the uncertainty from measurement repeatability was respectively estimated by dividing the repeatability by √5, as 0.128 ppm and 0.051 ppm.

(5) Measurement reproducibility $u(\delta_{\text{rep}})$

The FUT group delay (optical length) calibration was conducted more than twice by changing days. There were found the maximum difference of 2.5 ppm among the results. By assuming the difference as the maximum deviation, the uncertainty from the measurement reproducibility was estimated as:

2.5 ppm / √3 = 1.43 ppm.

Uncertainty budgets are summarized as follows:

1310 nm, 3 km

Factor x_i	deviation	PDF	divisor	Standard uncertainty $u(x_i)$	$c_i = \partial f / \partial x_i$	Standard uncertainty $c_i \cdot u(x_i)$	DoF
Freq. meas. $u(\tau_0)/\tau_0$	3.97E-10	normal	1	3.97E-10	1	3.97E-10	∞
Temp. dep. $u(\delta_{temp})$	1 K	rectan gular	√3	0.577 K	13.0 ppm/K	7.53E-6	∞
Wav. dep. $u(\delta_{wav})$	0.2 nm	rectan gular	√3	0.115 nm	0.18 ps/nm/km	4.28E-09	∞
Repeat-ability	2.86E-7	normal	√5	1.28E-7	1	1.28E-07	4
Reproduci-bility	2.50E-6	rectan gular	√3	1.43E-6	1	1.43E-06	∞
Combined std. unc.		normal				7.66E-06	5.17E+07
Expanded unc. (k=2)						0.0015%	

1310 nm, 13 km

Factor x_i	deviation	PDF	divisor	Standard uncertainty $u(x_i)$	$c_i = \partial f / \partial x_i$	Standard uncertainty $c_i \cdot u(x_i)$	DoF
Freq. meas. $u(\tau_0)/\tau_0$	3.13E-10	normal	1	3.13E-10	1	3.13E-10	∞
Temp. dep. $u(\delta_{temp})$	1 K	rectan gular	√3	0.577 K	13.0 ppm/K	7.53E-6	∞
Wav. dep. $u(\delta_{wav})$	0.2 nm	rectan gular	√3	0.115 nm	0.18 ps/nm/km	4.28E-09	∞
Repeat-ability	1.13E-7	normal	√5	5.05E-08	1	5.05E-08	4
Reproduci-bility	2.50E-6	rectan gular	√3	1.43E-6	1	1.43E-06	∞
Combined std. unc.		normal				7.66E-06	2.12E+09
Expanded unc. (k=2)						0.0015%	

1550 nm, 3 km

Factor x_i	deviation	PDF	divisor	Standard uncertainty $u(x_i)$	$c_i = \partial f / \partial x_i$	Standard uncertainty $c_i \cdot u(x_i)$	DoF
Freq. meas. $u(\tau_0)/\tau_0$	3.97E-10	normal	1	3.97E-10	1	3.97E-10	∞
Temp. dep. $u(\delta_{temp})$	1 K	rectan gular	√3	0.577 K	13.0 ppm/K	7.53E-6	∞
Wav. dep. $u(\delta_{wav})$	0.02 nm	rectan gular	√3	0.0115 nm	16.96 ps/nm/km	5.32E-08	∞
Repeat-ability	2.86E-7	normal	√5	1.28E-7	1	1.28E-07	4
Reproduci-bility	2.50E-6	rectan gular	√3	1.43E-6	1	1.43E-06	∞
Combined std. unc.		normal				7.66E-06	5.17E+07
Expanded unc. (k=2)						0.0015%	

1550 nm, 13 km

Factor x_i	deviation	PDF	divisor	Standard uncertainty $u(x_i)$	$c_i = \partial f / \partial x_i$	Standard uncertainty $c_i \cdot u(x_i)$	DoF
Freq. meas. $u(\tau_0)/\tau_0$	3.13E-10	normal	1	3.13E-10	1	3.13E-10	∞
Temp. dep. $u(\delta_{temp})$	1 K	rectan gular	√3	0.577 K	13.0 ppm/K	7.53E-6	∞
Wav. dep. $u(\delta_{wav})$	0.02 nm	rectan gular	√3	0.0115 nm	16.96 ps/nm/km	5.32E-08	∞
Repeat-ability	1.13E-7	normal	√5	5.05E-08	1	5.05E-08	4
Reproduci-bility	2.50E-6	rectan gular	√3	1.43E-6	1	1.43E-06	∞
Combined std. unc.		normal				7.66E-06	2.12E+09
Expanded unc. (k=2)						0.0015%	

1625 nm, 3 km

Factor x_i	deviation	PDF	divisor	Standard uncertainty $u(x_i)$	$c_i = \partial f / \partial x_i$	Standard uncertainty $c_i \cdot u(x_i)$	DoF
Freq. meas. $u(\tau_0)/\tau_0$	3.97E-10	normal	1	3.97E-10	1	3.97E-10	∞
Temp. dep. $u(\delta_{temp})$	1 K	rectan gular	√3	0.577 K	13.0 ppm/K	7.53E-6	∞
Wav. dep. $u(\delta_{wav})$	0.2 nm	rectan gular	√3	0.115 nm	20.94 ps/nm/km	4.96E-07	∞
Repeat-ability	2.86E-7	normal	√5	1.28E-7	1	1.28E-07	4
Reproduci-bility	2.50E-6	rectan gular	√3	1.43E-6	1	1.43E-06	∞
Combined std. unc.		normal				7.68E-06	5.21E+07
Expanded unc. (k=2)						0.0015%	

1625 nm, 13 km

Factor x_i	deviation	PDF	divisor	Standard uncertainty $u(x_i)$	$c_i = \partial f / \partial x_i$	Standard uncertainty $c_i \cdot u(x_i)$	DoF
Freq. meas. $u(\tau_0)/\tau_0$	3.13E-10	normal	1	3.13E-10	1	3.13E-10	∞
Temp. dep. $u(\delta_{temp})$	1 K	rectan gular	√3	0.577 K	13.0 ppm/K	7.53E-6	∞
Wav. dep. $u(\delta_{wav})$	0.2 nm	rectan gular	√3	0.115 nm	20.94 ps/nm/km	4.96E-07	∞
Repeat-ability	1.13E-7	normal	√5	5.05E-08	1	5.05E-08	4
Reproduci-bility	2.50E-6	rectan gular	√3	1.43E-6	1	1.43E-06	∞
Combined std. unc.		normal				7.68E-06	2.13E+09
Expanded unc. (k=2)						0.0015%	

4.3. METAS

Schweizerische Eidgenossenschaft
Confédération suisse
Confederazione Svizzera
Confederaziun svizra

Federal Institute of Metrology METAS

METAS results to APMP.PR-S8
Supplementary Inter-comparison on optical fibre length calibration
Part 1/2

Object	**Singlemode Length Reference Fibre** Manufacturer: METAS Serial Nr. LRF 2015.06 Approximate Fibre length: 12 km Connector: FC/UPC
Order	Calibration of the transit time of a light pulse propagating through the fibre at λ = 1310 nm, λ = 1550 nm and λ = 1625 nm. Determination of the fibre length for n_g = 1.46.
Traceability	The reported measurement values are traceable to national standards and thus to internationally supported realizations of the SI-units.
Date of calibration	27 March 2015
Date of control measurement	19 May 2016
Marking	Calibration label METAS 03. 2015

Photonics Time and Frequency Laboratory

Dr. Jacques Morel, Head of Laboratory

METAS
Lindenweg 50, 3003 Bern-Wabern, Switzerland, phone +41 58 387 50 11, www.metas.ch

METAS results to APMP.PR-S8

Object

The singlemode Length Reference Fibre (LRF) consists in a G.652D fibre spool with a length L_1. Two patch-cables of approximate length L = 2 m are fitted with FC UPC connectors and are fusion-spliced at both fibre ends. The internal structure of the LRF is shown in the figure below.

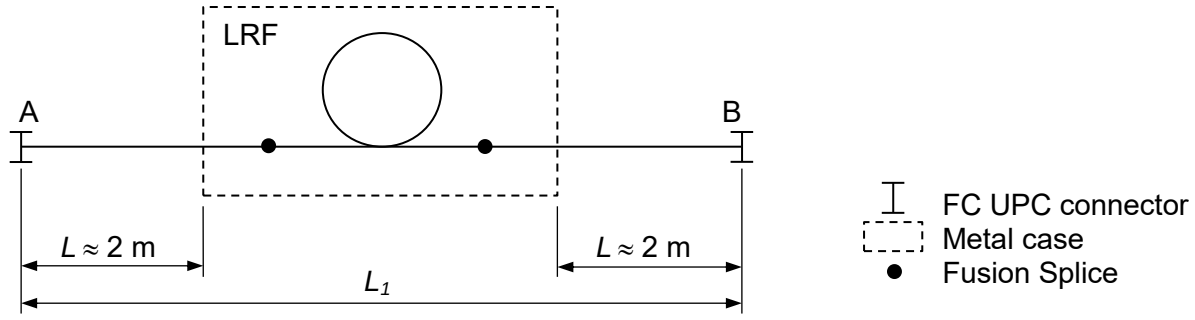

Extent of the calibration

Calibration of the transit time of a light pulse propagating through the fibre spool (measurement performed between points A and B) and calculation of the fibre length L_1 for a reference group refractive index n_g = 1.46. The measurements were done at the three wavelengths λ = 1310 nm, λ = 1550 nm and λ = 1625 nm.

Measurement procedure

The transit time t of a laser pulse propagating through the fibre was measured by using a modified version of the system as specified in the annex (A2) of the IEC 61746 document (Ed. 1).

The basic structure of the measuring setup is shown in figure 1, here below. A series of pulses with a repetition rate τ_{rep} is produced using different laser diodes (LD) and by modulating their injection currents directly or by modulating the optical CW power using a Mach Zehnder modulator. The optical pulses are then coupled into two different paths (Ref. and DUT) using a 3 dB coupler.

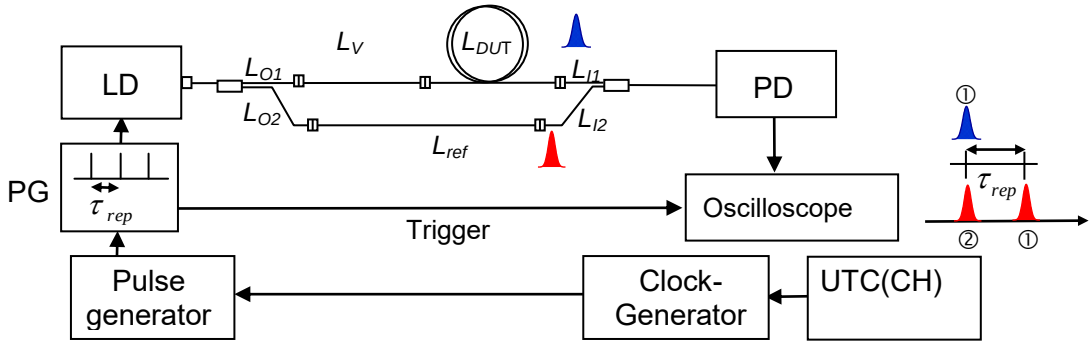

Fig. 1. METAS transit-time cailbration system.

The pulses having circulated through both paths are detected using a fast photodiode (PD).The repetition rate τ_{rep} is then adjusted until pulse 2 of Ref and pulse 1 of DUT paths are superimposed.

The length of the DUT is obtained from two successive measurements; the first one being performed with and the second one without the DUT. This yields:

METAS results to APMP.PR-S8

$L_{DUT} = \frac{c}{n_{eff}} \cdot \left\{ \tau_{\mathrm{rep}_{\mathrm{DUT}}} - \tau_{\mathrm{rep}_{\mathrm{cal}}} \right\}$, where $\tau_{\mathrm{rep}_{\mathrm{DUT}}}$ is the repetition rate measured with the DUT inserted in the system, and $\tau_{\mathrm{rep}_{\mathrm{cal}}}$ is the repetition rate measured without the DUT.

The clock generator is a pulse synthesizer, which is locked to UTC(CH).
The calibration setup is shown in figure 2, here below.

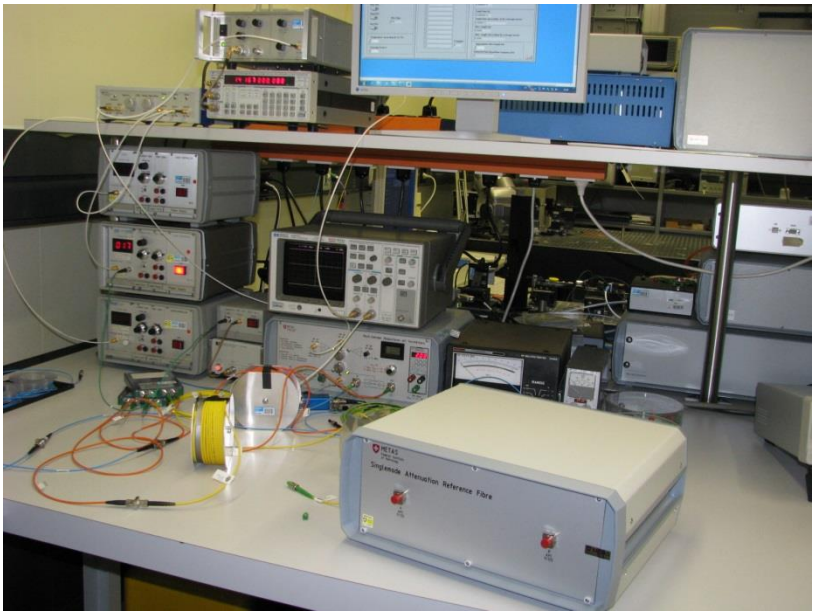

Fig. 2. Picture of the METAS transit-time calibration setup.

Measurement conditions

Ambient laboratory temperature: (23 ± 1) °C
Relative humidity: (45 ± 5 %) rH

The DUT was allowed to thermalize before starting the calibration.

The vacuum wavelengths of the laser sources are summarized in the table below.

Laser	$\lambda_{central}$ / nm	λ_{Peak} / nm	$U\lambda$
Fabry-Perot	1310.0	-	1.2 nm
DFB Extended cavity		1550.000	0.008 nm
DFB Extended cavity		1625.000	0.008 nm
DFB		1551.69	0.02 nm

METAS results to APMP.PR-S8

Measurement results

First measurements, dated 27th of March 2015

λ / nm	t / ns	U / ns	L_1 / m	U / m
1310.0	58949.54	0.43	12104.54	0.09
1550.000	58972.07	0.40	12109.17	0.09
1551.69	58972.39	0.40	12109.23	0.09
1625.000	58988.02	0.40	12112.44	0.09

Control measurements, dated 19th of May 2016

λ / nm	t / ns	U / ns	L_1 / m	U / m
1310.000	58949.53	0.43	12104.54	0.09
1550.000	58971.89	0.40	12109.13	0.09
1551.69	58972.39	0.40	12109.23	0.09
1625.000	58987.96	0.40	12112.43	0.09

Both sets of measurements are fully comparable within their measurement uncertainties.

Uncertainty of measurement

The uncertainty budget includes following contributions:

Uncertainty component	**Source of uncertainty**
u_{fgen}	Uncertainty of synthesizer frequency
u_{fA}	Type A uncertainty of the measured mean frequency. The frequency and the repetition rate are related through $f = 1/\tau_{rep}$
u_{fdisp}	Uncertainty arising from the fibre dispersion (chromatic dispersion and PMD)
u_T	Temperature stability of DUT (thermal expansion of glass and thermal dependency of the effective index of refraction)
u_{Lcal}	Uncertainty of reference path length calibration

The detailed uncertainty budgets for the first three calibrations performed on March 27, 2015 are shown in the next pages.

METAS results to APMP.PR-S8

Measurement setup: Optical fibre length (Transit-Time)

Wavelength	1310	nm
Source spectral width / wavelength uncertainty	4.00E+00	nm
Ref. index of refraction	1.46	
Estimated fibre length	12104.5396	m
Temperature coefficient of refractive index of fibre	1.00E-05	K^{-1}
Coeff. of lin. thermal expansion of fused silica	5.00E-07	K^{-1}
Reference path length	14.487	m

Equivalent synthesizer frequency 1.69434E+04 Hz

Uncertainty component	Source of uncertainty	*u*	[unit]	Distribution	n	Sens. coeff.	u_L / m	u_t /ns
u_{fgen}	Uncertainty of synthesizer frequency	1.694E-08	Hz	1.73	∞	0.71527	0.00000	0.00000
u_{fA}	Uncertainty of mean measured frequency	7.597E-04	Hz	1.00	9	0.71527	0.00054	0.00264
u_{fdisp}	Influence of fibre dispersion	2.408E-02	Hz	1.00	∞	0.71527	0.01722	0.08380
u_T	Temperature uncertainty of DUT	0.5	°C	1.00	∞	0.08323	0.04161	0.20252
u_{Lcal}	Uncertainty of reference path length	1.280E-03	m	1.00	9	1.00000	0.00128	0.00623
				Combined Standard uncertainty			0.04506	0.21928
						n eff.	6684134	6684134
						k 95%	1.960	1.960
						Expanded Uncertainty (U_{95})	**0.08831**	**0.4298**
						Rounded expanded uncertainty (U_{95})	**0.09**	**0.43**

$$U_{L_{tot}} = k_{95\%} \cdot \sqrt{\left(\frac{c}{n_{eff}} \cdot \frac{1}{f_{meas}^2}\right)^2 \cdot \left(u_{f_{gen}}^2 + u_{f_A}^2 + u_{f_{disp}}^2\right) + \left[\left(\frac{c}{f_{meas}} \cdot \frac{1}{n_{eff}^2} \cdot C_n\right)^2 + (\alpha \cdot L)^2\right] \cdot u_T^2 + u_{Lcal}^2}$$

$$U_{t_{tot}} = \frac{n_{eff}}{c} \cdot U_{L_{tot}}$$

METAS results to APMP.PR-S8

Dispersion contribution to the measurement uncertainty

$$\tau_{tot} = \sqrt{\tau_{CD}^2 + \tau_{IM}^2 + \tau_{PMD}^2}$$

$$\tau_{CD} = CD \cdot 1 \cdot 10^{-15} \cdot \Delta\lambda \cdot L$$ Chromatic dispersion — CD is in ps/nm/km; L is in m and $\Delta\lambda$ is in nm

$$\tau_{IM}^{-1} = \frac{MDB}{L} \cdot 1 \cdot 10^{9}$$ Inter-modal dispersion

$$\tau_{PMD} = PMD \cdot 1 \cdot 10^{-12} \cdot \sqrt{L/1000}$$ Polarisation Mode Dispersion

$$u_{\tau_{disp}} = \frac{1}{2 \cdot \sqrt{3}} \cdot \tau_{tot}$$

$$u_{f_{disp}} = f_{meas}^2 \cdot u_{\tau_{disp}}$$

Fibre Type	Wavelength λ (nm)	Chromatic Dispersion *CD* (ps/nm/km)	Modal Distorsion Bandwidth *MDB* (MHz·km)	PMD (ps·km$^{-1/2}$)	τ_{CD}	τ_{IM}	τ_{PMD}	τ_{tot}	$u_{\tau disp}$	u_{fdisp}
G.652 (Singlemode)	1310	6	---	0.06	2.91E-10	0	2.0875E-13	2.90509E-10	8.38627E-11	0.024075162
	1550	17	---	0.3	8.23E-10	0	1.0437E-12	8.23109E-10	2.37611E-10	0.068212997
	1625	20	---	0.5	9.80E-10	0	1.7396E-12	9.79661E-10	2.82804E-10	0.081186785
G.651 (Multimode)	850	120	200	0	5.81E-09	6.052E-08	0	6.08009E-08	1.75517E-08	5.038716649
	1300	6	200	0	2.91E-10	6.052E-08	0	6.05234E-08	1.74716E-08	5.015715286

METAS results to APMP.PR-S8

Measurement setup: Optical fibre length (Transit-Time)

Wavelength	1550	nm	
Source spectral width / wavelength uncertainty	8.00E-03	nm	DFB extended cavity
Ref. index of refraction	1.46		
Estimated fibre length	12109.17	m	
Temperature coefficient of refractive index of fibre	1.00E-05	K^{-1}	
Coeff. of lin. thermal expansion of fused silica	5.00E-07	K^{-1}	
Reference path length	14.496	m	

Equivalent synthesizer frequency 1.69369E+04 Hz

Uncertainty component	Source of uncertainty	*u*	[unit]	Distribution	n	Sens. coeff.	u_L / m	u_t /ns
u_{fgen}	Uncertainty of synthesizer frequency	1.694E-08	Hz	1.73	∞	0.71581	0.00000	0.00000
u_{fA}	Uncertainty of mean measured frequency	9.196E-04	Hz	1.00	9	0.71581	0.00066	0.00320
u_{fdisp}	Influence of fibre dispersion	1.615E-04	Hz	1.00	∞	0.71581	0.00012	0.00056
u_T	Temperature uncertainty of DUT	0.5	°C	1.00	∞	0.08326	0.04163	0.20260
u_{Lcal}	Uncertainty of reference path length	2.700E-04	m	1.00	9	1.00000	0.00027	0.00131
				Combined Standard uncertainty			0.04164	0.20263
						n eff.	9338919	9338919
						k 95%	1.960	1.960
						Expanded Uncertainty (U_{95})	**0.08160**	**0.3971**
						Rounded expanded uncertainty (U_{95})	**0.09**	**0.40**

$$U_{L_{tot}} = k_{95\%} \cdot \sqrt{\left(\frac{c}{n_{eff}} \cdot \frac{1}{f_{meas}^2}\right)^2 \cdot \left(u_{f_{gen}}^2 + u_{f_A}^2 + u_{f_{disp}}^2\right) + \left[\left(\frac{c}{f_{meas}} \cdot \frac{1}{n_{eff}^2} \cdot C_n\right)^2 + (\alpha \cdot L)^2\right] \cdot u_T^2 + u_{Lcal}^2}$$

$$U_{t_{tot}} = \frac{n_{eff}}{c} \cdot U_{L_{tot}}$$

METAS results to APMP.PR-S8

Dispersion contribution to the measurement uncertainty

$$\tau_{tot} = \sqrt{\tau_{CD}^2 + \tau_{IM}^2 + \tau_{PMD}^2}$$

$\tau_{CD} = CD \cdot 1 \cdot 10^{-15} \cdot \Delta\lambda \cdot L$ Chromatic dispersion CD is in ps/nm/km; L is in m and $\Delta\lambda$ is in nm

$\tau_{IM}^{-1} = \frac{MDB}{L} \cdot 1 \cdot 10^{9}$ Inter-modal dispersion

$\tau_{PMD} = PMD \cdot 1 \cdot 10^{-12} \cdot \sqrt{L/1000}$ Polarisation Mode Dispersion

$$u_{\tau_{disp}} = \frac{1}{2 \cdot \sqrt{3}} \cdot \tau_{tot}$$

$$u_{f_{disp}} = f_{meas}^2 \cdot u_{\tau_{disp}}$$

Fibre Type	Wavelength λ (nm)	Chromatic Dispersion *CD* (ps/nm/km)	Modal Distorsion Bandwidth *MDB* (MHz·km)	PMD (ps·km$^{-1/2}$)	τ_{CD}	τ_{IM}	τ_{PMD}	τ_{tot}	$u_{\tau disp}$	u_{fdisp}
G.652 (Singlemode)	1310	6	---	0.06	5.81E-13	0	2.0879E-13	6.17603E-13	1.78287E-13	5.1143E-05
	1550	17	---	0.3	1.65E-12	0	1.0439E-12	1.94985E-12	5.62874E-13	0.000161465
	1625	20	---	0.5	1.96E-12	0	1.7399E-12	2.62091E-12	7.56591E-13	0.000217035
G.651 (Multimode)	850	120	200	0	1.16E-11	6.055E-08	0	6.05459E-08	1.74781E-08	5.013736828
	1300	6	200	0	5.81E-13	6.055E-08	0	6.05459E-08	1.74781E-08	5.013736736

METAS results to APMP.PR-S8

Measurement setup: Optical fibre length (Transit-Time)

Wavelength	1551.69	nm	
Source spectral width / wavelength uncertainty	2.00E-02	nm	DFB
Ref. index of refraction	1.46		
Estimated fibre length	12109.23043	m	
Temperature coefficient of refractive index of fibre	1.00E-05	K^{-1}	
Coeff. of lin. thermal expansion of fused silica	5.00E-07	K^{-1}	
Reference path length	14.496	m	

Equivalent synthesizer frequency 1.69368E+04 Hz

Uncertainty component	Source of uncertainty	*u*	[unit]	Distribution	n	Sens. coeff.	u_L / m	u_t /ns
u_{fgen}	Uncertainty of synthesizer frequency	1.694E-08	Hz	1.73	∞	0.71582	0.00000	0.00000
u_{fA}	Uncertainty of mean measured frequency	1.691E-03	Hz	1.00	9	0.71582	0.00121	0.00589
u_{fdisp}	Influence of fibre dispersion	3.517E-04	Hz	1.00	∞	0.71582	0.00025	0.00123
u_T	Temperature uncertainty of DUT	0.5	°C	1.00	∞	0.08326	0.04163	0.20260
u_{Lcal}	Uncertainty of reference path length	1.560E-03	m	1.00	9	1.00000	0.00156	0.00759
				Combined Standard uncertainty			0.04168	0.20283
						n eff.	2520215	2520215
						k 95%	1.960	1.960
						Expanded Uncertainty (U_{95})	**0.08169**	**0.3975**
						Rounded expanded uncertainty (U_{95})	**0.09**	**0.40**

$$U_{L_{tot}} = k_{95\%} \cdot \sqrt{\left(\frac{c}{n_{eff}} \cdot \frac{1}{f_{meas}^2}\right)^2 \cdot \left(u_{f_{gen}}^2 + u_{f_A}^2 + u_{f_{disp}}^2\right) + \left[\left(\frac{c}{f_{meas}} \cdot \frac{1}{n_{eff}^2} \cdot C_n\right)^2 + (\alpha \cdot L)^2\right] \cdot u_T^2 + u_{Lcal}^2}$$

$$U_{t_{tot}} = \frac{n_{eff}}{c} \cdot U_{L_{tot}}$$

METAS results to APMP.PR-S8

Dispersion contribution to the measurement uncertainty

$$\tau_{tot} = \sqrt{\tau_{CD}^2 + \tau_{IM}^2 + \tau_{PMD}^2}$$

$\tau_{CD} = CD \cdot 1 \cdot 10^{-15} \cdot \Delta\lambda \cdot L$ Chromatic dispersion CD is in ps/nm/km; L is in m and $\Delta\lambda$ is in nm

$\tau_{IM}^{-1} = \frac{MDB}{L} \cdot 1 \cdot 10^{9}$ Inter-modal dispersion

$\tau_{PMD} = PMD \cdot 1 \cdot 10^{-12} \cdot \sqrt{L/1000}$ Polarisation Mode Dispersion

$$u_{\tau_{disp}} = \frac{1}{2 \cdot \sqrt{3}} \cdot \tau_{tot}$$

$$u_{f_{disp}} = f_{meas}^2 \cdot u_{\tau_{disp}}$$

Fibre Type	Wavelength λ (nm)	Chromatic Dispersion *CD* (ps/nm/km)	Modal Distorsion Bandwidth *MDB* (MHz·km)	PMD (ps·km$^{-1/2}$)	τ_{CD}	τ_{IM}	τ_{PMD}	τ_{tot}	$u_{\tau disp}$	u_{fdisp}
G.652 (Singlemode)	1310	6	---	0.06	1.45E-12	0	2.0879E-13	1.46803E-12	4.23784E-13	0.000121565
	1550	17	---	0.3	4.12E-12	0	1.0439E-12	4.24743E-12	1.22613E-12	0.000351722
	1625	20	---	0.5	4.90E-12	0	1.7399E-12	5.19992E-12	1.50109E-12	0.000430596
G.651 (Multimode)	850	120	200	0	2.91E-11	6.055E-08	0	6.05462E-08	1.74782E-08	5.013712592
	1300	6	200	0	1.45E-12	6.055E-08	0	6.05462E-08	1.74782E-08	5.013712016

METAS results to APMP.PR-S8

Measurement setup: Optical fibre length (Transit-Time)

Wavelength	1625	nm
Source spectral width / wavelength uncertainty	8.00E-03	nm
Ref. index of refraction	1.46	
Estimated fibre length	12112.43987	m
Temperature coefficient of refractive index of fibre	1.00E-05	K^{-1}
Coeff. of lin. thermal expansion of fused silica	5.00E-07	K^{-1}
Reference path length	14.498	m

Equivalent synthesizer frequency 1.69323E+04 Hz

Uncertainty component	Source of uncertainty	*u*	[unit]	Distribution	n	Sens. coeff.	u_L / m	u_t /ns
u_{fgen}	Uncertainty of synthesizer frequency	1.693E-08	Hz	1.73	∞	0.71620	0.00000	0.00000
u_{fA}	Uncertainty of mean measured frequency	9.146E-04	Hz	1.00	9	0.71620	0.00066	0.00319
u_{fdisp}	Influence of fibre dispersion	2.170E-04	Hz	1.00	∞	0.71620	0.00016	0.00076
u_T	Temperature uncertainty of DUT	0.5	°C	1.00	∞	0.08328	0.04164	0.20265
u_{Lcal}	Uncertainty of reference path length	1.910E-03	m	1.00	9	1.00000	0.00191	0.00930
				Combined Standard uncertainty			0.04169	0.20289
						n eff.	1678394	1678394
						k 95%	1.960	1.960
						Expanded Uncertainty (U_{95})	**0.08171**	**0.3977**
						Rounded expanded uncertainty (U_{95})	**0.09**	**0.40**

$$U_{L_{tot}} = k_{95\%} \cdot \sqrt{\left(\frac{c}{n_{eff}} \cdot \frac{1}{f_{meas}^2}\right)^2 \cdot \left(u_{f_{gen}}^2 + u_{f_A}^2 + u_{f_{disp}}^2\right) + \left[\left(\frac{c}{f_{meas}} \cdot \frac{1}{n_{eff}^2} \cdot C_n\right)^2 + (\alpha \cdot L)^2\right] \cdot u_T^2 + u_{Lcal}^2}$$

$$U_{t_{tot}} = \frac{n_{eff}}{c} \cdot U_{L_{tot}}$$

METAS results to APMP.PR-S8

Dispersion contribution to the measurement uncertainty

$$\tau_{tot} = \sqrt{\tau_{CD}^2 + \tau_{IM}^2 + \tau_{PMD}^2}$$

$$\tau_{CD} = CD \cdot 1 \cdot 10^{-15} \cdot \Delta\lambda \cdot L$$ Chromatic dispersion — CD is in ps/nm/km; L is in m and $\Delta\lambda$ is in nm

$$\tau_{IM}^{-1} = \frac{MDB}{L} \cdot 1 \cdot 10^{9}$$ Inter-modal dispersion

$$\tau_{PMD} = PMD \cdot 1 \cdot 10^{-12} \cdot \sqrt{L/1000}$$ Polarisation Mode Dispersion

$$u_{\tau_{disp}} = \frac{1}{2 \cdot \sqrt{3}} \cdot \tau_{tot}$$

$$u_{f_{disp}} = f_{meas}^2 \cdot u_{\tau_{disp}}$$

Fibre Type	Wavelength λ (nm)	Chromatic Dispersion *CD* (ps/nm/km)	Modal Distorsion Bandwidth *MDB* (MHz·km)	PMD (ps·km$^{-1/2}$)	τ_{CD}	τ_{IM}	τ_{PMD}	τ_{tot}	$u_{\tau disp}$	u_{fdisp}
G.652 (Singlemode)	1310	6	---	0.06	5.81E-13	0	2.0882E-13	6.1776E-13	1.78332E-13	5.11284E-05
	1550	17	---	0.3	1.65E-12	0	1.0441E-12	1.95031E-12	5.63005E-13	0.000161416
	1625	20	---	0.5	1.96E-12	0	1.7401E-12	2.62146E-12	7.5675E-13	0.000216963
G.651 (Multimode)	850	120	200	0	1.16E-11	6.056E-08	0	6.05622E-08	1.74828E-08	5.012385226
	1300	6	200	0	5.81E-13	6.056E-08	0	6.05622E-08	1.74828E-08	5.012385134

METAS results to APMP.PR-S8
Supplementary Inter-comparison on optical fibre length calibration
Part 2/2 / rev. 05.2019

Object	**Singlemode Length Reference Fibre** Manufacturer: METAS Serial Nr. LRF 2015.07 Approximate fibre length: 2.3 km Connector: FC/UPC
Order	Calibration of the transit time of a light pulse propagating through the fibre at λ = 1310 nm, λ = 1550 nm and λ = 1625 nm. Determination of the fibre length for n_g = 1.46.
Traceability	The reported measurement values are traceable to national standards and thus to internationally supported realizations of the SI-units.
Date of calibration	27 March 2015
Date of control measurement	19 May 2016
Marking	Calibration label METAS 03. 2015

Photonics Time and Frequency Laboratory

Dr. Jacques Morel, Head of Laboratory

Object

The singlemode Length Reference Fibre (LRF) consists in a G.652D fibre spool with a length L_1. Two patch-cables of approximate length L = 2 m are fitted with FC UPC connectors and are fusion-spliced at both fibre ends. The internal structure of the LRF is shown in the figure below.

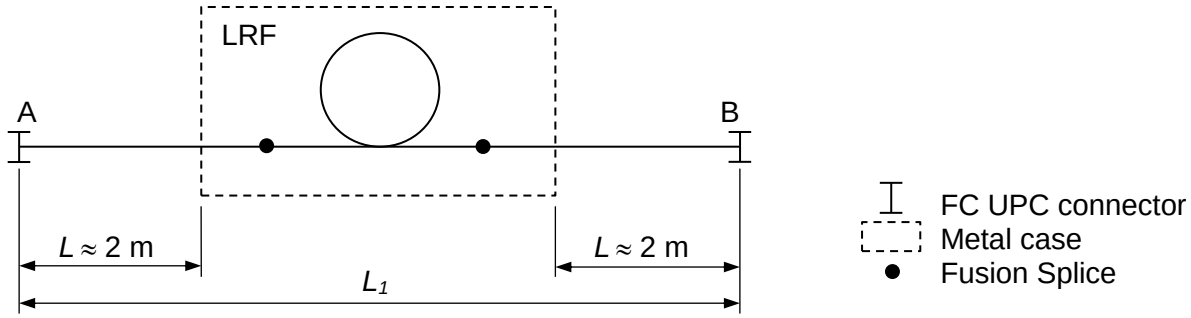

Extent of the calibration

Calibration of the transit time of a light pulse propagating through the fibre spool (measurement performed between points A and B) and calculation of the fibre length L_1 for a reference group refractive index n_g = 1.46. The measurements were done at the three wavelengths λ = 1310 nm, λ = 1550 nm and λ = 1625 nm.

Measurement procedure

The transit time t of a laser pulse propagating through the fibre was measured by using a modified version of the system as specified in the annex (A2) of the IEC 61746 document (Ed. 1).

The basic structure of the measuring setup is shown in figure 1, here below. A series of pulses with a repetition rate τ_{rep} is produced using different laser diodes (LD) and by modulating their injection currents directly or by modulating the optical CW power using a Mach Zehnder modulator. The optical pulses are then coupled into two different paths (Ref. and DUT) using a 3 dB coupler.

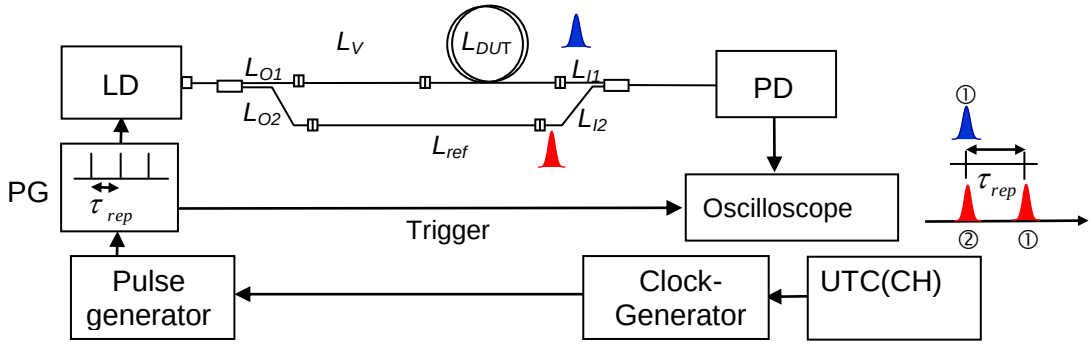

Fig. 1. METAS transit-time cailbration system.

The pulses having circulated through both paths are detected using a fast photodiode (PD).The repetition rate τ_{rep} is then adjusted until pulse 2 of Ref and pulse 1 of DUT paths are superimposed.

The length of the DUT is obtained from two successive measurements; the first one being performed with and the second one without the DUT. This yields:

$L_{DUT} = \frac{c}{n_{eff}} \cdot \left\{ \tau_{\mathrm{rep}_{\mathrm{DUT}}} - \tau_{\mathrm{rep}_{\mathrm{cal}}} \right\}$, where $\tau_{\mathrm{rep}_{\mathrm{DUT}}}$ is the repetition rate measured with the DUT inserted in the system, and $\tau_{\mathrm{rep}_{\mathrm{cal}}}$ is the repetition rate measured without the DUT.

The clock generator is a pulse synthesizer, which is locked to UTC(CH).
The calibration setup is shown in figure 2, here below.

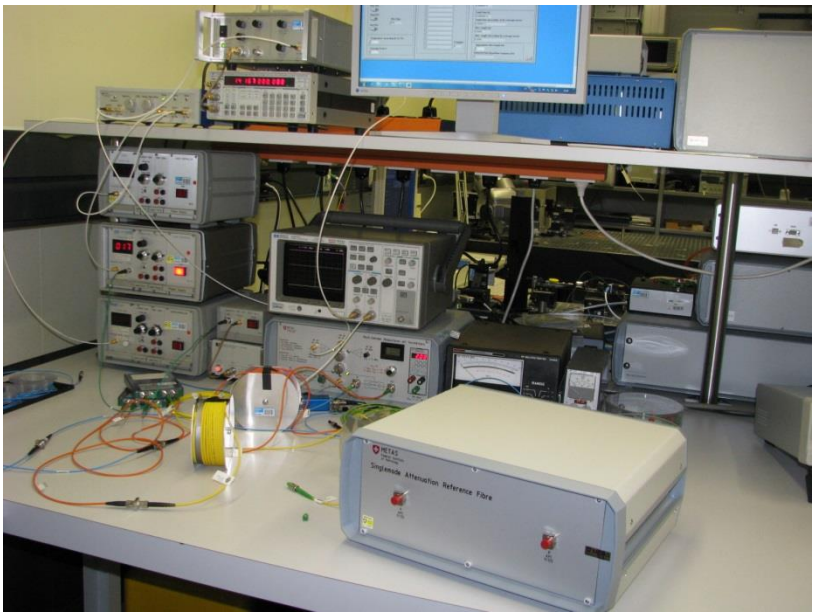

Fig. 2. Picture of the METAS transit-time calibration setup.

Measurement conditions

Ambient laboratory temperature: (23 ± 1) °C
Relative humidity: (45 ± 5 %) rH

The DUT was allowed to thermalize before starting the calibration.

The vacuum wavelengths of the laser sources are summarized in the table below.

Laser	$\lambda_{central}$ / nm	λ_{Peak} / nm	$U\lambda$
Fabry-Perot	1310.0	-	1.2 nm
DFB Extended cavity		1550.000	0.008 nm
DFB Extended cavity		1625.000	0.008 nm
DFB		1551.69	0.02 nm

Measurement results

First measurements, dated 27th of March 2015

λ / nm	t / ns	U / ns	L_1 / m	U / m
1310.000	11428.08	0.09	2346.612	0.018
1550.000	11432.58	0.08	2347.535	0.016
1551.69	11432.64	0.08	2347.547	0.017
1625.000	11435.72	0.08	2348.180	0.017

Control measurements, dated 19th of May 2016

λ / nm	t / ns	U / ns	L_1 / m	U / m
1310.000	11428.09	0.09	2346.612	0.018
1550.000	11432.53	0.09	2347.524	0.017
1551.69	11432.62	0.08	2347.544	0.017
1625.000	11435.70	0.09	2348.176	0.017

Both sets of measurements are fully comparable within their uncertainties.

Uncertainty of measurement

The uncertainty budget includes following contributions:

Uncertainty component	**Source of uncertainty**
u_{fgen}	Uncertainty of synthesizer frequency
u_{fA}	Type A uncertainty of the measured mean frequency. The frequency and the repetition rate are related through $f = 1/\tau_{rep}$
u_{fdisp}	Uncertainty arising from the fibre dispersion (chromatic dispersion and PMD)
u_T	Temperature stability of DUT (thermal expansion of glass and thermal dependency of the effective index of refraction)
u_{Lcal}	Uncertainty of reference path length calibration

The detailed uncertainty budgets for the first three calibrations performed on March 27, 2015 are shown in the next pages.

Measurement setup: Optical fibre length (Transit-Time)

Wavelength	1310	nm
Source spectral width / wavelength uncertainty	4.00E+00	nm
Ref. index of refraction	1.46	
Estimated fibre length	2346.6117	m
Temperature coefficient of refractive index of fibre	1.00E-05	K^{-1}
Coeff. of lin. thermal expansion of fused silica	5.00E-07	K^{-1}
Reference path length	14.487	m

Equivalent synthesizer frequency 8.69668E+04 Hz

Uncertainty component	**Source of uncertainty**	***u***	**[unit]**	**Distribution**	**n**	**Sens. coeff.**	**u_L / m**	**u_t /ns**
u_{fgen}	Uncertainty of synthesizer frequency	8.697E-08	Hz	1.73	∞	0.02715	0.00000	0.00000
u_{fA}	Uncertainty of mean measured frequency	3.768E-02	Hz	1.00	9	0.02715	0.00102	0.00498
u_{fdisp}	Influence of fibre dispersion	1.230E-01	Hz	1.00	∞	0.02715	0.00334	0.01625
u_T	Temperature uncertainty of DUT	0.5	°C	1.00	∞	0.01621	0.00811	0.03946
u_{Lcal}	Uncertainty of reference path length	1.280E-03	m	1.00	9	1.00000	0.00128	0.00623
				Combined Standard uncertainty			0.00892	0.04341
						n eff.	15056	15056
						k 95%	1.960	1.960
						Expanded Uncertainty (U_{95})	**0.01748**	**0.0851**
						Rounded expanded uncertainty (U_{95})	**0.018**	**0.09**

$$U_{L_{tot}} = k_{95\%} \cdot \sqrt{\left(\frac{c}{n_{eff}} \cdot \frac{1}{f_{meas}^2}\right)^2 \cdot \left(u_{f_{gen}}^2 + u_{f_A}^2 + u_{f_{disp}}^2\right) + \left[\left(\frac{c}{f_{meas}} \cdot \frac{1}{n_{eff}^2} \cdot C_n\right)^2 + (\alpha \cdot L)^2\right] \cdot u_T^2 + u_{Lcal}^2}$$

$$U_{t_{tot}} = \frac{n_{eff}}{c} \cdot U_{L_{tot}}$$

Dispersion contribution to the measurement uncertainty

$$\tau_{tot} = \sqrt{\tau_{CD}^2 + \tau_{IM}^2 + \tau_{PMD}^2}$$

$\tau_{CD} = CD \cdot 1 \cdot 10^{-15} \cdot \Delta\lambda \cdot L$ Chromatic dispersion CD is in ps/nm/km; L is in m and $\Delta\lambda$ is in nm

$\tau_{IM}^{-1} = \frac{MDB}{L} \cdot 1 \cdot 10^{9}$ Inter-modal dispersion

$\tau_{PMD} = PMD \cdot 1 \cdot 10^{-12} \cdot \sqrt{L/1000}$ Polarisation Mode Dispersion

$$u_{\tau_{disp}} = \frac{1}{2 \cdot \sqrt{3}} \cdot \tau_{tot}$$

$$u_{f_{disp}} = f_{meas}^2 \cdot u_{\tau_{disp}}$$

Fibre Type	Wavelength λ (nm)	Chromatic Dispersion *CD* (ps/nm/km)	Modal Distorsion Bandwidth *MDB* (MHz·km)	PMD (ps·km$^{-1/2}$)	τ_{CD}	τ_{IM}	τ_{PMD}	τ_{tot}	$u_{\tau disp}$	u_{fdisp}
G.652 (Singlemode)	1310	6	---	0.06	5.63E-11	0	9.1912E-14	5.63188E-11	1.62578E-11	0.122961696
	1550	17	---	0.3	1.60E-10	0	4.5956E-13	1.5957E-10	4.6064E-11	0.348392453
	1625	20	---	0.5	1.90E-10	0	7.6593E-13	1.8992E-10	5.48253E-11	0.414656373
G.651 (Multimode)	850	120	200	0	1.13E-09	1.173E-08	0	1.1787E-08	3.40261E-09	25.73475821
	1300	6	200	0	5.63E-11	1.173E-08	0	1.17332E-08	3.38708E-09	25.61728097

Wavelength	1550	nm
Source spectral width / wavelength uncertainty	8.00E-03	nm
Ref. index of refraction	1.46	
Estimated fibre length	2347.541	m
Temperature coefficient of refractive index of fibre	1.00E-05	K^{-1}
Coeff. of lin. thermal expansion of fused silica	5.00E-07	K^{-1}
Reference path length	14.496	m

DFB extended cavity

Equivalent synthesizer frequency 8.69323E+04 Hz

Uncertainty component	**Source of uncertainty**	***u***	**[unit]**	**Distribution**	**ν**	**Sens. coeff.**	**u_L / m**	**u_t /ns**
u_{fgen}	Uncertainty of synthesizer frequency	8.693E-08	Hz	1.73	∞	0.02717	0.00000	0.00000
u_{fA}	Uncertainty of mean measured frequency	2.357E-02	Hz	1.00	9	0.02717	0.00064	0.00312
u_{fdisp}	Influence of fibre dispersion	1.221E-03	Hz	1.00	∞	0.02717	0.00003	0.00016
u_T	Temperature uncertainty of DUT	0.5	°C	1.00	∞	0.01622	0.00811	0.03947
u_{Lcal}	Uncertainty of reference path length	2.700E-04	m	1.00	9	1.00000	0.00027	0.00131
				Combined Standard uncertainty			0.00814	0.03962
						ν eff.	222731	222731
						$k_{95\%}$	1.960	1.960
						Expanded Uncertainty (U_{95})	**0.01595**	**0.0776**
						Rounded expanded uncertainty (U_{95})	**0.016**	**0.08**

$$U_{L_{tot}} = k_{95\%} \cdot \sqrt{\left(\frac{c}{n_{eff}} \cdot \frac{1}{f_{meas}^2}\right)^2 \cdot \left(u_{f_{gen}}^2 + u_{f_A}^2 + u_{f_{disp}}^2\right) + \left[\left(\frac{c}{f_{meas}} \cdot \frac{1}{n_{eff}^2} \cdot C_n\right)^2 + (\alpha \cdot L)^2\right] \cdot u_T^2 + u_{Lcal}^2}$$

$$U_{t_{tot}} = \frac{n_{eff}}{c} \cdot U_{L_{tot}}$$

Dispersion contribution to the measurement uncertainty

$$\tau_{tot} = \sqrt{\tau_{CD}^2 + \tau_{IM}^2 + \tau_{PMD}^2}$$

$$\tau_{CD} = CD \cdot 1 \cdot 10^{-15} \cdot \Delta\lambda \cdot L$$ Chromatic dispersion — CD is in ps/nm/km; L is in m and $\Delta\lambda$ is in nm

$$\tau_{IM}^{-1} = \frac{MDB}{L} \cdot 1 \cdot 10^{9}$$ Inter-modal dispersion

$$\tau_{PMD} = PMD \cdot 1 \cdot 10^{-12} \cdot \sqrt{L/1000}$$ Polarisation Mode Dispersion

$$u_{\tau_{disp}} = \frac{1}{2 \cdot \sqrt{3}} \cdot \tau_{tot}$$

$$u_{f_{disp}} = f_{meas}^2 \cdot u_{\tau_{disp}}$$

Fibre Type	Wavelength λ (nm)	Chromatic Dispersion *CD* (ps/nm/km)	Modal Distorsion Bandwidth *MDB* (MHz·km)	PMD (ps·km$^{-1/2}$)	τ_{CD}	τ_{IM}	τ_{PMD}	τ_{tot}	$u_{\tau disp}$	u_{fdisp}
G.652 (Singlemode)	1310	6	---	0.06	1.13E-13	0	9.193E-14	1.45425E-13	4.19804E-14	0.000317257
	1550	17	---	0.3	3.19E-13	0	4.5965E-13	5.5965E-13	1.61557E-13	0.001220929
	1625	20	---	0.5	3.80E-13	0	7.6608E-13	8.55146E-13	2.46859E-13	0.00186558
G.651 (Multimode)	850	120	200	0	2.25E-12	1.174E-08	0	1.17377E-08	3.38837E-09	25.60683914
	1300	6	200	0	1.13E-13	1.174E-08	0	1.17377E-08	3.38837E-09	25.60683867

Measurement setup: Optical fibre length (Transit-Time)

Wavelength	1551.69	nm	
Source spectral width / wavelength uncertainty	2.00E-02	nm	DFB
Ref. index of refraction	1.46		
Estimated fibre length	2347.54716	m	
Temperature coefficient of refractive index of fibre	1.00E-05	K^{-1}	
Coeff. of lin. thermal expansion of fused silica	5.00E-07	K^{-1}	
Reference path length	14.497	m	

Equivalent synthesizer frequency 8.69320E+04 Hz

Uncertainty component	**Source of uncertainty**	***u***	**[unit]**	**Distribution**	**n**	**Sens. coeff.**	**u_L / m**	**u_t /ns**
u_{fgen}	Uncertainty of synthesizer frequency	8.693E-08	Hz	1.73	∞	0.02717	0.00000	0.00000
u_{fA}	Uncertainty of mean measured frequency	3.333E-02	Hz	1.00	9	0.02717	0.00091	0.00441
u_{fdisp}	Influence of fibre dispersion	2.009E-03	Hz	1.00	∞	0.02717	0.00005	0.00027
u_T	Temperature uncertainty of DUT	0.5	°C	1.00	∞	0.01622	0.00811	0.03947
u_{Lcal}	Uncertainty of reference path length	1.560E-03	m	1.00	9	1.00000	0.00156	0.00759
				Combined Standard uncertainty			0.00831	0.04044
						n eff.	6500	6500
						k 95%	1.960	1.960
						Expanded Uncertainty (U_{95})	**0.01629**	**0.0793**
						Rounded expanded uncertainty (U_{95})	**0.017**	**0.08**

$$U_{L_{tot}} = k_{95\%} \cdot \sqrt{\left(\frac{c}{n_{eff}} \cdot \frac{1}{f_{meas}^2}\right)^2 \cdot \left(u_{f_{gen}}^2 + u_{f_A}^2 + u_{f_{disp}}^2\right) + \left[\left(\frac{c}{f_{meas}} \cdot \frac{1}{n_{eff}^2} \cdot C_n\right)^2 + (\alpha \cdot L)^2\right] \cdot u_T^2 + u_{Lcal}^2}$$

$$U_{t_{tot}} = \frac{n_{eff}}{c} \cdot U_{L_{tot}}$$

Dispersion contribution to the measurement uncertainty

$$\tau_{tot} = \sqrt{\tau_{CD}^2 + \tau_{IM}^2 + \tau_{PMD}^2}$$

$\tau_{CD} = CD \cdot 1 \cdot 10^{-15} \cdot \Delta\lambda \cdot L$ Chromatic dispersion CD is in ps/nm/km; L is in m and $\Delta\lambda$ is in nm

$$\tau_{IM}^{-1} = \frac{MDB}{L} \cdot 1 \cdot 10^{9}$$ Inter-modal dispersion

$\tau_{PMD} = PMD \cdot 1 \cdot 10^{-12} \cdot \sqrt{L/1000}$ Polarisation Mode Dispersion

$$u_{\tau_{disp}} = \frac{1}{2 \cdot \sqrt{3}} \cdot \tau_{tot}$$

$$u_{f_{disp}} = f_{meas}^2 \cdot u_{\tau_{disp}}$$

Fibre Type	Wavelength λ (nm)	Chromatic Dispersion *CD* (ps/nm/km)	Modal Distorsion Bandwidth *MDB* (MHz·km)	PMD (ps·km$^{-1/2}$)	τ_{CD}	τ_{IM}	τ_{PMD}	τ_{tot}	$u_{\tau disp}$	u_{fdisp}
G.652 (Singlemode)	1310	6	---	0.06	2.82E-13	0	9.193E-14	2.96326E-13	8.5542E-14	0.000646456
	1550	17	---	0.3	7.98E-13	0	4.5965E-13	9.21058E-13	2.65887E-13	0.002009353
	1625	20	---	0.5	9.50E-13	0	7.6609E-13	1.22038E-12	3.52294E-13	0.002662351
G.651 (Multimode)	850	120	200	0	5.63E-12	1.174E-08	0	1.17377E-08	3.38839E-09	25.60668936
	1300	6	200	0	2.82E-13	1.174E-08	0	1.17377E-08	3.38839E-09	25.60668642

Measurement setup: Optical fibre length (Transit-Time)

Wavelength	1625	nm
Source spectral width / wavelength uncertainty	8.00E-03	nm
Ref. index of refraction	1.46	
Estimated fibre length	2348.17982	m
Temperature coefficient of refractive index of fibre	1.00E-05	K^{-1}
Coeff. of lin. thermal expansion of fused silica	5.00E-07	K^{-1}
Reference path length	14.498	m

Equivalent synthesizer frequency 8.69087E+04 Hz

Uncertainty component	Source of uncertainty	*u*	[unit]	Distribution	n	Sens. coeff.	u_L / m	u_t /ns
u_{fgen}	Uncertainty of synthesizer frequency	8.691E-08	Hz	1.73	∞	0.02719	0.00000	0.00000
u_{fA}	Uncertainty of mean measured frequency	3.727E-02	Hz	1.00	9	0.02719	0.00101	0.00493
u_{fdisp}	Influence of fibre dispersion	1.865E-03	Hz	1.00	∞	0.02719	0.00005	0.00025
u_T	Temperature uncertainty of DUT	0.5	°C	1.00	∞	0.01623	0.00811	0.03948
u_{Lcal}	Uncertainty of reference path length	1.910E-03	m	1.00	9	1.00000	0.00191	0.00930
				Combined Standard uncertainty			0.00840	0.04086
						n eff.	3113	3113
						k 95%	1.961	1.961
						Expanded Uncertainty (U_{95})	**0.01646**	**0.0801**
						Rounded expanded uncertainty (U_{95})	**0.017**	**0.08**

$$U_{L_{tot}} = k_{95\%} \cdot \sqrt{\left(\frac{c}{n_{eff}} \cdot \frac{1}{f_{meas}^2}\right)^2 \cdot \left(u_{f_{gen}}^2 + u_{f_A}^2 + u_{f_{disp}}^2\right) + \left[\left(\frac{c}{f_{meas}} \cdot \frac{1}{n_{eff}^2} \cdot C_n\right)^2 + (\alpha \cdot L)^2\right] \cdot u_T^2 + u_{Lcal}^2}$$

$$U_{t_{tot}} = \frac{n_{eff}}{c} \cdot U_{L_{tot}}$$

Dispersion contribution to the measurement uncertainty

$$\tau_{tot} = \sqrt{\tau_{CD}^2 + \tau_{IM}^2 + \tau_{PMD}^2}$$

$\tau_{CD} = CD \cdot 1 \cdot 10^{-15} \cdot \Delta\lambda \cdot L$ Chromatic dispersion CD is in ps/nm/km; L is in m and $\Delta\lambda$ is in nm

$\tau_{IM}^{-1} = \frac{MDB}{L} \cdot 1 \cdot 10^{9}$ Inter-modal dispersion

$\tau_{PMD} = PMD \cdot 1 \cdot 10^{-12} \cdot \sqrt{L/1000}$ Polarisation Mode Dispersion

$$u_{\tau_{disp}} = \frac{1}{2 \cdot \sqrt{3}} \cdot \tau_{tot}$$

$$u_{f_{disp}} = f_{meas}^2 \cdot u_{\tau_{disp}}$$

Fibre Type	Wavelength λ (nm)	Chromatic Dispersion *CD* (ps/nm/km)	Modal Distorsion Bandwidth *MDB* (MHz·km)	PMD (ps·km$^{-1/2}$)	τ_{CD}	τ_{IM}	τ_{PMD}	τ_{tot}	$u_{\tau disp}$	u_{fdisp}
G.652 (Singlemode)	1310	6	---	0.06	1.13E-13	0	9.1943E-14	1.45456E-13	4.19897E-14	0.000317153
	1550	17	---	0.3	3.19E-13	0	4.5971E-13	5.59752E-13	1.61586E-13	0.001220483
	1625	20	---	0.5	3.80E-13	0	7.6619E-13	8.55286E-13	2.469E-13	0.001864866
G.651 (Multimode)	850	120	200	0	2.25E-12	1.174E-08	0	1.17409E-08	3.38931E-09	25.59985901
	1300	6	200	0	1.13E-13	1.174E-08	0	1.17409E-08	3.38931E-09	25.59985854

4.4. LNE

LABORATOIRES DE TRAPPES
29, avenue Roger Hennequin – 78197 TRAPPES Cedex
Tél. : 01 30 69 10 00 – Fax : 01 30 69 12 34

Optical fiber length comparison

APMP PR-S8

LNE report

J. Dubard
November 16, 2015

Content

1 Introduction

This document reports on the measurements performed by LNE in the framework of the APMP PR-S8 comparison on optical fiber length piloted by KRISS.
The measurements were performed at wavelengths 1310 nm and 1550 nm in July and August 2015 on the two artefacts prepared by METAS.

2 Measurement results

The results are indicated in table 1. They are corrected for laser wavelength mismatch and room temperature mismatch

Fiber reference	Wavelength (nm)	Group delay (µs)	Group delay uncertainty (µs)	Fiber length (m) [n=1.46]
LRF 2015.06	1310	11.4281	0.0029	2346.62
	1550	11.4320	0.0029	2347.41
LRF 2015.07	1310	58.949	0.015	12104.5
	1550	58.968	0.015	12108.4

Table 1. LNE measurement results

3 Measurement technique

The technique used to measure the group delay of the fiber is the measurement of the time of flight of a short optical pulse in the fiber.

3.1 Measurement set-up

The schematic of the measurement set-up is shown on figure 1.

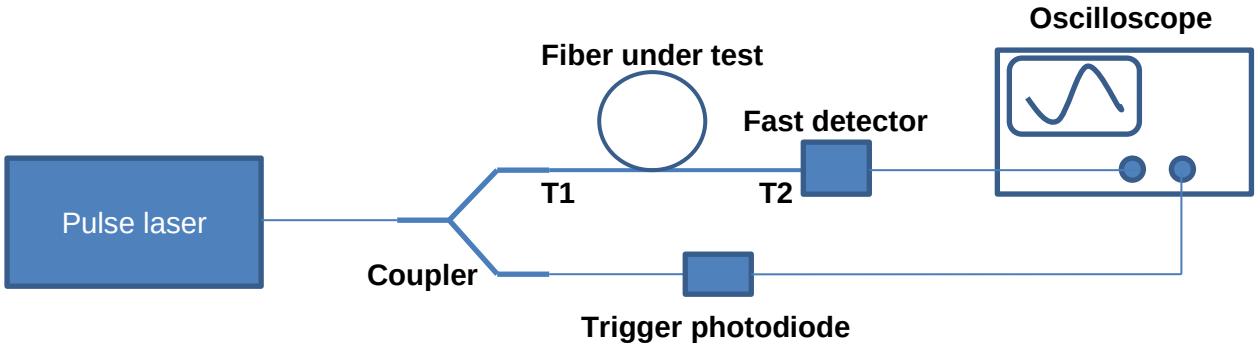

Figure 1: Schematic of the measurement set-up

This set-up includes:

- A laser source that emit 10 ns (FWHM) pulses at 1300 nm or 1550 nm
- A 1x2 fiber coupler. One side of the coupler is connected to the fiber under test. The other side is connected to InGaAs photodiode that is used as a signal trigger for the oscilloscope
- A fast detector that measures the laser pulse temporal shape
- An oscilloscope that displays the waveform of the signal from the fast detector

A picture of the set-up is shown on picture 1.

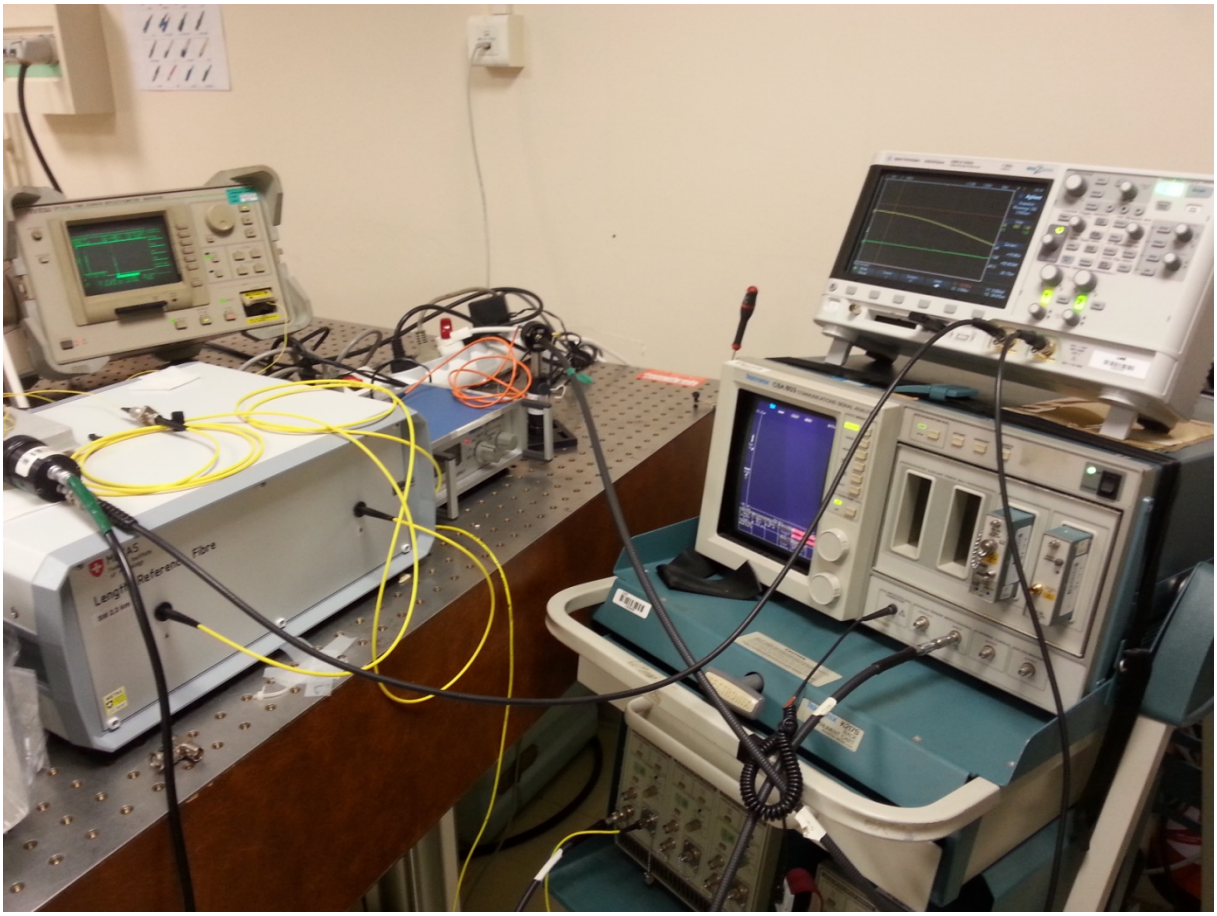

Picture 1: Measurement set-up

The characteristics of the instruments used are indicated in table 2

Instrument	Manufacturer	Type	Comments
Laser source	Anritsu	MW9040B (OTDR)	Pulse width: 10 ns (FWHM) See annex 1 for full description
Trigger photodiode	Hamamatsu	InGaAs	5 mm diameter. Photovoltaic mode, no bias
Fast detector	Antel	AR-S25	Bandwidth: 12 GHz
Oscilloscope	Agilent	DSO-X3102A	

Table 2. Characteristics of the instruments used

The set-up uses single-mode fiber to connect the different instruments except the fast detector that is equipped with a 1 meter long multimode fiber. This multimode fibre has a neglectable impact on the measurement results.

The pulse light of the laser source is injected in a fiber connected to a 1x2 coupler that separates the beam into two paths.

- One path is connected to a InGaAs detector that is used as a trigger for the oscilloscope
- The other path is connected to the fiber under test. The output of the fiber under test is connected to the fast detector which signal is measured by the oscilloscope.

Figure 2 shows the temporal shape of the pulse light (green curve) measured with the fast detector and part of the temporal shape of the trigger signal (yellow curve).

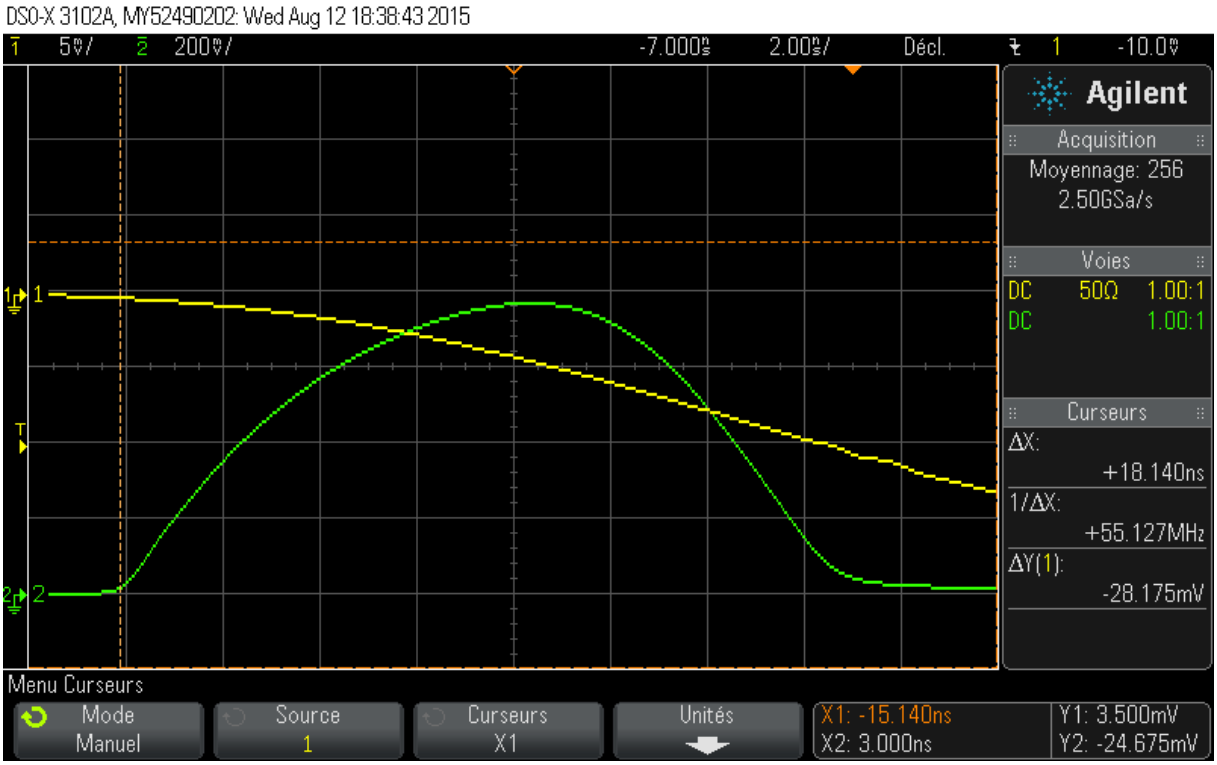

Figure 2: Trace of the laser pulse measured with the fast photodiode

The temperature of the laboratory is 22 °C.

3.2 Measurement procedure

The measurement of the group delay for a given fiber is performed according to the following steps:

- Step 1: measurement of the time T1 (see figure 1) corresponding to the pulse light measured at the input of the fiber under test (output of the coupler)
- Step 2: measurement of the time T2 (see figure 1) corresponding to the pulse light measured at the output of the fiber under test.

T1 and T2 are measured with respect to the trigger time position by use of a cursor as shown on figure 2 (brown vertical dashed line on figure 2).
The group delay τ_g is determined by the following equation:

$$\tau_g = T2 - T1$$

4 Uncertainty evaluation

4.1 Uncertainty analysis

Repeatability:
Measurement of the group delay is performed 10 times. Uncertainty due to the measurement repeatability is obtained by calculating the standard deviation of these 10 measurements. This uncertainty takes into account the following contributions:

- Positioning of the cursor to determine T1 and T2
- Jitter of the trigger signal

Time scale calibration:
This uncertainty is given by the calibration certificate of the oscilloscope used. For the time scale the relative uncertainty is 0.0125 % which gives an uncertainty on the group delay of::

- 0.0015 µs for the 2.3 km long fiber
- 0.0075 µs for the 12 km long fiber

Laser wavelength mismatch and accuracy
The wavelengths of the lasers are measured with an uncertainty of ± 0.25 nm (k=1). The group delay measurement is corrected for the wavelength mismatch of the sources taking into account the chromatic dispersion of the fiber at the reference wavelengths: 0 ps/nm/km at 1310 nm and 17 ps/nm/km at 1550 nm.
Therefore the uncertainty due to wavelength accuracy is neglected at 1310 nm.
At 1550 nm if Δλ is the uncertainty on the wavelength scale with a Gaussian distribution, the group delay uncertainty u(λ) is:

$$u(\lambda) = 17 \; x \; \Delta\lambda \; x \; L$$

Which gives:

- $U_{2.3}(\lambda)$= 9.8 x 10^{-6} µs for the 2.3 km long fiber
- $U_{12}(\lambda)$= 51 x 10^{-6} µs for the 12 km long fiber

Temperature mismatch and accuracy
The ambient temperature of the laboratory is 22°C ± 1°C. The measurement is corrected for the temperature mismatch taking into account a temperature coefficient for the fiber length of:

$$\alpha = 0.55 \; x \; 10^{-6} \; / °C$$

Considering a rectangular distribution for the uncertainty on the temperature ΔT then the uncertainty $\Delta\tau_g(T)$ on the time delay measurement is :

$$\Delta\tau_g(T) = \frac{\alpha \; \tau_g \; \Delta T}{\sqrt{3}}$$

For $\Delta T = 1 \; °C$ the time delay relative uncertainty u(T) is:

$$u(T) = 3.2 \; x \; 10^{-7}$$

Therefore the time delay uncertainty for each fiber is:

- $U_{2.3}(T)$= 3.7 x 10^{-6} µs for the 2.3 km long fiber
- $U_{12}(T)$= 19 x 10^{-6} µs for the 12 km long fiber

4.2 Uncertainty budget

	Fiber reference			
	LRF 2015.06		LRF 2015.07	
	Wavelength (nm)		Wavelength (nm)	
Uncertainty components	**1310**	**1550**	**1310**	**1550**
Repeatability	0.000061	0.000050	0.000081	0.000128
Calibration of the oscilloscope	0.001429	0.001429	0.007369	0.007371
Wavelength mismatch and accuracy	0.000000	0.000010	0.000000	0.000051
Temperature mismatch and accuracy	0.000011	0.000011	0.000056	0.000056
Combined uncertainty	0.0014	0.0014	0.0074	0.0074
Expanded uncertainty (k=2)	**0.0029**	**0.0029**	**0.015**	**0.015**

Annex 1

Characteristics of the laser sources

The laser source used is a dual laser from an OTDR. The centre wavelengths are 1301.5 nm for the nominal 1310 nm source and 1548.0 nm for the nominal 1550 nm source. The spectral power distributions of the sources are shown on figures 3 and 4.

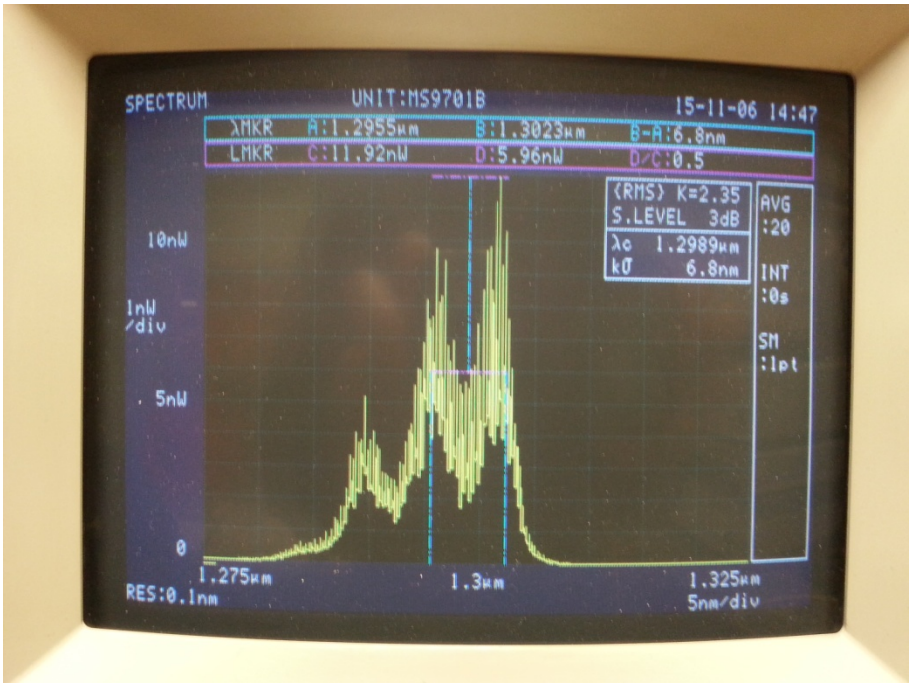

Figure 3: Spectral power distribution of the 1310 nm laser

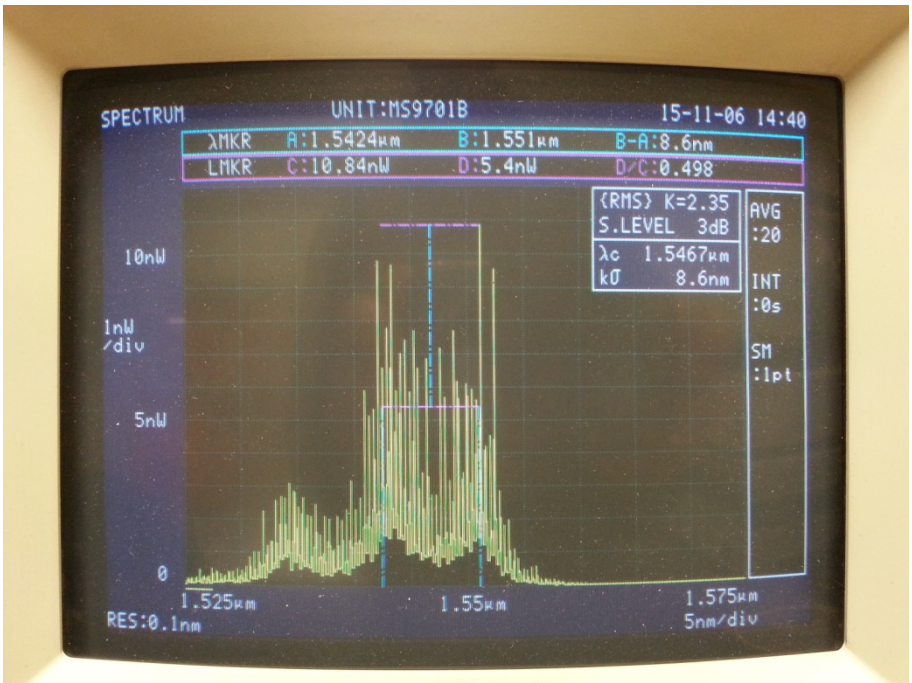

Figure 4: Spectral power distribution of the 1550 nm laser

* * * * *

4.5. VNIIOFI

Report of Results and Uncertainties VNIIOFI, Russia Federation

1. Facility (set)

The measurement set of group delay consist of:

1) Digital delay generator with rubidium standard frequency. Provides very accuracy time set interval between channels T0 and T1.

2) Optical sources with 1310, 1550 and 1625 nm DFB lasers are provides E/O conversation.

3) Sampling oscilloscope is provides O/E conversation and registration of pulse form from optical sources with 40 GHz wideband

4) OSA need for measurement wavelength of optical source for follow correction values group delay

5) Active thermostat using for stabilization temperature 23˚C.

6) Precision thermometer with 0,1˚C accuracy using for controlling temperature in the active thermostat.

All of the instruments (set) are describe above using to measurement of group delay in the artifact at 3 wavelengths.

Measurements carrying out in 3 stages.

First stage, determined internal delay of set. For it, conecting pathcord from couple through FC adapter to sampling oscilloscope (fig 1).

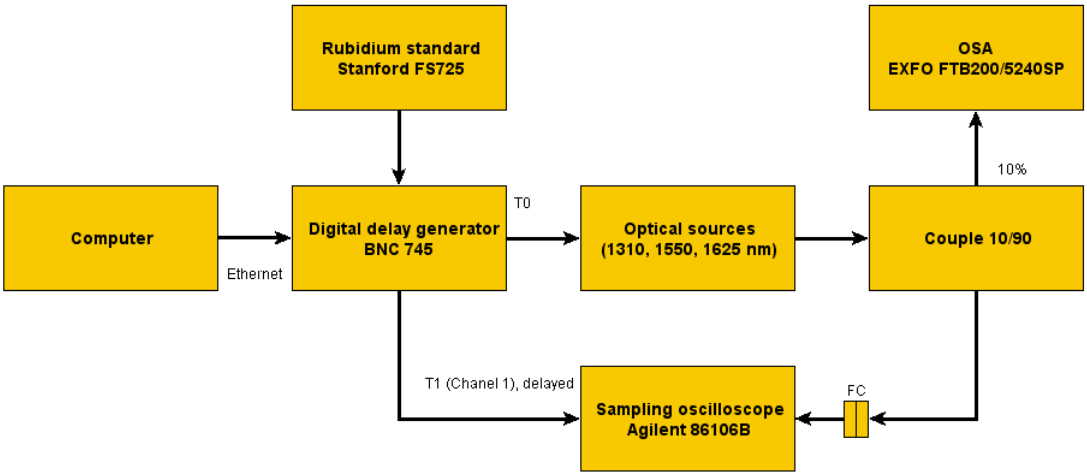

Figure 1 – Determine internal delay of set

Second stage, measurement a group delays combined group delay of artifact and internal delay of set, simultaneously measuring wavelength by OSA (Fig 2).

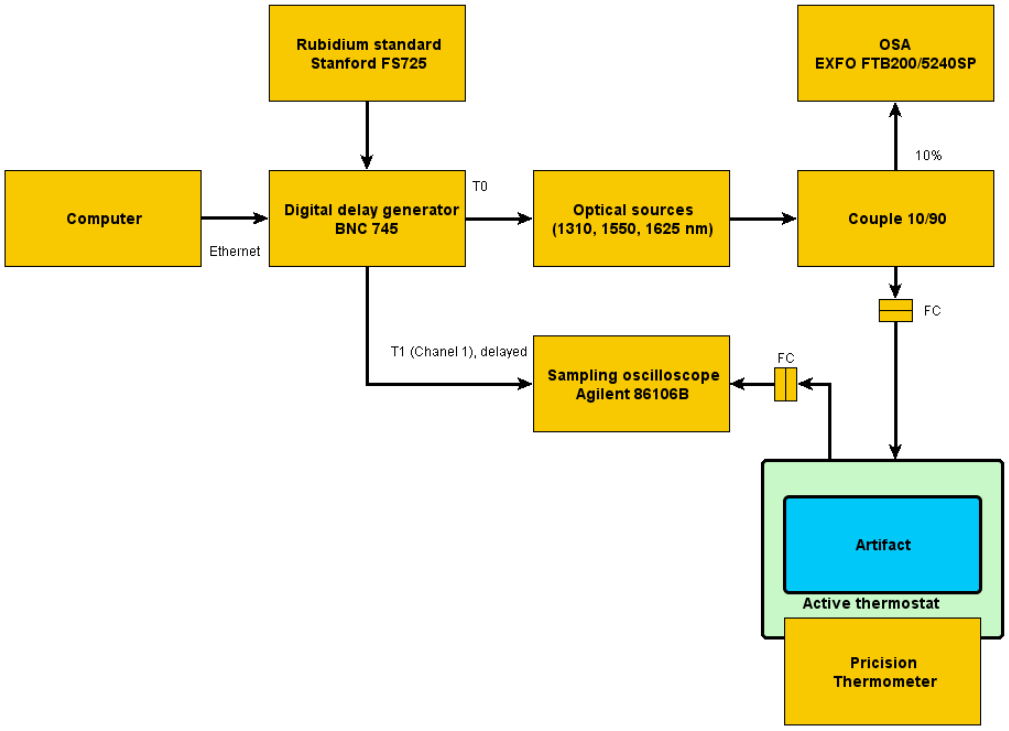

Figure 2 – Measurement group delay of artifact

Third stage, measurement chromatic dispersion of artifacts for correcting value group delay due to mismatch wavelength of source and value wavelength described in the Technical protocol (Fig 3).

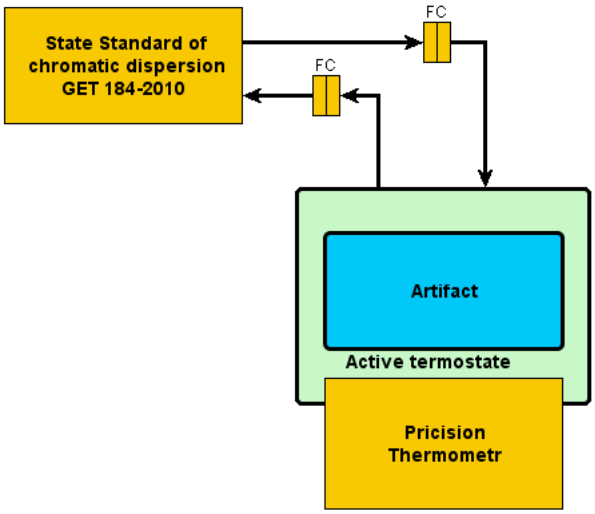

Figure 3 – Measurement chromatic dispersion of artifact

2. Traceability

Each measurement and facility (time interval, OSA, CD, thermometer) give units (frequency, wavelength, chromatic dispersion, temperature) from either State primary standard, or by means of calibration its according traceability chain.

Time interval (BNC745) – State primary standard of the time and frequency units and the national time scale GET 1-2012. Traceability chain GOST 8.129-2013.

Wavelength (OSA) - State primary special standard of units of signal propagation length and duration in the optical fiber of the average power, attenuation and wavelength for optical fiber communication systems and information transmission GET 170-2011. Traceability chain GOST 8.585-2013.

Chromatic dispersion - State primary special standard of chromatic dispersion unit in the optical fiber GET 184-2010. Traceability chain GOST 8.608-2012.

Temperature (precision thermometer) - State Primary Standard of temperature in range 0,8÷273,16K GET 35-91. Traceability chain GOST 8.558-2009.

3. Results and uncertainty budget

Tables 1 – 2 are show results measurements in Length and Time units for two artifacts.
Tables 3 – 6 are show uncertainty budgets in Length and Time units for two artifacts.

Table 1 – Results of measurements for artifact LRF2015.7

Wavelength, nm	Group delay, ns	Expanded Uncertainty, ns (k=2)	Length, m (n=1.460)	Expanded Uncertainty, m (k=2)
1310	11428.03	0.29	2346.601	0.059
1550	11432.52	0.29	2347.523	0.059
1625	11435.66	0.29	2348.168	0.060

Table 2 – Results of measurements for artifact LRF2015.6

Wavelength, nm	Group delay, ns	Expanded Uncertainty, ns (k=2)	Length, m (n=1.460)	Expanded Uncertainty, m (k=2)
1310	58949.57	0.31	12104.546	0.064
1550	58972.16	0.32	12109.184	0.066
1625	58988.09	0.33	12112.455	0.067

Table 3 – Uncertainty budget of Results of measurements for artifact LRF2015.7 (group delay)

Source of uncertainty	Standard uncertainty	Degree of freedom	Type
Time interval	144 ps	∞	B
Wavelength mismatch			
Chromatic dispersion	0.13 ps	$1.3 \cdot 10^3$	B
Wavelength	0.4 ps for 1310 7.4 ps for 1550 9.4 ps for 1625	∞	B
Temperature	11 ps	9	B
Jitter	5 ps	9	A
Combined uncertainty	144.5 ps for 1310 144.7 ps for 1550 144.8 ps for 1625		
Expanded uncertainty	289.0 ps for 1310		

(k=2)	289.4 ps for 1550 289.6 ps for 1625

Table 4 – Uncertainty budget of Results of measurements for artifact LRF2015.6 (group delay)

Source of uncertainty	Standard uncertainty	Degree of freedom	Type
Time interval	144 ps	∞	B
Wavelength mismatch			
Chromatic dispersion	0.13 ps	$1.3 \cdot 10^3$	B
Wavelength	2.6 ps for 1310 37.4 ps for 1550 47.4 ps for 1625	∞	B
Temperature	59 ps	9	B
Jitter	5 ps	9	A
Combined uncertainty	155.7 ps for 1310 160.1 ps for 1550 162.8 ps for 1625		
Expanded uncertainty (k=2)	311.4 ps for 1310 320.2 ps for 1550 325.6 ps for 1625		

Table 5 – Uncertainty budget of Results of measurements for artifact LRF2015.7 (length)

Source of uncertainty	Standard uncertainty	Degree of freedom	Type
Time interval	29.6 mm	∞	B
Wavelength mismatch			
Chromatic dispersion	0.03 mm	$1.3 \cdot 10^3$	B
Wavelength	0.08 mm for 1310 1.5 mm for 1550 1.9 mm for 1625	∞	B
Temperature	2.3 mm	9	B
Jitter	1 mm	9	A
Combined uncertainty	29.7 mm for 1310 29.7 mm for 1550 29.7 mm for 1625		
Expanded uncertainty (k=2)	59.3 mm for 1310 59.4 mm for 1550 59.5 mm for 1625		

Table 6 – Uncertainty budget of Results of measurements for artifact LRF2015.6 (length)

Source of uncertainty	Standard uncertainty	Degree of freedom	Type
Time interval	29.6 mm	∞	B
Wavelength mismatch			
Chromatic dispersion	0.03 mm	$1.3 \cdot 10^3$	B

Wavelength	0.5 mm for 1310 7.7 mm for 1550 9.7 mm for 1625	∞	B
Temperature	12.1 mm	9	B
Jitter	1 mm	9	A
Combined uncertainty	32.0 mm for 1310 32.9 mm for 1550 33.4 mm for 1625		
Expanded uncertainty (k=2)	64.0 mm for 1310 65.8 mm for 1550 66.8 mm for 1625		

4.6. NMISA

APMP.PR-S8 Supplementary Comparison Optical length

National Metrology institute of South Africa, NMISA

Mariesa Nel (MNel@nmisa.org) and Pritesh Jivan (PJivan@nmisa.org)

Introduction:

The measurements were performed in the Fibre Optics laboratory at NMISA. The laboratory is temperature and humidity controlled, the temperature is controlled at 23℃ ±2℃ and the humidity at 50 % RH ± 15 %RH. The facility also uses dust filters to filter out air incoming from the air conditioning ducts.

The optical fibre length artefacts prepared by KRISS, consists of two spools with step index single mode optical fibre (SMF) and predetermined lengths, approximately 3 km and 13 km. NMISA measured in the third round, on the 6th and 7th of June 2016.

The box was opened at a lab environment of 23 °C and 35 %RH. Visual inspection of the fibre ends were performed when the items arrived at NMISA and just before sending the artefacts. A microscope inspection probe was used to inspect the fibre ends. Items were in good order.

Traceability:

Temperature is traceable to the South African national measurement standards for humidity and temperature.

Length measurements of the time interval counter was referenced to the South African national measurement standard for time and frequency, a Caesium beam atomic clock.

Wavelength measurements traceable to the absorption wavelengths of acetylene gas ($^{12}C_2H_2$) as listed for NIST standard reference material 2517a).

Description of measurement: NMISA

At the NMISA we measure the delay within a fibre by measuring the transmitted pulse through the fibre: Method A: Delay measuring [1].

Measurement procedure:

With the optical delay line (DUT) connected and the attenuator adjusted to minimum attenuation, adjust the delay on the delay generator until the pulse appears on the oscilloscope screen. Note the delay (t_1). Store the trace in the Digital Sampling Oscilloscope (DSO) memory.

Remove the optical delay line (DUT) and inter-connect the two fibre patch cords. Adjust the delay on the delay generator to get the peak of the pulse. Adjust the attenuator so that the pulse amplitude matches that of the initial pulse. Note the delay (t_0).

Connect the delay generator to the counter/timer referenced to the caesium clock, the initial and delayed outputs connected to the start and finish inputs (Channel 1 and 2) of the time interval counter.

With the delay generator set to t_1, measure the corresponding delay on the counter/timer (t_1'). Repeat for setting t_0 to get the reading t_0'.

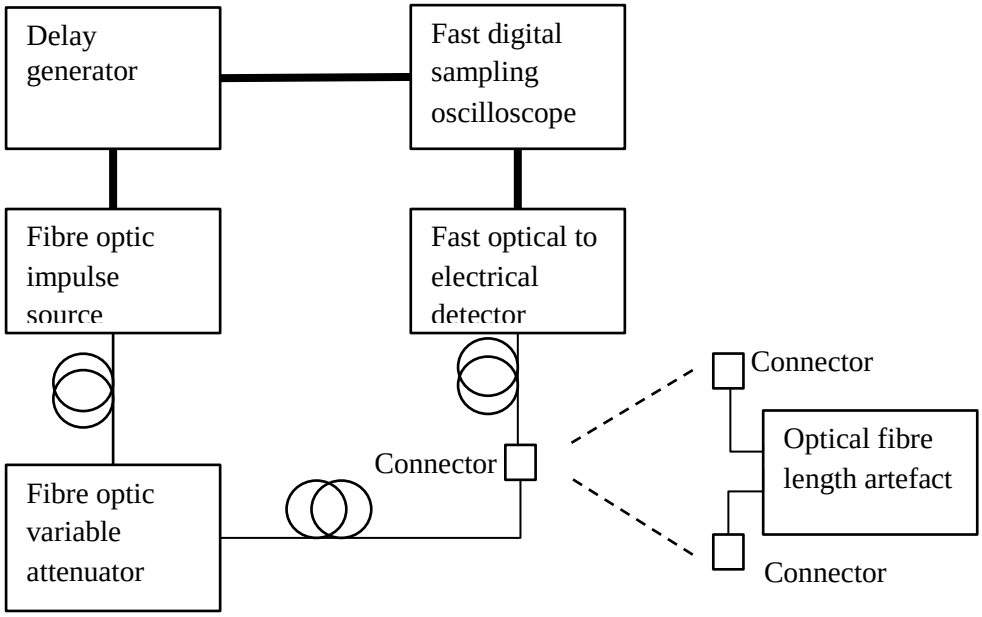

Figure 1: Measurement setup

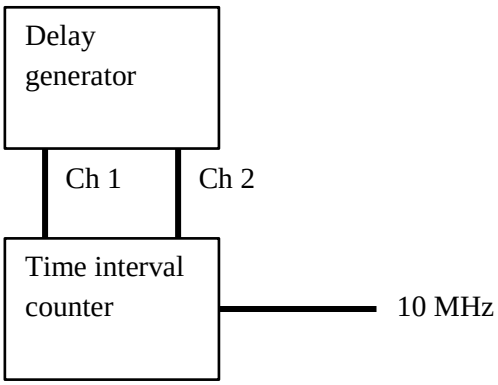

Figure 2: Delay generator calibration

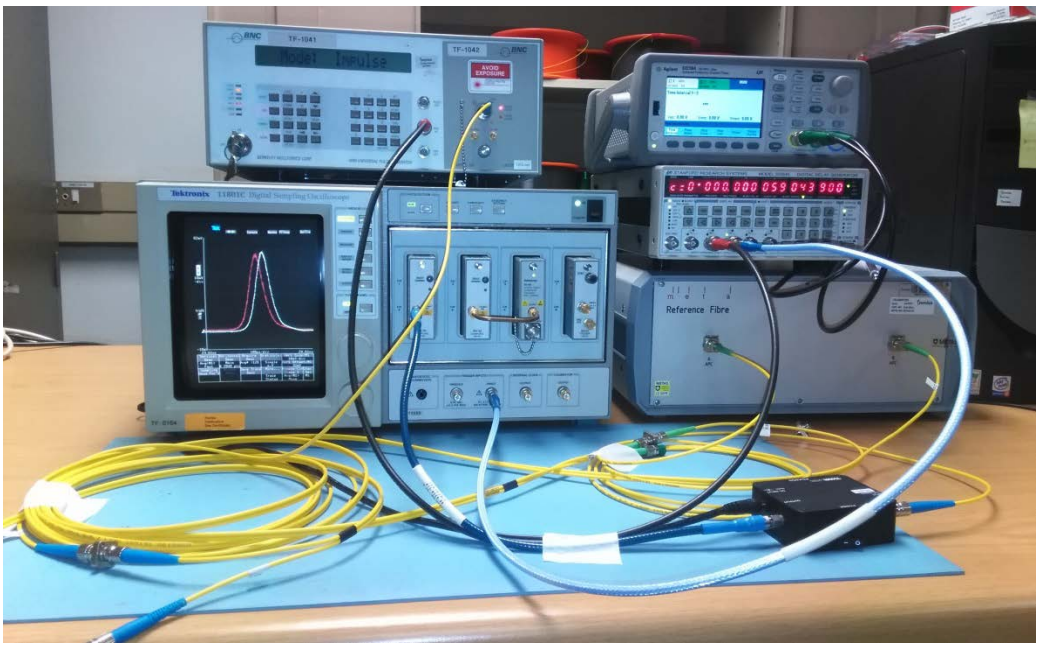

Figure 3: Photo of the measurement setup.

Table 1: List of sources

Source detail	**Measured centre wavelength [nm]**	**Uncertainty [nm]**
Berkeley Nucleonics Corp model 6040 with model 130 plug-in, set to impulse mode.	1 313,9	±0,3
Berkeley Nucleonics Corp model 6040 with model 155 plug-in, set to impulse mode.	1 552,0	±0,8
Berkeley Nucleonics Corp model 6040 with model 155-11 plug-in, set to impulse mode.	1 612,0	±0,3

Uncertainty budget :

Under the headings below the Uncertainty contributions for the measurement are discussed. The uncertainties were calculated and expressed in accordance with the GUM [2].

Caesium clock: Serving as reference oscillator for the counter: Relative stability
Sensitivity factor is the measured time delay.

Counter specification: Counter's relative time-base error, worst case option 10 Agilent 53230A

Counter channel: Counter channel difference and trigger error, worst case.

Temperature effect: Temperature coefficient of 40 ps·km^{-1}K^{-1} [3] for a difference of 0,4 °C from 23 °C the uncertainty contribution for 3,25 km is 0,052 ns and for 13,31 km is 0,213 ns.

Wavelength Effect:
1310 nm: 0.3 nm wavelength uncertainty for the wavelength measurement. No correction for 1310 nm on the measurement. Typical values for typical single mode fibre.
Sensitivity coefficient (Ci): 1313 nm <1 ps/(nm·km) absolute value [4]
$C1 = 0{,}001\ ns/(nm \cdot km) \times 3{,}25\ km$ and $C2 = 0{,}001\ ns/(nm \cdot km) \times 13{,}13\ km.$
1550 nm: 0,8 nm wavelength uncertainty for the wavelength measurement. 2 nm difference in wavelength contribution: $\sqrt{(0{,}8^2 + 2^2)}$ .Typical values for typical single mode fibre.
Sensitivity coefficient (Ci):1550 nm 17ps/(nm·km) absolute value [4]
$C1 = 0{,}017\ ns/(nm \cdot km) \times 3{,}250\ km$ and $C2 = 0{,}017\ ns/(nm \cdot km) \times 13{,}13\ km.$
1625 nm: 0,3 nm wavelength uncertainty for the wavelength measurement. Correction for 1612 nm to 1625 nm of 0,79 ns will be applied for 3,25 km and 3,3 ns for 13,31 km. Typical values for typical single mode fibre.
Sensitivity coefficient (Ci) :1625 nm <22 ps/(nm·km) absolute value [4]
$C1 = 0{,}022\ ns/(nm \cdot km) \times 3{,}25\ km$ and $C2 = 0.022\ ns/(nm \cdot km) \times 13{,}13\ km.$

Delay generator resolution: Delay generator resolution = 0,05 ns/2

Pulse peak alignment (Oscilloscope): 1/4 of a block on scope (DSO) with 200 ps/div setting for the 1310 nm and 1550 nm laser and 500 ps/div for the 1625 nm laser.

Table 2: Artefact 1: 1310 nm

Source of uncertainty	**Estimated uncertainty**	**Probability distribution**	**Sensitivity coefficient**	**Standard uncertainty**	**Degrees of freedom**
Caesium clock	1,5E-10 rel	Normal k= 1	15835,34 ns	2,374E-06 ns	Infinite
Counter specification	0,01 ns	Rectangular	1	5,774E-03 ns	Infinite
Counter channel	0,1440 ns	Rectangular	1	8,314E-02 ns	Infinite
Temperature effect	0,05 ns	Rectangular	1	3,002E-02 ns	Infinite
Wavelength Effect	0,3 nm	Normal k= 2	0,00325 ns/nm	4,875E-04 ns	Infinite
Delay generator resolution	0,025 ns	Rectangular	1	1,443E-02 ns	Infinite
Pulse peak alignment (Oscilloscope)	0,05 ns	Rectangular	1	2,887E-02 ns	Infinite
Type A ESDM	0,02148 ns	Normal k= 1	1	2,148E-02 ns	2
The expanded uncertainty of measurement with a coverage factor of k=2 for a normal distribution that approximates to a level of confidence of 95,45%				**±0,194 ns**	**Effective degrees of freedom =** Infinite
Claimed uncertainty: $1x10^{-5}$(t[ns]) + 0,2 ns = $1x10^{-5}$(15838 ns) + 0,2 ns = 0,36 ns				**±0,36 ns**	

Table 3: Artefact 1, 1550 nm

Source of uncertainty	**Estimated uncertainty**	**Probability distribution**	**Sensitivity coefficient**	**Standard uncertainty**	**Degrees of freedom**
Caesium clock	1,5E-10 rel	Normal k= 1	15835.34 ns	2,375E-06 ns	Infinite
Counter specification	0,01 ns	Rectangular	1	5,774E-03 ns	Infinite
Temperature effect	0,05 ns	Rectangular	1	3,002E-02 ns	Infinite
Wavelength Effect	2,15 nm	Normal k= 2	0.06 ns/nm	5,951E-02 ns	Infinite
Delay generator resolution	0,03 ns	Rectangular	1	1,443E-02 ns	Infinite
Pulse peak alignment (Oscilloscope)	0,05 ns	Rectangular	1	2,887E-02 ns	Infinite
Counter channel	0,14 ns	Rectangular	1	8,314E-02 ns	Infinite
Type A ESDM	0,02 ns	Normal k= 1	1	1,849E-02 ns	2
The expanded uncertainty of measurement with a coverage factor of k=2 for a normal distribution that approximates to a level of confidence of 95,45%				**±0,226 ns**	**Effective degrees of freedom =** Infinite
Claimed uncertainty: $1x10^{-5}$(t[ns]) + 0,2 ns = $1x10^{-5}$(15838 ns) + 0,2 ns = 0,36 ns				**±0,36 ns**	

Table 4: Artefact 1, 1625 nm

Source of uncertainty	**Estimated uncertainty**	**Probability distribution**	**Sensitivity coefficient**	**Standard uncertainty**	**Degrees of freedom**
Caesium clock	1,5E-10 rel	Normal k= 1	15838,98 ns	2,376E-06 ns	Infinite
Counter specification	0,01 ns	Rectangular	1	5,774E-03 ns	Infinite
Temperature effect	0,05 ns	Rectangular	1	3,002E-02 ns	Infinite
Wavelength Effect	0,30 nm	Normal k= 2	0,07 ns/nm	1,073E-02 ns	Infinite
Delay generator resolution	0,03 ns	Rectangular	1	1,443E-02 ns	Infinite
Pulse peak alignment (Oscilloscope)	0,13 ns	Rectangular	1	7,217E-02 ns	Infinite
Counter channel	0,14 ns	Rectangular	1	8,314E-02 ns	Infinite
Type A ESDM	0,02 ns	Normal k= 1	1	2,023E-02 ns	2
The expanded uncertainty of measurement with a coverage factor of k=2 for a normal distribution that approximates to a level of confidence of 95,45%				**±0,235 ns**	**Effective degrees of freedom =** Infinite
Claimed uncertainty: $1x10^{-5}$(t[ns]) + 0,2 ns = $1x10^{-5}$(15838 ns) + 0,2 ns = 0,36 ns				**±0,36 ns**	

Table 5: Artefact 2, 1310 nm

Source of uncertainty	**Estimated uncertainty**	**Probability distribution**	**Sensitivity coefficient**	**Standard uncertainty**	**Degrees of freedom**
Caesium clock	1,5E-10 rel	Normal k= 1	64800,44 ns	9,72E-06 ns	Infinite
Counter specification	0,01 ns	Rectangular	1	5,77E-03 ns	Infinite
Temperature effect	0,21 ns	Rectangular	1	1,23E-01 ns	Infinite
Wavelength Effect	0,30 nm	Normal k= 2	0,01 ns/nm	2,00E-03 ns	Infinite
Delay generator resolution	0,03 ns	Rectangular	1	1,44E-02 ns	Infinite
Pulse peak alignment (Oscilloscope)	0,05 ns	Rectangular	1	2,89E-02 ns	Infinite
Counter channel	0,19 ns	Rectangular	1	1,11E-01 ns	Infinite
Type A ESDM	0,02 ns	Normal k= 1	1	2,046E-02 ns	2
The expanded uncertainty of measurement with a coverage factor of k=2 for a normal distribution that approximates to a level of confidence of 95,45%				**±0,340 ns**	**Effective degrees of freedom =** Infinite
Claimed uncertainty: $1x10^{-5}$(t[ns]) + 0,2 ns = $1x10^{-5}$(64845 ns) + 0,2 ns = 0,85 ns				**±0,85 ns**	

Table 6: Artefact 2, 1550 nm

Source of uncertainty	**Estimated uncertainty**	**Probability distribution**	**Sensitivity coefficient**	**Standard uncertainty**	**Degrees of freedom**
Caesium clock	1,5E-10 rel	Normal k= 1	64829,38 ns	9,724E-06 ns	Infinite
Counter specification	0,01 ns	Rectangular	1	5,774E-03 ns	Infinite
Temperature effect	0,21 ns	Rectangular	1	1,230E-01 ns	Infinite
Wavelength Effect	2,15 nm	Normal k= 2	0,23 ns/nm	2,437E-01 ns	Infinite
Delay generator resolution	0,03 ns	Rectangular	1	1,443E-02 ns	Infinite
Pulse peak alignment (Oscilloscope)	0,05 ns	Rectangular	1	2,887E-02 ns	Infinite
Counter channel	0,19 ns	Rectangular	1	1,109E-01 ns	Infinite
Type A ESDM	0,02 ns	Normal k= 1	1	2,012E-02 ns	2
The expanded uncertainty of measurement with a coverage factor of k=2 for a normal distribution that approximates to a level of confidence of 95,45%				**±0,595 ns**	**Effective degrees of freedom =** Infinite
Claimed uncertainty: $1x10^{-5}$(t[ns]) + 0,2 ns = $1x10^{-5}$(64845 ns) + 0,2 ns = 0,85 ns				**±0,85 ns**	

Table 7: Artefact 2, 1625 nm

Source of uncertainty	**Estimated uncertainty**	**Probability distribution**	**Sensitivity coefficient**	**Standard uncertainty**	**Degrees of freedom**
Caesium clock	1,5E-10 rel	Normal k= 1	64844,60 ns	9,727E-06 ns	Infinite
Counter specification	0,01 ns	Rectangular	1	5,774E-03 ns	Infinite
Temperature effect	0,21 ns	Rectangular	1	1,230E-01 ns	Infinite
Wavelength Effect	0,30 nm	Normal k= 2	0,29 ns/nm	4,392E-02 ns	Infinite
Delay generator resolution	0,03 ns	Rectangular	1.00	1,443E-02 ns	Infinite
Pulse peak alignment (Oscilloscope)	0,13 ns	Rectangular	1.00	7,217E-02 ns	Infinite
Counter channel	0,19 ns	Rectangular	1.00	1,109E-01 ns	Infinite
Type A ESDM	0,02 ns	Normal k= 1	1	1,964E-02 ns	2
The expanded uncertainty of measurement with a coverage factor of k=2 for a normal distribution that approximates to a level of confidence of 95,45%				**±0,376 ns**	**Effective degrees of freedom =** Infinite
Claimed uncertainty: $1x10^{-5}$(t[ns]) + 0,2 ns = $1x10^{-5}$(64845 ns) + 0,2 ns = 0,85 ns				**±0,85 ns**	

Correction for wavelength mismatch

A straight line approximation between the measured time delay at 1552,0 nm and 1612,0 nm were used and extrapolated to 1625 nm to get the delay for 1625 nm for both the artefacts. For the 3 km fibre the correction was 0,79 ns and for the 13 km delay line the correction was calculated to be 3,3 ns. No correction was applied to the 1550 nm delay measurements.

Measurement results and uncertainties

The group delay of the fibres was measured in seconds at 1310 nm, 1550 nm and 1625 nm (optional). Measurements were performed at 23,4 °C. No correction was applied for temperature mismatch. The wavelength sources NMISA has are close to 1310 nm and 1550 nm. The 1625 nm a correction to the time of flight are necessary as our wavelength is detuned from the nominal wavelength.

Fibre length is reported using the refractive index of 1,460.

Table 8: Artefact 1, uncorrected time of flight

Wavelength [nm]	Temperature [°C]	Measurement [ns]	Uncertainty [ns] k=2	Length [m]
1313,9	23,4	15 828,39	±0,20	3 250,16
1552,0	23,4	15 835,34	±0,23	3 251,59
1612,0	23,4	15 838,98	±0,24	3 252,33

Table 9: Artefact 1, corrected time of flight

Wavelength [nm]	Temperature [°C]	Measurement [ns]	Uncertainty [ns] k=2	Length [m]
1310	23	15 828,39	±0,36	3 250,16
1550	23	15 835,34	±0,36	3 251,59
1625	23	15 839,77	±0,36	3 252,50

Table 10: Artefact 2, uncorrected time of flight

Wavelength [nm]	Temperature [°C]	Measurement [ns]	Uncertainty [ns] k=2	Length [m]
1313,9	23,4	64 800,44	±0,34	13 305,95
1552,0	23,4	64 829,38	±0,60	13 311,89
1612,0	23,4	64 844,60	±0,38	13 315,02

Table 11: Artefact 2, corrected time of flight

Wavelength [nm]	Temperature [°C]	Measurement [ns]	Uncertainty [ns] k=2	Length [m]
1310	23	64 800,44	±0,85	13 305,95
1550	23	64 829,38	±0,85	13 311,89
1625	23	64 847,90	±0,85	13 315,69

References

[1] SABS IEC 60793-1-22 Ed 1: 2001 Specification, Optical fibres Part 1-22 Measurement methods and test procedures, length measurement.

[2] "*A Guide to the expression of uncertainty in measurement, International organisation for standardisation"*, Geneva, Switzerland, 1993.

[3] A.H. Hartog, A.J. Conduit, D.N. Payne, "*Variation of pulse delay with stress and temperature in Jacketed and unjacketed optical fibres*", Optical and quantum electronics Vol 11, 1979, p 265-273.

[4] Corning Optical fibre, "*Single mode dispersion: measurement method*", September 2001

4.7. NIS

APMP Supplementary Comparison on

Optical Fiber Length

(NIS, Egypt)

Length of artifact (3 km) = L1 **Length of artifact (13 km)** = L2

Status at arrival: Attenuation: L1= 0.70 dB L2= 2.60 dB

Fiber end faces:

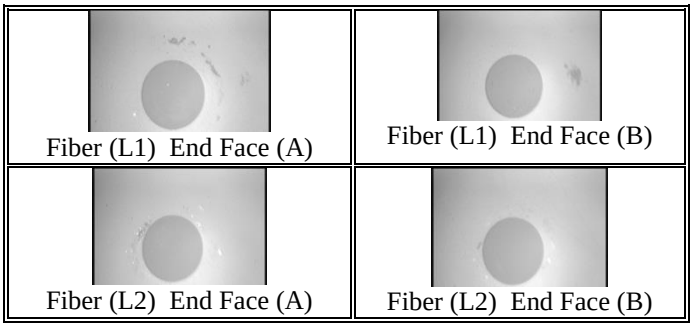

Status at departure: Attenuation: L1= 0.72 dB L2= 2.65 dB

Fiber end faces:

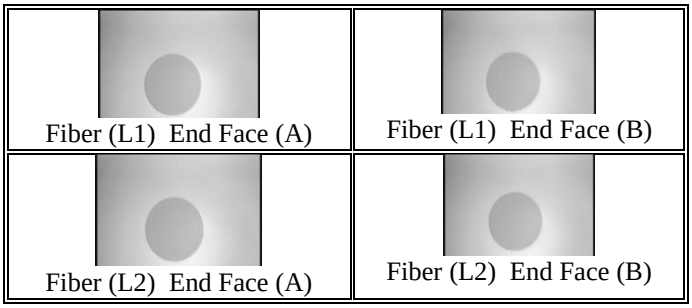

Technique: *Delay:* time-of-flight technique.

Sensitivity coefficients: Phase shift of a 200 MHz sinusoidal modulation wave.

Reference: O. Terra, H. Hussein, "*Accurate Fiber Length Measurement Using the Time-of-Flight Technique*", Journal of Optical Communications. Volume 37, Issue 2, Pages 187–191, November 2015.

Sensitivity coefficients equation: - Temperature: $\frac{\partial L}{\partial T} = \frac{\partial \tau}{\partial T}\frac{c}{n}$ **(**for 1 meter**)**

- Wavelength: $\frac{\partial L}{\partial \lambda} = \frac{\partial \tau}{\partial \lambda}\frac{c}{n}$ **(**for 1 meter**)**

(Delay change is resulting from the refractive index change due to wavelength and temperature)

Traceability: - Time interval counter (BNC 1105) (which is used to measure the delay) is calibrated at the time and frequency laboratory to achieve traceability to the SI unit of time, the second. The certificate of calibration is available on request.

- The temperature monitor (HUMLOG20) has been calibrated at the thermometry department to achieve traceability to the SI unit of temperature, the Kelvin. The certificate of calibration is available on request.

System Photograph

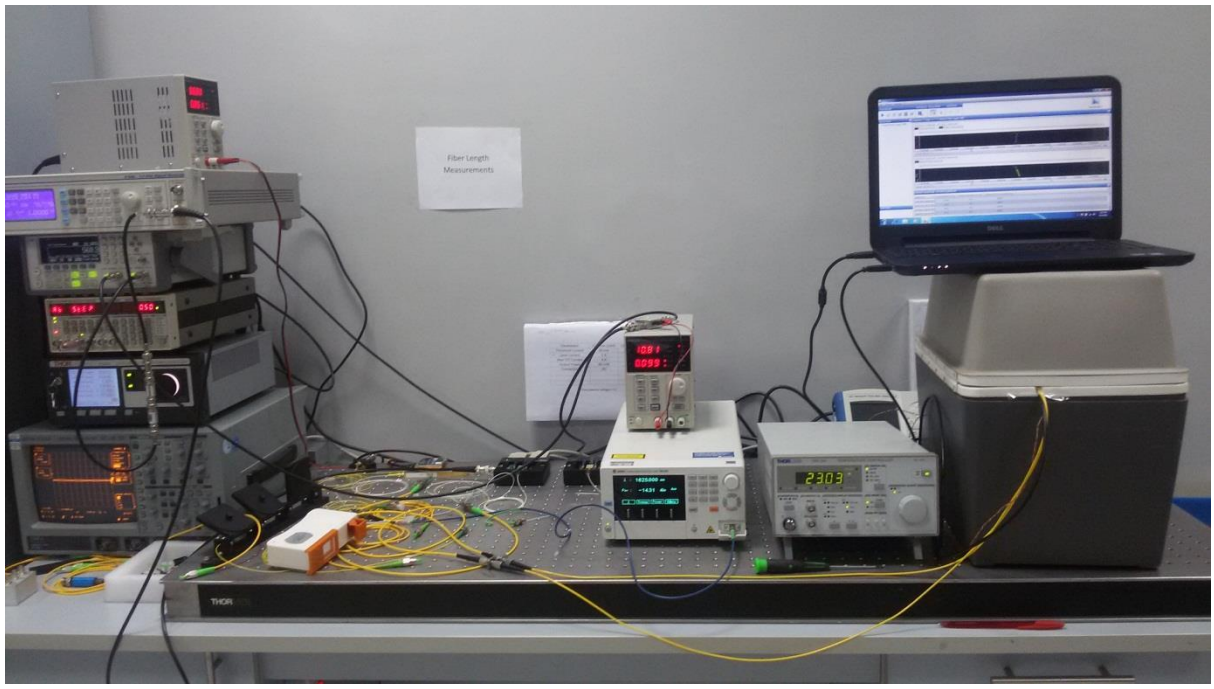

Contact Persons

Dr. Osama Terra (e-mail: osama.terra@gmail.com, osama.terra@nis.sci.eg, +201141172900)

Prof. Dr. Hatem Hussein (e-mail: Hatem_hussein@hotmail.com)

Length and Precision Engineering Division, National Institute for standards (NIS)
Tersa street, Haram, 12211 Giza; P.O.Box: 136 Giza, Egypt

Measurement Results

-*Temperature is fluctuated from (22.63* ^{o}C *to 23.51* ^{o}C) through all the 120 measurements.

-*Results are reported at Temperature of (T* = 23 ^{o}C) and wavelengths of (1310 nm, 1550 nm, 1625 nm) *after correction of temperature and wavelength mismatch.*

- Refractive index: 1.46

- Number of measurements: 20

- The effective degree of freedom is calculated from: $\nu_{eff} = u_c^4(y)/\sum_{i=1}^{N}(u_i^4(y)/\nu_i)$ where, u_c is the combined uncertainty, u_i is the uncertainty in each component.

λ= 1310 nm

L1 = 3250.046 m Standard deviation = 2.5 cm

L2 = 13305.791 m Standard deviation = 5.4 cm

Sensitivity Coefficients: Temperature: $\frac{\partial L}{\partial T}$ = 4.8 × 10^{-6} /^{o}C.

Wavelength: $\frac{\partial L}{\partial \lambda}$ = **0** /nm (not detectable with 1 nm shift)

λ= 1550 nm

L1 = 3251.562 m Standard deviation = 1.3 cm

L2 = 13311.907 m Standard deviation = 2.6 cm

Sensitivity Coefficients: Temperature: $\frac{\partial L}{\partial T}$ = 6.9 × 10^{-6} /^{o}C.

Wavelength: $\frac{\partial L}{\partial \lambda}$ = 3.5 × 10^{-6} /nm.

λ= 1625 nm

L1 = 3252.505 m Standard deviation = 1.6 cm

L2 = 13315.801 m Standard deviation = 2.6 cm

Sensitivity Coefficients: Temperature: $\frac{\partial L}{\partial T}$ = 9.0 × 10^{-6} /^{o}C.

Wavelength: $\frac{\partial L}{\partial \lambda}$ = 4.6 × 10^{-6} /nm.

Uncertainty Calculation

λ= 1310 nm

For L1:

Source of uncertainty	Value (±)	PD	DIV	DOF	Sensitivity Coefficient	Standard Uncertainty
Time interval counter	1×10^{-11} s	Rectangular	$\sqrt{3}$	∞	2.05×10^{8}	± 1 mm
Modulation rise time	1×10^{-10} s	Rectangular	$\sqrt{3}$	∞	2.05×10^{8}	± 12 mm
Wavelength	0.1 nm	Triangle	$\sqrt{6}$	∞	0	± 0 mm
Temperature	0.5 ^{o}C	Triangle	$\sqrt{6}$	∞	0.016	± 3 mm
Repeatability	25 mm	Normal	1	19	1	± 25 mm
Combined uncertainty						± 28 mm
Effective degrees of freedom						**30**
Expanded uncertainty (k ≈ 2)						**± 56 mm**

Div: Divisor, DOF: degrees-of-freedom, PD: Probability distribution

For L2:

Source of uncertainty	Value (±)	PD	DIV	DOF	Sensitivity Coefficient	Standard Uncertainty
Time interval counter	1×10^{-10} s	Rectangular	$\sqrt{3}$	∞	2.05×10^{8}	± 12 mm
Modulation rise time	1×10^{-10} s	Rectangular	$\sqrt{3}$	∞	2.05×10^{8}	± 12 mm
Wavelength	0.1 nm	Triangle	$\sqrt{6}$	∞	0	± 0 mm
Temperature	0.5 ^{o}C	Triangle	$\sqrt{6}$	∞	0.064	± 13 mm
Repeatability	54 mm	Normal	1	19	1	± 54 mm
Combined uncertainty						± 58 mm
Effective degrees of freedom						**25**
Expanded uncertainty (k ≈ 2)						**± 116 mm**

Div: Divisor, DOF: degrees-of-freedom, PD: Probability distribution

λ= 1550 nm

For L1:

Source of uncertainty	Value (±)	PD	DIV	DOF	Sensitivity Coefficient	Standard Uncertainty
Time interval counter	1×10^{-11} s	Rectangular	$\sqrt{3}$	∞	2.05×10^{8}	± 1 mm
Modulation rise time	5×10^{-11} s	Rectangular	$\sqrt{3}$	∞	2.05×10^{8}	± 6 mm
Wavelength	0.1 nm	Triangle	$\sqrt{6}$	∞	0.011	± 1 mm
Temperature	0.5 ^{o}C	Triangle	$\sqrt{6}$	∞	0.022	± 5 mm
Repeatability	13 mm	Normal	1	19	1	± 13 mm
Combined uncertainty						± 15 mm
Effective degrees of freedom						**34**
Expanded uncertainty (k ≈ 2)						**± 30 mm**

Div: Divisor, DOF: degrees-of-freedom, PD: Probability distribution

For L2:

Source of uncertainty	Value (±)	PD	DIV	DOF	Sensitivity Coefficient	Standard Uncertainty
Time interval counter	1×10^{-10} s	Rectangular	$\sqrt{3}$	∞	2.05×10^{8}	± 12 mm
Modulation rise time	5×10^{-11} s	Rectangular	$\sqrt{3}$	∞	2.05×10^{8}	± 6 mm
Wavelength	0.1 nm	Triangle	$\sqrt{6}$	∞	0.047	± 2 mm
Temperature	0.5 ^{o}C	Triangle	$\sqrt{6}$	∞	0.092	± 19 mm
Repeatability	26 mm	Normal	1	19	1	± 26 mm
Combined uncertainty						± 35 mm
Effective degrees of freedom						**62**
Expanded uncertainty (k ≈ 2)						**± 70 mm**

Div: Divisor, DOF: degrees-of-freedom, PD: Probability distribution

λ= 1625 nm

For L1:

Source of uncertainty	Value (±)	PD	DIV	DOF	Sensitivity Coefficient	Standard Uncertainty
Time interval counter	1×10^{-11} s	Rectangular	$\sqrt{3}$	∞	2.05×10^{8}	± 1 mm
Modulation rise time	5×10^{-11} s	Rectangular	$\sqrt{3}$	∞	2.05×10^{8}	± 6 mm
Wavelength	0.1 nm	Triangle	$\sqrt{6}$	∞	0.015	± 1 mm
Temperature	0.5 ^{o}C	Triangle	$\sqrt{6}$	∞	0.0128	± 6 mm
Repeatability	16 mm	Normal	1	19	1	± 16 mm
Combined uncertainty						± 18 mm
Effective degrees of freedom						**30**
Expanded uncertainty (k ≈ 2)						**± 36 mm**

Div: Divisor, DOF: degrees-of-freedom, PD: Probability distribution

For L2:

Source of uncertainty	Value (±)	PD	DIV	DOF	Sensitivity Coefficient	Standard Uncertainty
Time interval counter	1×10^{-10} s	Rectangular	$\sqrt{3}$	∞	2.05×10^{8}	± 12 mm
Modulation rise time	5×10^{-11} s	Rectangular	$\sqrt{3}$	∞	2.05×10^{8}	± 6 mm
Wavelength	0.1 nm	Triangle	$\sqrt{6}$	∞	0.0613	± 3 mm
Temperature	0.5 ^{o}C	Triangle	$\sqrt{6}$	∞	0.0524	± 25 mm
Repeatability	26 mm	Normal	1	19	1	± 26 mm
Combined uncertainty						± 39 mm
Effective degrees of freedom						**96**
Expanded uncertainty (k ≈ 2)						**± 78 mm**

Div: Divisor, DOF: degrees-of-freedom, PD: Probability distribution

4.8. CENAM

SE
SECRETARÍA DE ECONOMÍA

CENAM
CENTRO NACIONAL DE METROLOGÍA

"2017, Año del Centenario de la Promulgación de la Constitución Política de los Estados Unidos Mexicanos"

APMP Supplementary Comparison on

Optical Fiber Length

Report of Results of the National Metrology Center of México (CENAM)

31 January, 2017

km 4.5 Carretera a Los Cués, El Marqués, Querétaro, C.P. 76246, México

Tel. (442) 211-0500 al 04 www.cenam.mx

Table of Contents

km 4.5 Carretera a Los Cués, El Marqués, Querétaro, C.P. 76246, México

Tel. (442) 211-0500 al 04 www.cenam.mx

Introduction

1.1 At the APMP TCPR meeting in Kuala Lumpur, Malaysia in 2009, the APMP international supplementary comparison on optical fiber length was agreed to be conducted and KRISS agreed to act as a pilot lab.

1.2 The aim of this comparison is to access the equivalence of the optical fiber length scales among the participants and to underpin the relevant claim of the Calibration and Measurement Capability in BIPM KCDB.

1.3 This technical protocol has been prepared by KRISS under the supervision of the Task Group on OTDR of CCPR Working Group Strategic Planning and follows the guidelines established by BIPM and CCPR.

Participant

About CENAM:

CENAM is the national reference laboratory in the area of measurements in Mexico.

It is responsible for establishing and maintaining national standards, provides metrological services such as calibration of instruments and standards, certification and development of reference materials, specialized courses in metrology, consulting and sale of publications. CENAM maintains a close relationship with other national laboratories and international organizations involved in metrology, in order to assure the international recognition of the national standards of Mexico and, as a result, promote the acceptance of the products and services of our country.

CENAM's mission is to support the various sectors of society in meeting their present and future metrological needs, establishing national standards of measurement, developing reference materials and disseminating its accuracy through technology services of the highest quality, to increase the competitiveness of the country, contribute to sustainable development and improve the quality of life of the people in Mexico.

Participant detail

The metrologist of CENAM in charge for this comparison was the following:

km 4.5 Carretera a Los Cués, El Marqués, Querétaro, C.P. 76246, México

Tel. (442) 211-0500 al 04 www.cenam.mx

Participant	Correspondence	E-mail address Phone number	Address
CENAM (México)	MSc. Zeus Efrain Ruiz Gutierrez	zruiz@cenam.mx; +52 (442) 2110500 Ext. 3354	Optics and Radiometry Direction, National Metrology Center of México (CENAM) km 4.5 Carretera a Los Cués, Municipio El Marqués, Qro. C.P. 76246 México

Description of the participant measurement facility

Our optical fiber length characterization system is based on the phase shift method according to the international standard CEI/IEC 60793-1-22:2001: "Measurement methods and test procedures-Length measurement". According to this method the length is determined from the phase shift that occurs when a predetermined modulation frequency is applied.

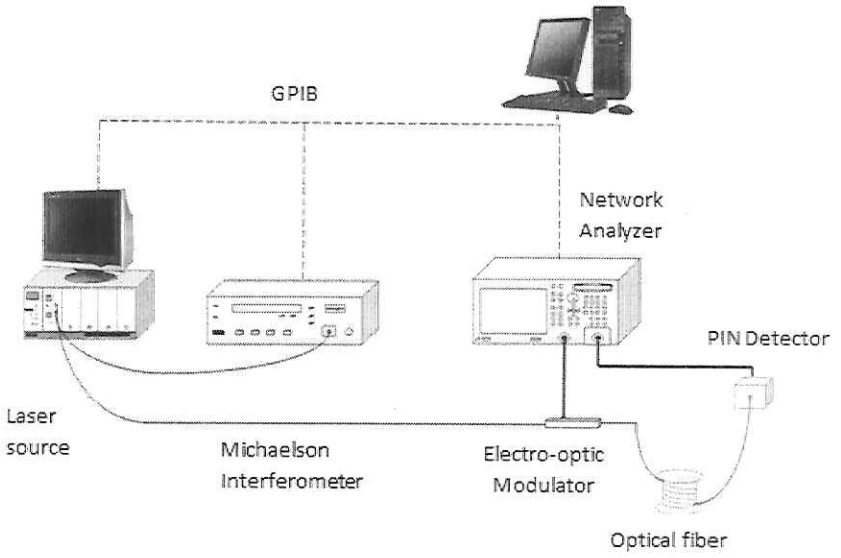

Figure 1. Length characterization system of CENAM.

Our system is composed by one network analyzer, one Lithium Niobate electro-optic modulator, one PIN detector, one Michaelson interferometer, two tunable laser sources (1 310 nm and 1 550

nm) and one 1 629 nm fabry-perot source (see Figure 1). A computer is also needed for the purposes of equipment control, data acquisition and numerical evaluation data. The details of the main standards and equipment used in our length characterization system are the following:

- Network Analyzer.
  Brand: Agilent Technologies
  Model: E5061A
  Serial Number: MY44203205
  Certificate number: CNM-CC-440-021/2015
  Traceability: National standard of reflection coefficient and dispersion parameters – CNM-PNE-14.

- Michaelson Interferometer.
  Brand: Anritsu
  Model: MF9630A
  Serial Number: M14049
  Certificate number: CNM-CC-520-006/2015
  Traceability: National Standard of length – CNM-PNM-2.

- Tunable laser source.
  Brand: New Focus
  Model: TLB-6600
  Serial Number: 10-OPM4200-01-11
  Certificate number: CNM-CC-520-021/2015
  Traceability: National Standard of length – CNM-PNM-2.

- Tunable laser source.
  Brand: EXFO
  Model: IQS-2600B-00-EA-EUI-89
  Serial Number: 230764
  Certificate number: CNM-CC-520-020/2015
  Traceability: National Standard of length – CNM-PNM-2.

- Fabry-perot laser source.
  Brand: JDSU
  Model: MAPL+1F067FP
  Serial Number: MY44203205
  Certificate number: CNM-CC-520-195/2016
  Traceability: National Standard of length – CNM-PNM-2.

According to the Figure 1, a network analyzer generates a RF signal; this signal modulates the laser source. The modulated optical signal produced by the laser travels through the optical fiber under

km 4.5 Carretera a Los Cués, El Marqués, Querétaro, C.P. 76246, México

Tel. (442) 211-0500 al 04 www.cenam.mx

test and is detected by a PIN photodiode. The phase meter of the network analyzer compares the phase of the signal coming from the photodiode (ϕ_{sig}) with a reference phase (ϕ_{ref}) introduced by the measurement system. To determine the reference phase (ϕ_{ref}) the phase calibration fiber (short fiber) is connected directly to the laser source and to the PIN photodiode.

The method provides the optical length of the fiber under test based on the modulation frequency and the optical signal wavelength. Starting at one wavelength the modulation frequency f_i is increased from 0.5 MHz up to 50 MHz, then the modulated signal phase is measured for every frequency and the process is repeated for the different wavelengths. The total phase shift change introduced by the fiber under test is given by:

$$\phi_{tot(i)} = \phi_i' + m_i \cdot 2\pi \tag{1}$$

Where:

ϕ_i': $\phi_{sig\,(i)} - \phi_{ref(i)}$

m_i: is the number of periods(phase shift changes of 2π) at the frequency f_i

The optical length of the fiber under test is given by:

$$L = \left(m + \frac{\phi_i'}{2\pi}\right) \cdot L_p + L_T + L_\lambda = \left(m + \frac{\phi_i'}{2\pi}\right) \cdot \frac{c}{N \cdot f} + L_T + L_\lambda \tag{2}$$

Where:

L: is the optical length of the fiber under test

ϕ_i': $\phi_{sig\,(i)} - \phi_{ref(i)}$

L_p: is the length of one period

m: is the number of periods (phase shift changes of 2π) at the frequency f

c: is the vacuum speed of light

N: is the group index of the fiber

f: is the modulation frequency

L_T: is the temperature mismatch correction

km 4.5 Carretera a Los Cués, El Marqués, Querétaro, C.P. 76246, México

Tel. (442) 211-0500 al 04 www.cenam.mx

$L\lambda$: is the wavelength mismatch correction

In this method the calculation of m requires a previous rough estimation of L. The risk of an error in calculating m, due to the previous estimation of L, increases with frequency because L_p decreases. An iterative method was used to achieve the necessary accuracy in the previous estimation of L: the calculation of m_i for the frequency f_i uses the length L_{i-1} estimated in the previous step, in this way the accuracy in the estimation of L increases in every step as the frequency increases.

$$m_i = Integer\left[\frac{(L_{i-1}\cdot N\cdot f_i)}{c}\right] \qquad L_i = \frac{(\phi_i' + m_i\cdot 2\pi)\cdot c}{N\cdot f_i\cdot 2\pi} \tag{3}$$

Where L_0 was measured with an OTDR and Integer is the truncated value

Figure 2 shows the results obtained for one of the 25 measurements of the artifact 1 at 1 550 nm.

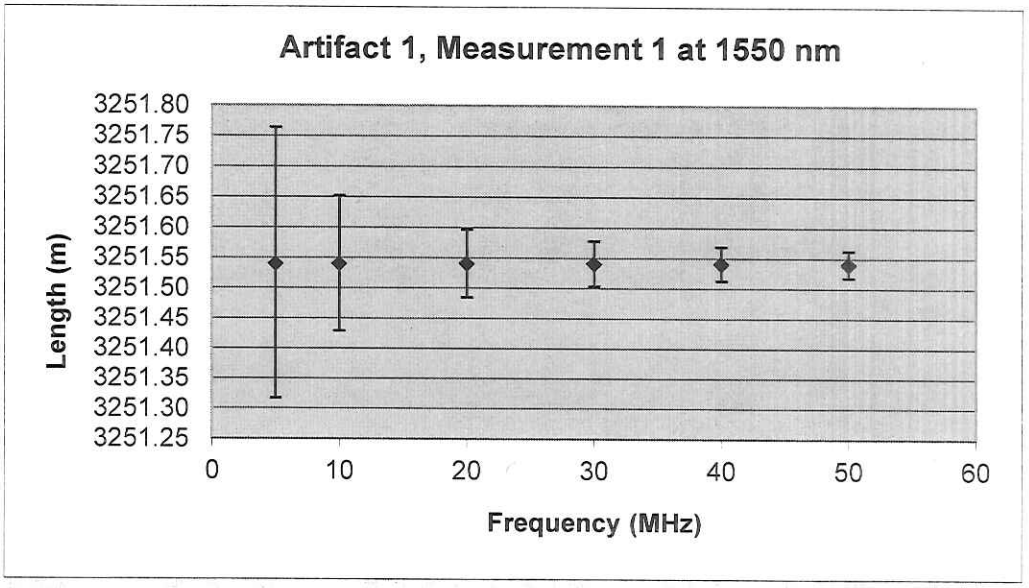

Figure 2. Measurement 1for the artifact 1 at 1 550 nm.

The transit time of the fiber under test at each wavelength is estimated by the equation:

km 4.5 Carretera a Los Cués, El Marqués, Querétaro, C.P. 76246, México

Tel. (442) 211-0500 al 04 www.cenam.mx

$$t = \frac{L}{c} \tag{4}$$

Where:

t: is the transit time

L: is the optical length of the fiber under test

c: is the vacuum speed of light

The Figure 3 shows some pictures of the system implemented.

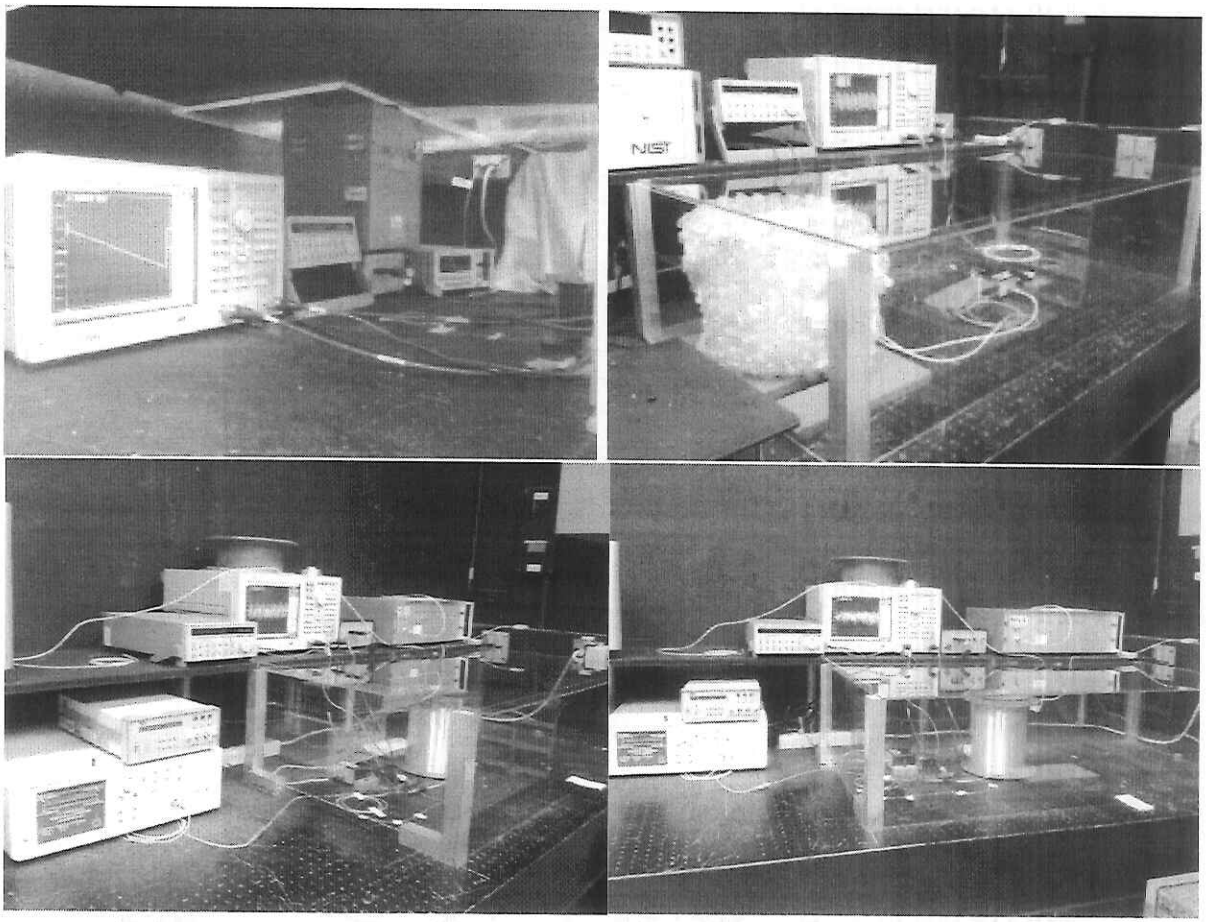

Figure 3 Length characterization system photographs.

km 4.5 Carretera a Los Cués, El Marqués, Querétaro, C.P. 76246, México

Tel. (442) 211-0500 al 04 www.cenam.mx

Traceability

All the measurements made with the length characterization system of CENAM have traceability to the S.I. unities according to the following chart:

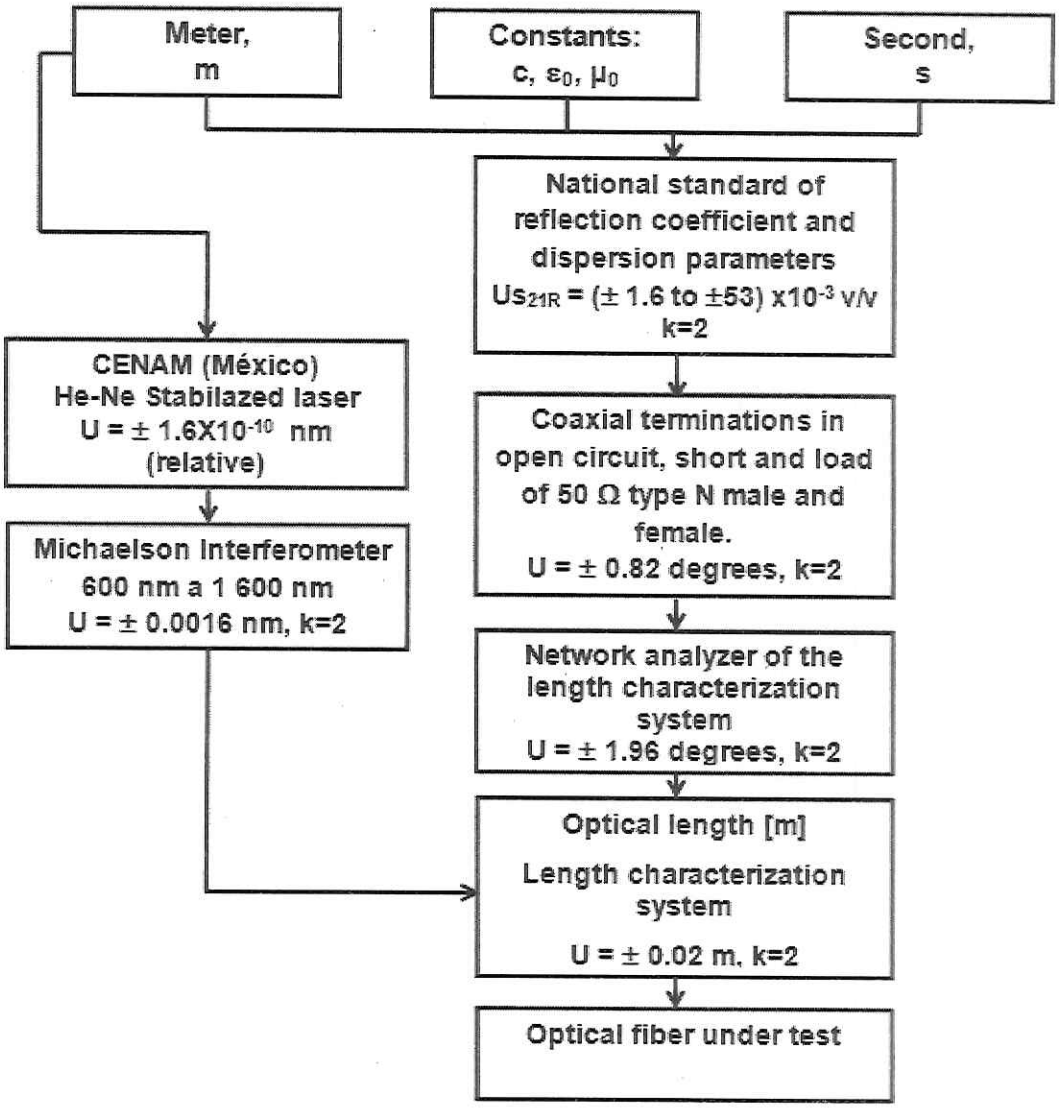

Figure 4 Traceability chart of optical length.

km 4.5 Carretera a Los Cués, El Marqués, Querétaro, C.P. 76246, México

Tel. (442) 211-0500 al 04 www.cenam.mx

Results

For this comparison we measured two different artifacts from KRISS. The artifacts were two spools of step-index single mode optical fiber (SMF) with approximately 3 km and 13 km, respectively. Both ends of each artifact were spliced to FC/PC connector cables of about 1.5 m of length.

Prior to the calibration, the reference standards, the equipment and the artifact under test were subjected to a passive process of conditioning and stabilization to the ambient conditions of the laboratory.

Each artifact was measured 25 times from both ends at 3 different wavelengths: 1 310 nm, 1 550 nm and 1 625 nm and during the measurement process, the artifact under test was placed inside a plastic cabinet fitted with a temperature sensor and a humidity sensor to measure its variations independently. The variations in temperature did not exceed ± 0.6 ºC and the variations for the humidity did not exceed ± 10%.

The table 1 shows the optical length results for the artifact 1 at 1 310 nm, 1 550 nm and 1 625 nm. The table 2 shows the transit time results for the artifact 1 for the same wavelengths. The results of CENAM for each artifact are in the "Mean" column.

Table 1. Optical length of the artifact 1.

Wavelength	Side A	Side B	Mean
1 310 nm	(3250.14 ± 0.04) m (k=2)	(3250.14 ± 0.04) m (k=2)	(3250.14 ± 0.04) m (k=2)
1 550 nm	(3251.54 ± 0.04) m (k=2)	(3251.55 ± 0.04) m (k=2)	(3251.54 ± 0.04) m (k=2)
1 625 nm	(3252.59 ± 0.04) m (k=2)	(3252.60 ± 0.04) m (k=2)	(3252.60 ± 0.04) m (k=2)

Table 2. Transit time of the artifact 1.

Wavelength	Side A	Side B	Mean
1 310 nm	(15828.30 ± 0.16) ns (k=2)	(15828.30 ± 0.16) ns (k=2)	(15828.30 ± 0.16) ns (k=2)
1 550 nm	(15835.13 ± 0.16) ns (k=2)	(15835.14 ± 0.16) ns (k=2)	(15835.13 ± 0.16) ns (k=2)
1 625 nm	(15840.25 ± 0.16) ns (k=2)	(15840.25 ± 0.16) ns (k=2)	(15840.25 ± 0.16) ns (k=2)

km 4.5 Carretera a Los Cués, El Marqués, Querétaro, C.P. 76246, México

Tel. (442) 211-0500 al 04 www.cenam.mx

The table 3 shows the optical length results for the artifact 2 at 1 310 nm, 1 550 nm and 1 625 nm. The table 4 shows the transit time results for the artifact 2 for the same wavelengths.

Table 3. Optical length of the artifact 2.

Wavelength	Side A	Side B	Mean
1 310 nm	(13305.87 ± 0.04) m (k=2)	(13305.88 ± 0.04) m (k=2)	(13305.88 ± 0.04) m (k=2)
1 550 nm	(13311.77 ± 0.04) m (k=2)	(13311.76 ± 0.04) m (k=2)	(13311.77 ± 0.04) m (k=2)
1 625 nm	(13316.08 ± 0.04) m (k=2)	(13316.07 ± 0.04) m (k=2)	(13316.07 ± 0.04) m (k=2)

Table 4. Transit time of the artifact 2.

Wavelength	Side A	Side B	Mean
1 310 nm	(64800.07 ± 0.20) ns (k=2)	(64800.12 ± 0.20) ns (k=2)	(64800.09 ± 0.20) ns (k=2)
1 550 nm	(64828.79 ± 0.20) ns (k=2)	(64828.77 ± 0.20) ns (k=2)	(64828.78 ± 0.20) ns (k=2)
1 625 nm	(64849.80 ± 0.20) ns (k=2)	(64849.70 ± 0.20) ns (k=2)	(64849.75 ± 0.20) ns (k=2)

These results are at 23 °C and include the corrections for temperature and wavelength mismatch. These corrections were made from the temperature sensitivity coefficient C_{Trel} =(7.15 ± 0.25)x10^{-03} m/°C·km and the wavelength sensitivity coefficients $C_{\lambda 1\ 310}$=(0.397 ±0.19)x10^{-03} m/nm·km and $C_{\lambda 1\ 550}$=(3.22 ±0.10)x10^{-03} m/nm·km estimated by some previous tests made to one Corning SMF28e single mode optical fiber spool at different temperatures in the range of 21.6 °C to 25.1 °C and different optical signal wavelengths in the range of 1530 nm to 1552.2 nm and 1301 nm at 3111 nm.[1]

The optical length of the artifacts were calculated assuming a group index of N = 1.46000.

Also note that all the laser sources used were previously characterized prior to the measurements. The values of the central wavelength of the sources are shown in the table 5

[1] J. C. Bermudez, "Development of an optical fiber standard for OTDRs distance scale calibration", Proc. SPIE 6046, Fifth Symposium Optics in Industry, México (2006)

km 4.5 Carretera a Los Cués, El Marqués, Querétaro, C.P. 76246, México

Tel. (442) 211-0500 al 04 www.cenam.mx

Table 5. Wavelength values and uncertainties

Nominal Wavelength λ_{NOM}	Central wavelength. λ_{MED}	Wavelength Uncertainty [k=2]
1 310 nm	1 309.896 31 nm	0.002 1 nm
1 550 nm	1550.014 56 nm	0.002 2 nm
1 625 nm	1 629.47 nm	0.09 nm

The results of the measurements subject to this inform are expressed in terms of the International System of Units and therefore in accordance with the General System of Units of Measure in Mexico. The national measurement standards are the references with which these units are experimentally carried out in Mexico.

Uncertainty

The following sources of uncertainty are considered in estimating the artifacts length: signal phase (ϕ_{sig}), reference phase (ϕ_{ref}), modulation frequency (f_i), temperature T, and wavelength λ. The uncertainty of the modulation frequency includes contributions due to resolution, stability and calibration of the network analyzer. The values for m_i must be unambiguously determined and therefore it is considered with zero uncertainty. According to the model described by equation 2, the combined standard uncertainty, assuming the null correlations between variables is:

$$u_L^2 = \left(\frac{c}{N \cdot f \cdot 2\pi}\right)^2 u_{phase}^2 + \left(-\frac{\left(\phi_{sig} - \phi_{ref} + m \cdot 2\pi\right) \cdot c}{N \cdot f^2 \cdot 2\pi}\right)^2 u_{freq}^2 + u_{LT}^2 + u_{L\lambda}^2 + u_{rep}^2 \qquad (5)$$

Were:

u_{phase}^2: Is the phase uncertainty and includes the contributions for the signal phase ($u\phi_{sig}$), reference phase ($u\phi_{ref}$), phase resolution ($u\phi_{res}$) and phase calibration ($u\phi_{cal}$)

u_{freq}^2: Is the frequency uncertainty and includes the contributions for the frequency stability (uf_{st}) and the frequency resolution (uf_{res})

u_{LT}^2: Is the uncertainty for the temperature mismatch correction

$u_{L\lambda}^2$: Is the uncertainty for the wavelength mismatch correction

u_{rep}^2: Is the uncertainty for the measurements reproducibility

The table 6 shows in detail the uncertainty budget for a single measurement at a frequency f_i.

km 4.5 Carretera a Los Cués, El Marqués, Querétaro, C.P. 76246, México

Tel. (442) 211-0500 al 04 www.cenam.mx

Table 6. Uncertainty budget for a single measurement at a frequency f_i

Source of Uncertainty	Standard Uncertainty	Type	Distribution	Sensibility coefficients	Contribution	Degree of freedom
Signal phase repeatability	$u\phi_{sig}$	A	Normal	$\frac{c}{N2\pi f}$	$\frac{s}{\sqrt{n}}$	60
Reference phase repeatability	$u\phi_{ref}$	A	Normal	$\frac{c}{N2\pi f}$	$\frac{s}{\sqrt{n}}$	60
Phase resolution	$u\phi_{res}$	B	Uniform	$\frac{c}{N2\pi f}$	$\frac{\phi_{resolution}}{\sqrt{12}}$	60
Phase calibration	$u\phi_{cal}$	B	Normal	$\frac{c}{N2\pi f}$	$\frac{f_{\ calibration}}{\sqrt{12}}$	60
Frequency resolution	uf_{res}	B	Uniform	$-\frac{\Delta\emptyset c}{2\pi N f^2}$	$\frac{f_{\ resolution}}{\sqrt{12}}$	60
Frequency stability	uf_{st}	B	Uniform	$-\frac{\Delta\emptyset c}{2\pi N f^2}$	$\frac{f_{stability}}{\sqrt{12}}$	60
Temperature mismatch correction	u_{LT}^2	B	Normal	1	u_{LT}	10
Wavelength mismatch correction	$u_{L\lambda}^2$	B	Normal	1	$u_{L\lambda}$	100
Measurement reproducibility	u_{rep}^2	A	Normal	1	$\frac{s_L}{\sqrt{n}}$	49
Combined standard uncertainty	--	--	Normal	$u_c = \sqrt{\sum_i [c_i \cdot u(x_i)]^2}$		>100
Expanded uncertainty	$U=u_{c.k}\ (m)$					

Table 7 shows the uncertainty budget for the artifact 1 at 1 550 nm at a frequency of 50 MHz

km 4.5 Carretera a Los Cués, El Marqués, Querétaro, C.P. 76246, México

Tel. (442) 211-0500 al 04 www.cenam.mx

Table 7 Uncertainty budget of for the artifact 1 at 1 550 nm at a frequency of 50 MHz

Source of Uncertainty	Original Uncertainty	Type	Distribution	Standard Uncertainty	Sensibility coefficients	Contribution	Degree of freedom
Signal phase repeatability	2.45E-05	A	Normal	2.45E-05	6.54E-01	1.60E-05	60
Reference phase repeatability	2.45E-05	A	Normal	2.45E-05	6.54E-01	1.60E-05	60
Phase resolution	1.75E-04	B	Uniform	5.04E-05	6.54E-01	3.29E-05	60
Phase calibration	3.42E-02	B	Normal	3.42E-02	6.54E-01	2.24E-02	60
Frequency resolution	1.00E00	B	Uniform	2.89E-01	6.51E-05	1.88E-05	60
Frequency stability	5.00E-06	B	Uniform	1.44E-06	6.51E-05	9.39E-11	60
Temperature mismatch correction	3.51E-03	B	Normal	3.51E-03	1	3.51E-03	10
Wavelength mismatch correction	5.09E-07	B	Normal	5.09E-07	1	5.09E-07	100
Measurement reproducibility	9.54E-04	A	Normal	9.54E-04	1	9.54E-04	49
Combined standard uncertainty	--	--	--	Normal	u_c=2.3E-02		>100
Expanded uncertainty	$U=u_c k$ U= (2.3E-02) (2)= 4.5E-02 m (k=2)						

km 4.5 Carretera a Los Cués, El Marqués, Querétaro, C.P. 76246, México

Tel. (442) 211-0500 al 04 www.cenam.mx

The uncertainty of the measurement was obtained by multiplying the combined standard uncertainty by a coverage factor k = 2, which corresponds to a confidence level of approximately 95% under the assumption that the probability density function of the measurand is normal.

The repeatability source of uncertainty is contained in the measurement reproducibility source of the uncertainty budget.

The measurement uncertainty was estimated according to NMX-CH-140-IMNC 2002 Guideline for the Expression of Uncertainty in Measurements, equivalent to JCGM 100: 2008 (GUM 1995 with minor corrections) Evaluation of measurement data - Guide to the expression of uncertainty in measurement. BIPM. First edition - September 2008.

MSc. Zeus Efraín Ruíz Gutiérrez
Optics and Radiometry Metrologist
National Metrology Center of México (CENAM)

MSc. Carlos H. Matamoros Garcia
Optics and Radiometry Manager
National Metrology Center of México (CENAM)

km 4.5 Carretera a Los Cués, El Marqués, Querétaro, C.P. 76246, México

Tel. (442) 211-0500 al 04 www.cenam.mx

5. Results and Discussion

5.1. Artifact drift

Artifact drift was checked by the KRISS for round 1 and 3, and by the METAS for round 2. KRISS artifacts were delivered from the KRISS to one of the participating labs and were delivered back to the KRISS at the end of the rounds (for round 1 and 3). METAS artifacts were delivered from the METAS to one of the participating labs and were delivered back to the METAS at the end of the round (for round 2). The measurements to check the artifact drift were made before and after the rounds. Therefore, there were four data sets with KRISS and two data sets with METAS. Each data set has 6 data points, and they are 'fiber length' measured at 1310 nm, 1550 nm, and 1625 nm for two different artifacts.

Table 5-1-1 and 5-1-2 show the KRISS and the METAS artifacts drift check results, and the difference of fiber length measured were plotted in Fig. 5-1-1 and 5-1-2. From all the plots, we made a conclusion that there were no significant changes in the artifacts during the each round. Nevertheless, it was decided to add the uncertainty arising from this change in the overall uncertainty evaluation.

Table 5-1-1. KRISS Artifacts drift check results

	Artifact 1 fiber length (m) / Uncertainty (k=2) (m)			Artifact 2 fiber length (m) / Uncertainty (k=2) (m)			Date
	1310 nm	1550 nm	1625 nm	1310 nm	1550 nm	1625 nm	
1	3250.1274	3251.5361	3252.4821	13305.8634	13311.8005	13315.6851	2015-02-24
	0.0283	0.0283	0.0282	0.1097	0.1098	0.1100	
2	3250.1216	3251.5312	3252.4821	13305.9489	13311.8170	13315.6851	2016-03-15 2016-03-16
	0.0282	0.0282	0.0282	0.1097	0.1098	0.1100	
3	3250.1389	3251.5419	3252.4807	13305.9500	13311.8124	13315.6859	2017-02-03
	0.0446	0.0365	0.0282	0.1097	0.1098	0.1098	
4	3250.1230	3251.5314	3252.4491	13305.8172	13311.7725	13315.6859	2017-11-20
	0.0282	0.0283	0.0282	0.1100	0.1423	0.1098	
A*	0.0050	0.0031	0.0095	0.0383	0.0128	0.0002	

A*: Artifact drift value: (Max –Min)/(2×sqrt(3))

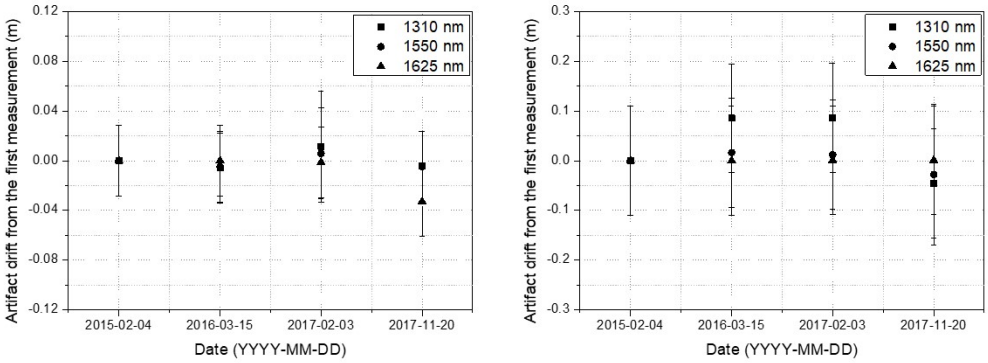

Fig. 5-1-1. Artifact drift for the KRISS artifact 1 and 2

Table 5-1-2. METAS Artifacts drift check results

	Artifact 1 fiber length (m) / Uncertainty (k=2) (m)			Artifact 2 fiber length (m) / Uncertainty (k=2) (m)			Date
	1310 nm	1550 nm	1625 nm	1310 nm	1550 nm	1625 nm	
1	2346.6120	2347.5350	2348.1800	12104.5400	12109.1700	12112.4400	2015-03-27
	0.0180	0.0170	0.0170	0.0900	0.0900	0.0900	
2	2346.6120	2347.5240	2348.1760	12104.5400	12109.1300	12112.4300	2016-05-19
	0.0180	0.0160	0.0170	0.0900	0.0900	0.0900	
A*	0	0.0031	0.0012	0	0.0115	0.0029	

A*: Artifact drift value: (Max –Min)/(2×sqrt(3))

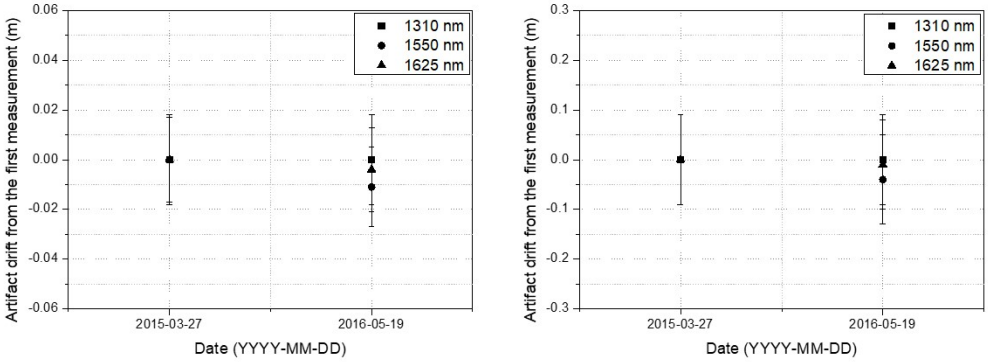

Fig. 5-1-2 Artifact drift for the METAS artifact 1 and 2

5.2. Difference from pilot

The difference Δ_i of fiber lengths (m) between the participant *i* and the pilot (*i*=0) is calculated by

$$\Delta_i = C_i - C_0 \tag{5-2-1}$$

and its standard uncertainty $u(\Delta_i)$ by

$$u(\Delta_i) = \sqrt{\left(u^2(C_i) + u^2(C_0) + u_{add}^2(C_i)\right)} \tag{5-2-2}$$

The additional uncertainty due to non-ideal characteristics of the artifacts is denoted by $u_{add}(C_i)$. This uncertainty was calculated from the maximum difference between measurements taken at the beginning and end of the round, which is expressed in Eq. (5-2-3) for round 1&3 and Eq. (5-2-4) for round 2.

$$u_{add}(C_i) = \left(Max(C_{KRISS}) - Min(C_{KRISS})\right) / \left(2\sqrt{3}\right) \quad \text{for round 1 \& 3} \tag{5-2-3}$$

$$u_{add}(C_i) = \left(Max(C_{METAS}) - Min(C_{METAS})\right) / \left(2\sqrt{3}\right) \quad \text{for round 2} \tag{5-2-4}$$

, where C_{KRISS} is the values measured by KRISS for KRISS artifacts and C_{METAS} is the values measured by METAS for METAS artifacts. These values can be also referred in Table 5-1-1 for Round 1 and 3 and in Table 5-1-2 for Round 2. The fiber length differences between the participants and the pilot for Round 1 and 3 are tabulated in Table 5-2-1, Table 5-2-2, Table 5-2-3, Table 5-2-4, Table 5-2-5, and Table 5-2-6. They are plotted in Fig. 5-2-1, Fig. 5-2-2, and Fig. 5-2-3 with their corresponding standard uncertainties. The fiber length differences between the participants and the pilot for Round 2 are tabulated in Table 5-2-7, Table 5-2-8, Table 5-2-9, Table 5-2-10, Table 5-2-11 and Table 5-2-12. They are also plotted in Fig. 5-2-4, Fig. 5-2-5, and Fig. 5-2-6 with their corresponding standard uncertainties.

Table 5-2-1. Difference from Pilot (KRISS artifact 1, Round 1&3, 1310 nm).

Participant	C_i	$u(C_i)$	$u_{add}(C_i)$	Δ_i	$u(\Delta_i)$
KRISS	3250.1274	0.0142	0.0050	0.0000	0.0150
NMIJ	3250.1470	0.0244		0.0196	0.0286
NMC	3250.1250	0.0104		-0.0024	0.0183
NMISA	3250.1590	0.0370		0.0316	0.0399
NIS	3250.0460	0.0280		-0.0814	0.0318
CENAM	3250.1400	0.0200		0.0126	0.0250

Table 5-2-2. Difference from Pilot (KRISS artifact 2, Round 1&3, 1310 nm).

Participant	C_i	$u(C_i)$	$u_{add}(C_i)$	Δ_i	$u(\Delta_i)$
KRISS	13305.8634	0.0549	0.0383	0.0000	0.0669
NMIJ	13305.9700	0.0998		0.1066	0.1202
NMC	13305.8580	0.0260		-0.0054	0.0718
NMISA	13305.9500	0.0900		0.0866	0.1122
NIS	13305.7910	0.0580		-0.0724	0.0886
CENAM	13305.8800	0.0200		0.0166	0.0698

Table 5-2-3. Difference from Pilot (KRISS artifact 1, Round 1&3, 1550 nm).

Participant	C_i	$u(C_i)$	$u_{add}(C_i)$	Δ_i	$u(\Delta_i)$
KRISS	3251.5361	0.0142	0.0031	0.0000	0.0145
NMIJ	3251.5440	0.0244		0.0079	0.0284
NMC	3251.5300	0.0104		-0.0061	0.0178
NMISA	3251.5860	0.0370		0.0499	0.0397
NIS	3251.5620	0.0150		0.0259	0.0209
CENAM	3251.5400	0.0200		0.0039	0.0247

Table 5-2-4. Difference from Pilot (KRISS artifact 2, Round 1&3, 1550 nm).

Participant	C_i	$u(C_i)$	$u_{add}(C_i)$	Δ_i	$u(\Delta_i)$
KRISS	13311.8005	0.0549	0.0128	0.0000	0.0564
NMIJ	13311.8500	0.0999		0.0495	0.1147
NMC	13311.7620	0.0260		-0.0385	0.0621
NMISA	13311.8900	0.0900		0.0895	0.1062
NIS	13311.9070	0.0350		0.1065	0.0664
CENAM	13311.7700	0.0200		-0.0305	0.0598

Table 5-2-5. Difference from Pilot (KRISS artifact 1, Round 1&3, 1625 nm).

Participant	C_i	$u(C_i)$	$u_{add}(C_i)$	Δ_i	$u(\Delta_i)$
KRISS	3252.4821	0.0141	0.0095	0.0000	0.0170
NMIJ	3252.4850	0.0244		0.0029	0.0297
NMC					
NMISA	3252.4960	0.0370		0.0139	0.0407
NIS	3252.5050	0.0180		0.0229	0.0248
CENAM	3252.6000	0.0200		0.1179	0.0263

Table 5-2-6. Difference from Pilot (KRISS artifact 2, Round 1&3, 1625 nm).

Participant	C_i	$u(C_i)$	$u_{add}(C_i)$	Δ_i	$u(\Delta_i)$
KRISS	13315.6851	0.0550	0.0002	0.0000	0.0550
NMIJ	13315.7400	0.0999		0.0549	0.1140
NMC					
NMISA	13315.6900	0.0900		0.0049	0.1055
NIS	13315.8010	0.0390		0.1159	0.0674
CENAM	13316.0700	0.0200		0.3849	0.0585

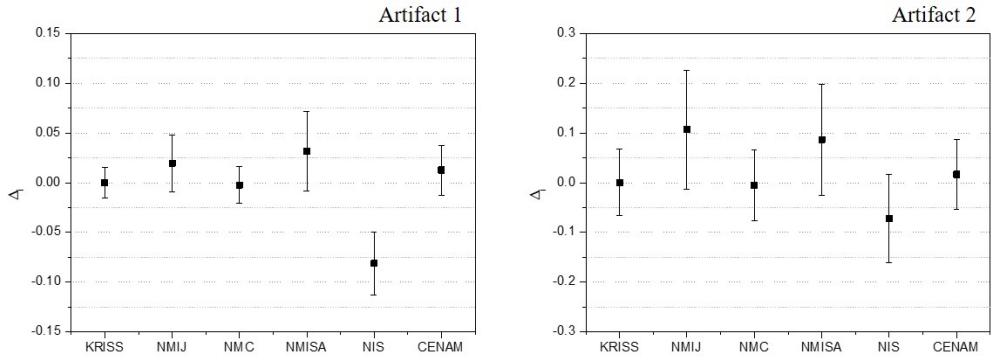

Fig. 5-2-1. Length difference between participants and the pilot at 1310 nm for round 1 and 3.

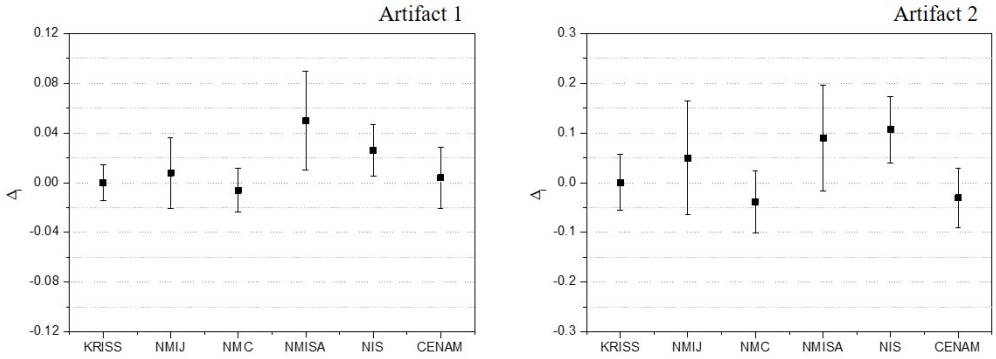

Fig. 5-2-2. Length difference between participants and the pilot at 1550 nm for round 1 and 3.

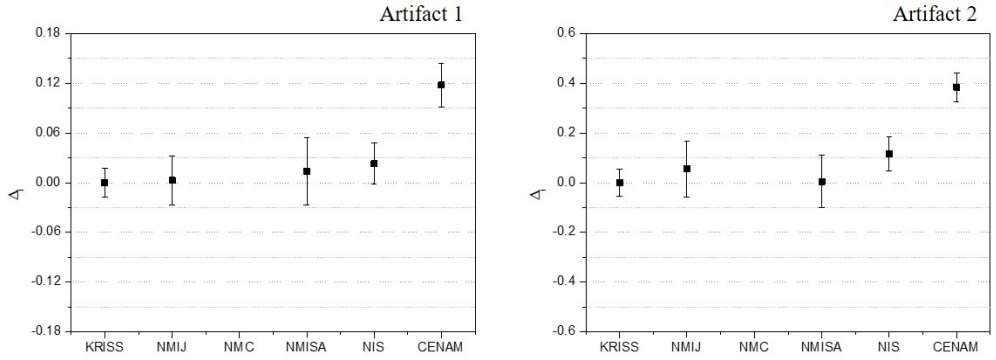

Fig. 5-2-3. Length difference between participants and the pilot at 1625 nm for round 1 and 3.

Table 5-2-7. Difference from Pilot (METAS artifact 1, Round 2, 1310 nm).

Participant	C_i	$u(C_i)$	$u_{add}(C_i)$	Δ_i	$u(\Delta_i)$
METAS	2346.6120	0.0090	0.0000	0.0170	0.0151
LNE	2346.6200	0.2950		0.0250	0.2952
VNIIOFI	2346.6010	0.0295		0.0060	0.0319
KRISS	2346.5950	0.0121		0.0000	0.0121

Table 5-2-8. Difference from Pilot (METAS artifact 2, Round 2, 1310 nm).

Participant	C_i	$u(C_i)$	$u_{add}(C_i)$	Δ_i	$u(\Delta_i)$
METAS	12104.5400	0.0450	0.0000	0.0810	0.0739
LNE	12104.5000	1.5000		0.0410	1.5011
VNIIOFI	12104.5460	0.0320		0.0870	0.0668
KRISS	12104.4590	0.0586		0.0000	0.0586

Table 5-2-9. Difference from Pilot (METAS artifact 1, Round 2, 1550 nm).

Participant	C_i	$u(C_i)$	$u_{add}(C_i)$	Δ_i	$u(\Delta_i)$
METAS	2347.5350	0.0085	0.0032	-0.0050	0.0140
LNE	2347.4100	0.2950		-0.1300	0.2952
VNIIOFI	2347.5230	0.0295		-0.0170	0.0315
KRISS	2347.5400	0.0106		0.0000	0.0111

Table 5-2-10. Difference from Pilot (METAS artifact 2, Round 2, 1550 nm).

Participant	C_i	$u(C_i)$	$u_{add}(C_i)$	Δ_i	$u(\Delta_i)$
METAS	12109.1700	0.0450	0.0115	0.0810	0.0747
LNE	12108.4000	1.5000		-0.6890	1.5012
VNIIOFI	12109.1840	0.0330		0.0950	0.0681
KRISS	12109.0890	0.0585		0.0000	0.0596

Table 5-2-11. Difference from Pilot (METAS artifact 1, Round 2, 1625 nm).

Participant	C_i	$u(C_i)$	$u_{add}(C_i)$	Δ_i	$u(\Delta_i)$
METAS	2348.1800	0.0085	0.0012	0.0050	0.0136
LNE					
VNIIOFI	2348.1680	0.0300		-0.0070	0.0318
KRISS	2348.1750	0.0106		0.0000	0.0107

Table 5-2-12. Difference from Pilot (METAS artifact 2, Round 2, 1625 nm).

Participant	C_i	$u(C_i)$	$u_{add}(C_i)$	Δ_i	$u(\Delta_i)$
METAS	12112.4350	0.0450	0.0029	0.0840	0.0674
LNE					
VNIIOFI	12112.4550	0.0335		0.0990	0.0603
KRISS	12112.3560	0.0501		0.0000	0.0502

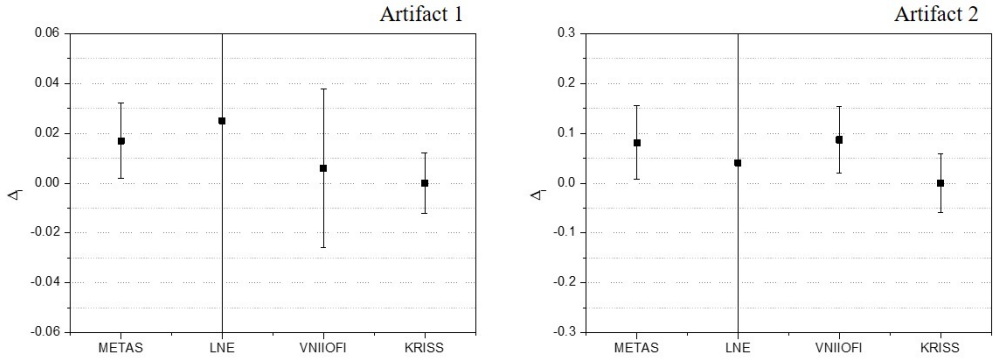

Fig. 5-2-4. Length difference between participants and the pilot at 1310 nm for round 2.

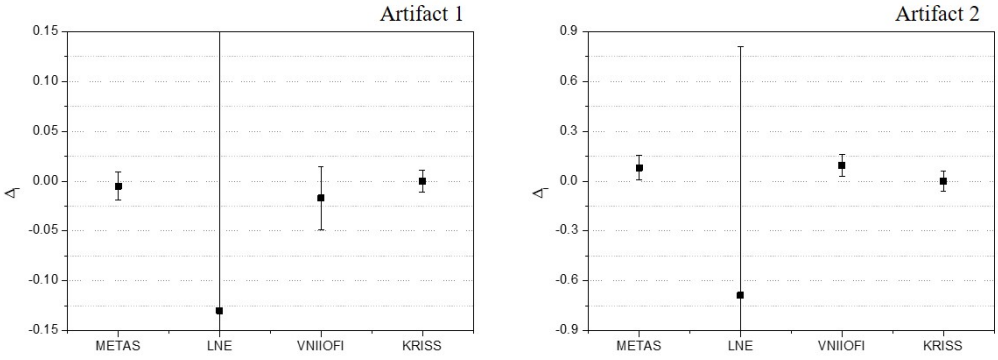

Fig. 5-2-5. Length difference between participants and the pilot at 1550 nm for round 2.

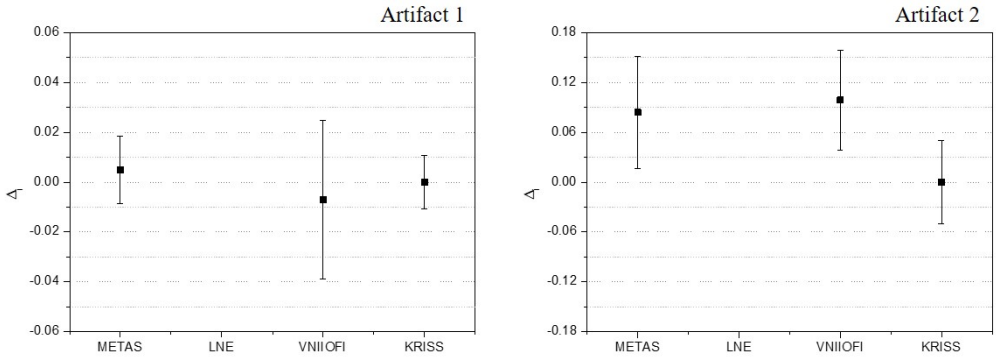

Fig. 5-2-6. Length difference between participants and the pilot at 1625 nm for round 2.

5.3. Comparison reference value

In calculation of comparison reference value, that is SCRV (supplementary comparison reference value), the cut-off value is determined as follows.

$$u_{cut-off} = \text{average}\left\{u\left(C_i\right)\right\} \quad \text{for} \quad u\left(C_i\right) \le \text{median}\left\{u\left(C_i\right)\right\} \quad (i = 0 \text{ to } N) \tag{5-3-1}$$

, where N is the number of participants excluding the pilot.

Then the reported uncertainty of each NMI is adjusted by the cut-off to be

$$\begin{matrix} u_{adj}(C_i) = u\left(C_i\right) \\ u_{adj}(C_i) = u_{cut-off} \end{matrix} \quad \text{for} \quad \begin{matrix} u\left(C_i\right) \ge u_{cut-off} \\ u\left(C_i\right) < u_{cut-off} \end{matrix} \quad (i = 0 \text{ to } N) \tag{5-3-2}$$

The uncertainty of the difference Δ_i after applying the cut-off is also adjusted to be

$$u_{adj}(\Delta_i) = \sqrt{u_{adj}^2(C_i) + u_T^2(\Delta_i)} \tag{5-3-3}$$

, where the transfer uncertainty component can be denoted by

$$u_T(\Delta_i) = \sqrt{u^2(\Delta_i) - u^2(C_i)} \tag{5-3-4}$$

The weights w_i is then calculated by

$$w_i = u_{adj}^{-2}(\Delta_i) / \sum_{j=0}^{N} u_{adj}^{-2}(\Delta_j) \tag{5-3-5}$$

Now the SCRV, Δ_{SCRV} is determined by

$$\Delta_{\text{SCRV}} = \sum_{i=0}^{N} w_i \Delta_i \tag{5-3-6}$$

The uncertainty of the SCRV is given by

$$u\left(\Delta_{\text{SCRV}}\right) = \sqrt{\sum_{i=0}^{N} \frac{u^2(\Delta_i)}{u_{adj}^4(\Delta_i)}} \Bigg/ \sum_{i=0}^{N} u_{adj}^{-2}(\Delta_i) \tag{5-3-7}$$

The expanded uncertainty of the SCRV is $U(\Delta_{\text{SCRV}}) = k \cdot u(\Delta_{\text{SCRV}})$. Here, a coverage factor of $k = 2$ is used at approximately the 95 % confidence level.

The calculated values are summarized in Table 5-3-1 to Table 5-3-12.

Table 5-3-1. SCRV and its uncertainty (round 1 and 3 with KRISS artifact 1 at 1310 nm)

$u_{cut-off}$ =0.0149

Participant	Δ_i	$u(\Delta_i)$	$u_{adj}(C_i)$	$u_{adj}(\Delta_i)$	w_i	Δ_{SCRV}	$U(\Delta_{\mathrm{SCRV}})$
KRISS	0.0000	0.0150	0.0149	0.0157	0.3787	-0.0021	0.0166
NMIJ	0.0196	0.0286	0.0244	0.0286	0.1135		
NMC	-0.0024	0.0183	0.0149	0.0211	0.2086		
NMISA	0.0316	0.0399	0.0370	0.0399	0.0583		
NIS	-0.0814	0.0318	0.0280	0.0318	0.0921		
CENAM	0.0126	0.0250	0.0200	0.0250	0.1487		

Table 5-3-2. SCRV and its uncertainty (round 1 and 3 with KRISS artifact 2 at 1310 nm)

$u_{cut-off}$ =0.0336

Participant	Δ_i	$u(\Delta_i)$	$u_{adj}(C_i)$	$u_{adj}(\Delta_i)$	w_i	Δ_{SCRV}	$U(\Delta_{\mathrm{SCRV}})$
KRISS	0.0000	0.0669	0.0549	0.0669	0.2608	0.0082	0.0453
NMIJ	0.1066	0.1202	0.0998	0.1202	0.0809		
NMC	-0.0054	0.0718	0.0336	0.0749	0.2083		
NMISA	0.0866	0.1122	0.0900	0.1122	0.0929		
NIS	-0.0724	0.0886	0.0580	0.0886	0.1489		
CENAM	0.0166	0.0698	0.0336	0.0749	0.2083		

Table 5-3-3. SCRV and its uncertainty (round 1 and 3 with KRISS artifact 1 at 1550 nm)

$u_{cut-off}$ =0.0132

Participant	Δ_i	$u(\Delta_i)$	$u_{adj}(C_i)$	$u_{adj}(\Delta_i)$	w_i	Δ_{SCRV}	$U(\Delta_{\mathrm{SCRV}})$
KRISS	0.0000	0.0145	0.0142	0.0145	0.3611	0.0069	0.0148
NMIJ	0.0079	0.0284	0.0244	0.0284	0.0943		
NMC	-0.0061	0.0178	0.0132	0.0196	0.1976		
NMISA	0.0499	0.0397	0.0370	0.0397	0.0481		
NIS	0.0259	0.0209	0.0150	0.0209	0.1745		
CENAM	0.0039	0.0247	0.0200	0.0247	0.1244		

Table 5-3-4. SCRV and its uncertainty (round 1 and 3 with KRISS artifact 2 at 1550 nm)

$u_{cut-off}$ =0.0270

Participant	Δ_i	$u(\Delta_i)$	$u_{adj}(C_i)$	$u_{adj}(\Delta_i)$	w_i	Δ_{SCRV}	$U(\Delta_{\mathrm{SCRV}})$
KRISS	0.0000	0.0564	0.0549	0.0564	0.2582	0.0149	0.0395
NMIJ	0.0495	0.1147	0.0999	0.1147	0.0624		
NMC	-0.0385	0.0621	0.0270	0.0625	0.2101		
NMISA	0.0895	0.1062	0.0900	0.1062	0.0728		
NIS	0.1065	0.0664	0.0350	0.0664	0.1864		
CENAM	-0.0305	0.0598	0.0270	0.0625	0.2101		

Table 5-3-5. SCRV and its uncertainty (round 1 and 3 with KRISS artifact 1 at 1625 nm)

$u_{cut-off}$ =0.0174

Participant	Δ_i	$u(\Delta_i)$	$u_{adj}(C_i)$	$u_{adj}(\Delta_i)$	w_i	Δ_{SCRV}	$U(\Delta_{\mathrm{SCRV}})$
KRISS	0.0000	0.0170	0.0141	0.0170	0.4178	0.0266	0.0177
NMIJ	0.0029	0.0297	0.0244	0.0297	0.1367		
NMC							
NMISA	0.0139	0.0407	0.0370	0.0407	0.0729		
NIS	0.0229	0.0248	0.0180	0.0248	0.1972		
CENAM	0.1179	0.0263	0.0200	0.0263	0.1754		

Table 5-3-6. SCRV and its uncertainty (round 1 and 3 with KRISS artifact 2 at 1625 nm)

$u_{cut-off}$ =0.0295

Participant	Δ_i	$u(\Delta_i)$	$u_{adj}(C_i)$	$u_{adj}(\Delta_i)$	w_i	Δ_{SCRV}	$U(\Delta_{\mathrm{SCRV}})$
KRISS	0.0000	0.0550	0.0550	0.0550	0.3394	0.1324	0.0497
NMIJ	0.0549	0.1140	0.0999	0.1140	0.0789		
NMC							
NMISA	0.0049	0.1055	0.0900	0.1055	0.0923		
NIS	0.1159	0.0674	0.0390	0.0674	0.2258		
CENAM	0.3849	0.0585	0.0295	0.0624	0.2636		

Table 5-3-7. SCRV and its uncertainty (round 2 with METAS artifact 1 at 1310 nm)

$u_{cut-off}$ =0.0106

Participant	Δ_i	$u(\Delta_i)$	$u_{adj}(C_i)$	$u_{adj}(\Delta_i)$	w_i	Δ_{SCRV}	$U(\Delta_{\mathrm{SCRV}})$
METAS	0.0170	0.0151	0.0106	0.0161	0.3315	0.0062	0.0165
LNE	0.0250	0.2952	0.2950	0.2952	0.0010		
VNIIOFI	0.0060	0.0319	0.0295	0.0319	0.0840		
KRISS	0.0000	0.0121	0.0121	0.0121	0.5835		

Table 5-3-8. SCRV and its uncertainty (round 2 with METAS artifact 2 at 1310 nm)

$u_{cut-off}$ =0.0385

Participant	Δ_i	$u(\Delta_i)$	$u_{adj}(C_i)$	$u_{adj}(\Delta_i)$	w_i	Δ_{SCRV}	$U(\Delta_{\mathrm{SCRV}})$
METAS	0.0810	0.0739	0.0450	0.0739	0.2701	0.0480	0.0605
LNE	0.0410	1.5011	1.5000	1.5011	0.0007		
VNIIOFI	0.0870	0.0668	0.0385	0.0701	0.2999		
KRISS	0.0000	0.0586	0.0586	0.0586	0.4294		

Table 5-3-9. SCRV and its uncertainty (round 2 with METAS artifact 1 at 1550 nm)

$u_{cut-off}$ =0.0096

Participant	Δ_i	$u(\Delta_i)$	$u_{adj}(C_i)$	$u_{adj}(\Delta_i)$	w_i	Δ_{SCRV}	$U(\Delta_{\mathrm{SCRV}})$
METAS	-0.0050	0.0140	0.0096	0.0146	0.3376	-0.0030	0.0147
LNE	-0.1300	0.2952	0.2950	0.2952	0.0008		
VNIIOFI	-0.0170	0.0315	0.0295	0.0315	0.0727		
KRISS	0.0000	0.0111	0.0106	0.0111	0.5888		

Table 5-3-10. SCRV and its uncertainty (round 2 with METAS artifact 2 at 1550 nm)

$u_{cut-off}$ =0.0390

Participant	Δ_i	$u(\Delta_i)$	$u_{adj}(C_i)$	$u_{adj}(\Delta_i)$	w_i	Δ_{SCRV}	$U(\Delta_{\mathrm{SCRV}})$
METAS	0.0810	0.0747	0.0450	0.0747	0.2724	0.0500	0.0604
LNE	-0.6890	1.5012	1.5000	1.5012	0.0007		
VNIIOFI	0.0950	0.0681	0.0390	0.0712	0.2994		
KRISS	0.0000	0.0596	0.0585	0.0596	0.4275		

Table 5-3-11. SCRV and its uncertainty (round 2 with METAS artifact 1 at 1625 nm)

$u_{cut-off}$ =0.0096

Participant	Δ_i	$u(\Delta_i)$	$u_{adj}(C_i)$	$u_{adj}(\Delta_i)$	w_i	Δ_{SCRV}	$U(\Delta_{\mathrm{SCRV}})$
METAS	0.0050	0.0136	0.0096	0.0143	0.3329	0.0012	0.0148
LNE							
VNIIOFI	-0.0070	0.0318	0.0300	0.0318	0.0673		
KRISS	0.0000	0.0107	0.0106	0.0107	0.5997		

Table 5-3-12. SCRV and its uncertainty (round 2 with METAS artifact 2 at 1625 nm)

$u_{cut-off}$ =0.0393

Participant	Δ_i	$u(\Delta_i)$	$u_{adj}(C_i)$	$u_{adj}(\Delta_i)$	w_i	Δ_{SCRV}	$U(\Delta_{\mathrm{SCRV}})$
METAS	0.0840	0.0674	0.0450	0.0674	0.2549	0.0497	0.0561
LNE							
VNIIOFI	0.0990	0.0603	0.0393	0.0637	0.2853		
KRISS	0.0000	0.0502	0.0501	0.0502	0.4598		

The Chi-square value χ^2_{obs} is calculated by using Eq. (5-3-8) for consistency check.

$$\chi^2_{\mathrm{obs}} = \sum_{i=0}^{N} \frac{(\Delta_i - \Delta_{\mathrm{RV}})^2}{u^2_{adj}(\Delta_i)} \tag{5-3-8}$$

, where i = 0 represents the pilot lab, and the values are as shown in Table 5-3-13.

Table 5-3-13. Calculated Chi-square values.

Round	Artifact	Wavelength (nm)	$\nu\ (=N-1)$	χ^2_{obs}	$\chi^2_{0.05}(\nu)$
1 & 3	1	1310	4	7.880	9.488
		1550	4	2.680	9.488
		1625	3	15.286	7.815
	2	1310	4	2.048	9.488
		1550	4	3.817	9.488
		1625	3	24.145	7.815

Round	Artifact	Wavelength (nm)	$\nu\ (=N-1)$	χ^2_{obs}	$\chi^2_{0.05}(\nu)$
2	1	1310	2	0.719	5.991
		1550	2	0.475	5.991
		1625	1	0.149	3.841
	2	1310	2	1.180	5.991
		1550	2	1.517	5.991
		1625	1	1.839	3.841

The consistency is satisfied for all measurements except for the measurements at 1625 nm of round 1 and 3 because of $\chi^2_{\text{obs}} > \chi^2_{0.05}(\nu)$. It was found that the deviations from the KCRV for one participant are greater than 2 times their associated expanded uncertainties with k = 2. So, we discussed and agreed to assume that the values are outliers, even though the CCPR-G2 only addressed it when the deviation is larger than 3 times. Then, the Table 5-3-5 and Table 5-3-6 are modified as follows.

Table 5-3-14. SCRV and its uncertainty (round 1 and 3 with KRISS artifact 1 at 1625 nm)

$u_{cut-off}$ =0.0161

Participant	Δ_i	$u(\Delta_i)$	$u_{adj}(C_i)$	$u_{adj}(\Delta_i)$	w_i	Δ_{SCRV}	$U(\Delta_{\text{SCRV}})$
KRISS	0.0000	0.0170	0.0161	0.0077	0.1189	0.0079	0.0209
NMIJ	0.0029	0.0297	0.0244	0.0029	0.8315		
NMC							
NMISA	0.0139	0.0407	0.0370	0.0139	0.0362		
NIS	0.0229	0.0248	0.0180	0.0229	0.0133		
CENAM							

Table 5-3-15. SCRV and its uncertainty (round 1 and 3 with KRISS artifact 2 at 1625 nm)

$u_{cut-off}$ =0.0295

Participant	Δ_i	$u(\Delta_i)$	$u_{adj}(C_i)$	$u_{adj}(\Delta_i)$	w_i	Δ_{SCRV}	$U(\Delta_{\text{SCRV}})$
KRISS	0.0000	0.0550	0.0550	0.0550	0.4608	0.0420	0.0641
NMIJ	0.0549	0.1140	0.0999	0.1140	0.1072		
NMC							
NMISA	0.0049	0.1055	0.0900	0.1055	0.1253		
NIS	0.1159	0.0674	0.0390	0.0674	0.3067		
CENAM							

Now, the consistency is satisfied at 1625 nm of round 1 and 3 as follows.

Table 5-3-16. Recalculated Chi-square values for round 1and 3 at 1625 nm

Round	Artifact	Wavelength (nm)	ν (= $N-1$)	χ^2_{obs}	$\chi^2_{0.05}(\nu)$
1&3	1	1625	2	0.596	5.991
	2	1625	2	1.921	5.991

5.4. Degree of equivalence

The unilateral degree of equivalence (DoE) of the participant *i* is definded by

$$D_i = \Delta_i - \Delta_{\mathrm{SCRV}} \tag{5-4-1}$$

and the uncertainty of DoE is given by

$$u_i = \sqrt{u^2(\Delta_i) + u^2(\Delta_{\mathrm{SCRV}}) - 2\left[\frac{u^2(\Delta_i)}{u_{adj}^2(\Delta_i)} \Big/ \sum_{j=0}^{N} u_{adj}^{-2}(\Delta_i)\right]} \quad , \tag{5-4-2}$$

and its expanded uncertainty is written by

$$U_i = k u_i \tag{5-4-3}$$

with a coverage factor of $k = 2$ at the level of confidence of approximately 95 %.

Table 5-4-1, 5-4-2, 5-4-3, and 5-4-4 summarize the calculation results based on the solution 1 (removal of the outlier), and they are plotted in Fig. 5-4-1, Fig. 5-4-2, Fig. 5-4-3, Fig. 5-4-4, Fig. 5-4-5, and 5-4-6 with their corresponding expanded uncertainties.

Table 5-4-1. Unilateral degree of equivalence and its uncertainty of each participant for round 1 and 3 with KRISS artifact 1

Participant	1310 nm		1550 nm		1625 nm	
	D_i	U_i	D_i	U_i	D_i	U_i
KRISS	0.0021	0.0222	-0.0069	0.0213	-0.0079	0.0230
NMIJ	0.0217	0.0530	0.0009	0.0532	-0.0050	0.0519
NMC	-0.0003	0.0325	-0.0131	0.0315		
NMISA	0.0337	0.0769	0.0429	0.0770	0.0060	0.0761
NIS	-0.0793	0.0597	0.0189	0.0368	0.0150	0.0401
CENAM	0.0147	0.0451	-0.0031	0.0453	0.1100	0.0437

Table 5-4-2. Unilateral degree of equivalence and its uncertainty of each participant for round 1 and 3 with KRISS artifact 2.

Participant	1310 nm		1550 nm		1625 nm	
	D_i	U_i	D_i	U_i	D_i	U_i
KRISS	-0.0082	0.1030	-0.0149	0.1011	-0.0420	0.0711
NMIJ	0.0984	0.2246	0.0345	0.2284	0.0129	0.2121
NMC	-0.0136	0.1186	-0.0535	0.1163		
NMISA	0.0784	0.2074	0.0745	0.2111	-0.0371	0.1935
NIS	-0.0806	0.1551	0.0915	0.1260	0.0739	0.1056
CENAM	0.0084	0.1159	-0.0455	0.1135	0.3429	0.0895

Table 5-4-3. Unilateral degree of equivalence and its uncertainty of each participant for round 2 with METAS artifact 1

Participant	1310 nm		1550 nm		1625 nm	
	D_i	U_i	D_i	U_i	D_i	U_i
METAS	0.0108	0.0196	-0.0020	0.0180	0.0038	0.0178
LNE	0.0188	0.5899	-0.1270	0.5900		
VNIIOFI	-0.0002	0.0586	-0.0140	0.0589	-0.0082	0.0599
KRISS	-0.0062	0.0110	0.0030	0.0088	-0.0012	0.0084

Table 5-4-4. Unilateral degree of equivalence and its uncertainty of each participant for round 2 with METAS artifact 2.

Participant	1310 nm		1550 nm		1625 nm	
	D_i	U_i	D_i	U_i	D_i	U_i
METAS	0.0330	0.0859	0.0310	0.0871	0.0343	0.0845
LNE	-0.0070	3.0000	-0.7390	3.0000		
VNIIOFI	0.0390	0.0924	0.0450	0.0941	0.0493	0.0926
KRISS	-0.0480	0.0821	-0.0500	0.0830	-0.0497	0.0679

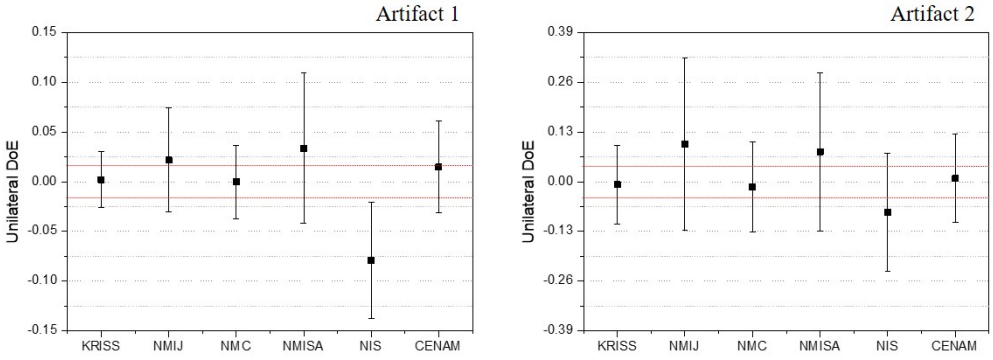

Fig. 5-4-1. Unilateral degree of equivalence and its uncertainty of each participant for round 1&3 with KRISS artifacts at 1310 nm. Red dotted lines indicate the uncertainty boundaries of SCRV.

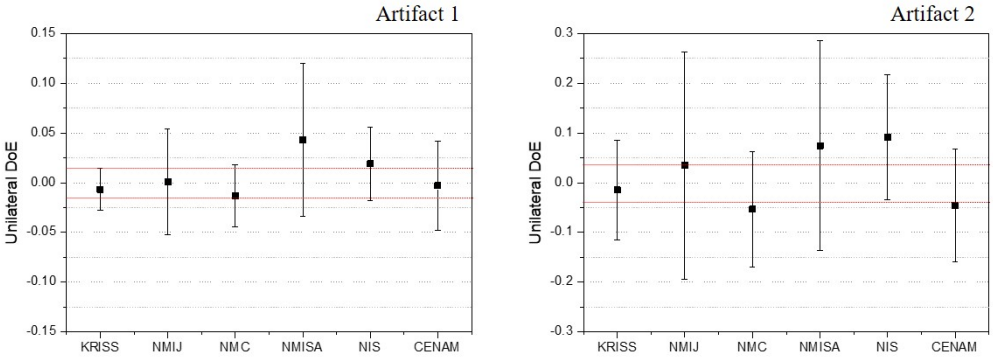

Fig. 5-4-2. Unilateral degree of equivalence and its uncertainty of each participant for round

1&3 with KRISS artifacts at 1550 nm. Red dotted lines indicate the uncertainty boundaries of SCRV.

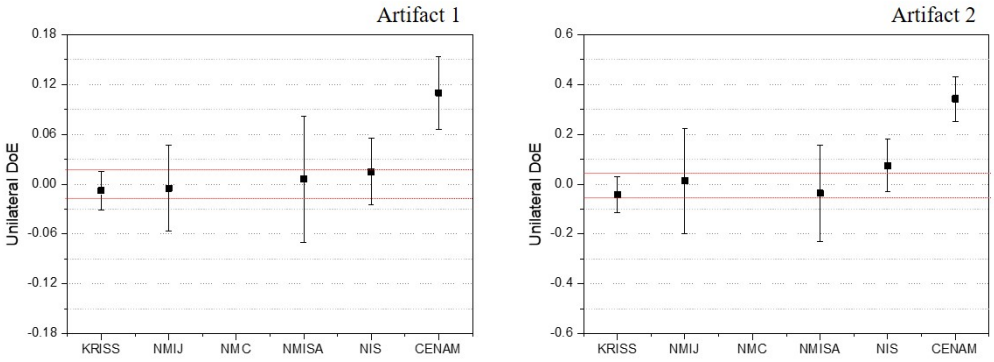

Fig. 5-4-3. Unilateral degree of equivalence and its uncertainty of each participant for round 1&3 with KRISS artifacts at 1625 nm. Red dotted lines indicate the uncertainty boundaries of SCRV.

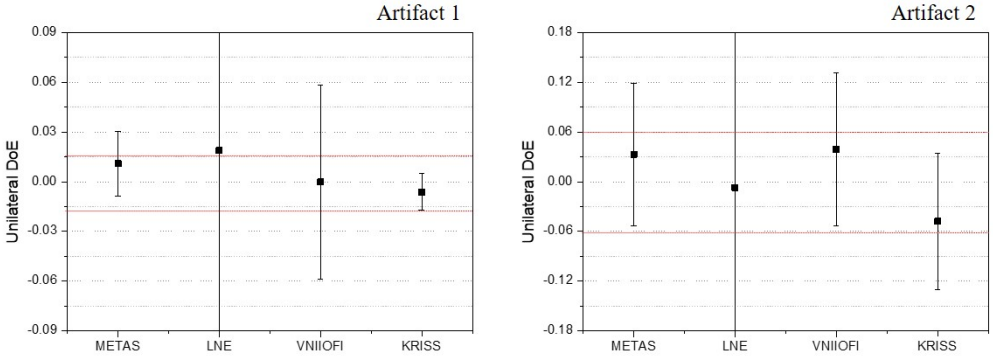

Fig. 5-4-4. Unilateral degree of equivalence and its uncertainty of each participant for round 2 with METAS artifacts at 1310 nm. Red dotted lines indicate the uncertainty boundaries of SCRV.

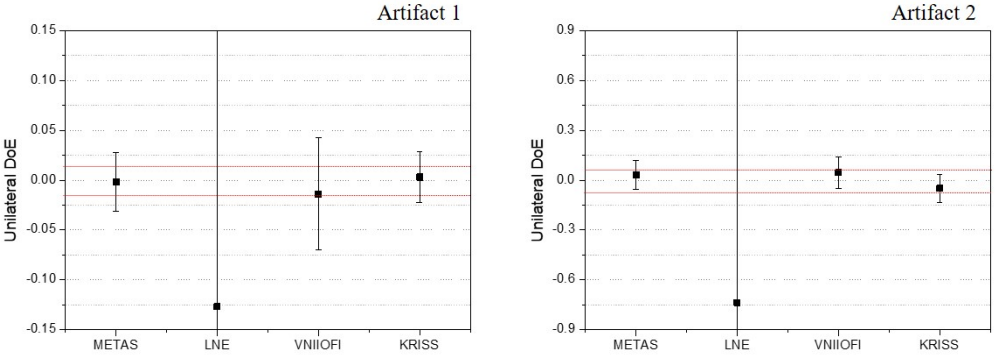

Fig. 5-4-5. Unilateral degree of equivalence and its uncertainty of each participant for round 2

with METAS artifacts at 1550 nm. Red dotted lines indicate the uncertainty boundaries of SCRV.

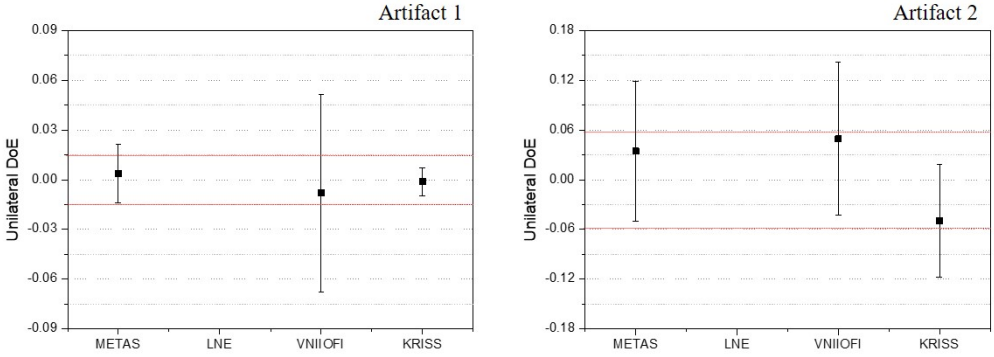

Fig. 5-4-6. Unilateral degree of equivalence and its uncertainty of each participant for round 2 with METAS artifacts at 1625 nm. Red dotted lines indicate the uncertainty boundaries of SCRV.

5.5. Discussion

Instead of removing one participant as an outlier for round 1 at 1625 nm, we can add s^2 term in Eq. (5-3-3) following the Mandel-Paule method to make the comparison consistent as below.

$$u_{adj}(\Delta_i) = \sqrt{u_{adj}^2(C_i) + u_T^2(\Delta_i) + s^2} \tag{5-5-3}$$

Here, s is determined by iteratively increasing from zero until $\chi^2_{\text{obs}} = \chi^2_{0.05}(\nu)$. The new SCRV and its uncertainty are summarized in Table 5-5-1 and 5-5-2.

Table 5-5-1. SCRV and its uncertainty (round 1 and 3 with KRISS artifact 1 at 1625 nm)

$$u_{cut-off} = 0.0174, \quad s \cong 0.0240, \quad \chi^2_{\text{obs}} = 7.815$$

Participant	Δ_i	$u(\Delta_i)$	$u_{adj}(C_i)$	$u_{adj}(\Delta_i)$	w_i	Δ_{SCRV}	$U(\Delta_{\text{SCRV}})$
KRISS	0.0000	0.0170	0.0141	0.0294	0.2950	0.0308	0.0184
NMIJ	0.0029	0.0297	0.0244	0.0382	0.1746		
NMC							
NMISA	0.0139	0.0407	0.0370	0.0473	0.1141		
NIS	0.0229	0.0248	0.0180	0.0345	0.2145		
CENAM	0.1179	0.0263	0.0200	0.0355	0.2016		

Table 5-5-2. SCRV and its uncertainty (round 1 and 3 with KRISS artifact 2 at 1625 nm)

$$u_{cut-off} = 0.0295, \quad s \cong 0.0918, \quad \chi^2_{\text{obs}} = 7.815$$

Participant	Δ_i	$u(\Delta_i)$	$u_{adj}(C_i)$	$u_{adj}(\Delta_i)$	w_i	Δ_{SCRV}	$U(\Delta_{\text{SCRV}})$
KRISS	0.0000	0.0550	0.0550	0.1070	0.2543	0.1252	0.0523
NMIJ	0.0549	0.1140	0.0999	0.1464	0.1359		
NMC							
NMISA	0.0049	0.1055	0.0900	0.1398	0.1490		
NIS	0.1159	0.0674	0.0390	0.1139	0.2245		
CENAM	0.3849	0.0585	0.0295	0.1110	0.2363		

Comparing Table 5-3-5 and 5-3-6 with Table 5-5-1 and 5-5-2, we can notice that the SCRV changes 15.8 % and -5.4 % for the KRISS artifact 1 and 2 at 1625 nm, respectively. The uncertainty also varies -4.0 % and 5.2 % for the KRISS artifact 1 and 2, respectively.

6. Conclusion

We have reported the results of the supplementary comparison of APMP.PR-S8 on optical fiber length at wavelengths of 1310 nm, 1550 nm, and 1625 nm. The comparison artifacts provided by KRISS and METAS showed reasonably low drift during each round, which overall resulted in consistent comparison results. The degrees of equivalence calculated in this comparison are to be used within the framework of the Mutual Recognition Arrangement, for example, as the supporting evidence for the item 7.10.0 of the CCPR service category that is Length, Optical fibre.

Reference

The Guidelines for CCPR Key Comparison Report Preparation (CCPR-G2 Rev.4 – *approved by WG-KC on January 8, 2019*)

Appendix

CENAM reported their large degree of equivalence (DoE) at 1625 nm originated from a simple arithmetic mistake in their data process. They explained the details, and the corrections are documented in this appendix according to the guidelines (CCPR-G2 Rev.4) as below.

Report

In general, our measurements for all artifacts were well performed, but we made a mistake when we applied the wavelength sensitivity coefficient to correct our measurements at this specific wavelength. Our laser sources for 1310 nm and 1550 nm were DFB tunable lasers and the wavelength correction we applied was practically negligible because we tried to tune them as close as possible to the nominal wavelength value. On the other hand, our laser at 1625 nm was a Fabry-Perot laser with a central wavelength of 1629.47 nm ± 0.09 nm (k=2), which give us a difference of 4.47 nm from the nominal value. If we apply this difference to our wavelength sensitivity coefficient of $C_\lambda=(3.22 \pm 0.10)\times10^{-3}$ m/(nm·km), we obtain a wavelength correction of 0.047 m or 0.23 ns for the artifact 1 and 0.192 m or 0.94 ns for the artifact 2. The problem in our report was that instead of subtracting this value because our wavelength value is beyond the nominal wavelength value, we add it and this give us our discrepancy. Table 1 and Table 2 show the reported results and the correct results for the artifact 1 and Table 3 and Table 4 show the results at 1625 nm for the artifact 2 respectively.

Table 1. Optical length of the artifact 1.

Wavelength	Side A			Side B			Mean	
1625 nm	Values without wavelength correction	Reported values (adding the value of the correction)	Correct values (subtracting the value of the correction)	Values without wavelength correction	Reported values (adding the value of the correction)	Correct values (subtracting the value of the correction)	Reported values (adding the value of the correction)	Correct vales (subtracting the value of the correction)
	(3252.55 ± 0.04) m (k=2)	(3252.59 ± 0.04) m (k=2)	(3252.50 ± 0.04) m (k=2)	(3252.55 ± 0.04) m (k=2)	(3252.60 ± 0.04) m (k=2)	(3252.50 ± 0.04) m (k=2)	(3252.60 ± 0.04) m (k=2)	(3252.50 ± 0.04) m (k=2)

Table 2. Transit time of the artifact 1.

Wavelength	Side A			Side B			Mean	
1625 nm	Values without wavelength correction	Reported values (adding the value of the correction)	Correct values (subtracting the value of the correction)	Values without wavelength correction	Reported values (adding the value of the correction)	Correct values (subtracting the value of the correction)	Reported values (adding the value of the correction)	Correct vales (subtracting the value of the correction)
	(15840.02 ± 0.16) ns (k=2)	(15840.25 ± 0.16) ns (k=2)	(15839.79 ± 0.16) ns (k=2)	(15840.02 ± 0.16) ns (k=2)	(15840.25 ± 0.16) ns (k=2)	(15839.80 ± 0.16) ns (k=2)	(15840.25 ± 0.16) ns (k=2)	(15839.79 ± 0.16) ns (k=2)

Table 3. Optical length of the artifact 2.

Wavelength	Side A			Side B			Mean	
1625 nm	Values without wavelength correction	Reported values (adding the value of the correction)	Correct values (subtracting the value of the correction)	Values without wavelength correction	Reported values (adding the value of the correction)	Correct values (subtracting the value of the correction)	Reported values (adding the value of the correction)	Correct vales (subtracting the value of the correction)
	(13315.89 ± 0.04) m (k=2)	(13316.08 ± 0.04) m (k=2)	(13315.70 ± 0.04) m (k=2)	(13315.87 ± 0.04) m (k=2)	(13316.07 ± 0.04) m (k=2)	(13315.68 ± 0.04) m (k=2)	(13316.07 ± 0.04) m (k=2)	(13315.69 ± 0.04) m (k=2)

Table 4. Transit time of the artifact 2.

Wavelength	Side A			Side B			Mean	
1625 nm	Values without wavelength correction	Reported values (adding the value of the correction)	Correct values (subtracting the value of the correction)	Values without wavelength correction	Reported values (adding the value of the correction)	Correct values (subtracting the value of the correction)	Reported values (adding the value of the correction)	Correct vales (subtracting the value of the correction)
	(64848.87 ± 0.20) ns (k=2)	(64849.80 ± 0.20) ns (k=2)	(64847.93 ± 0.20) ns (k=2)	(64848.77 ± 0.20) ns (k=2)	(64849.70 ± 0.20) ns (k=2)	(64847.84 ± 0.20) ns (k=2)	(64849.75 ± 0.20) ns (k=2)	(64847.88 ± 0.20) ns (k=2)

Additionally, Table 5 and Table 6 show the differences between the Pilot and CENAM for artifact 1 and artifact 2 respectively using the corrected values.

Table 5. Difference between Pilot and CENAM (KRISS artifact 1, Round 1&3, 1625 nm).

Participant	C_i	$u(C_i)$	$u_{ad}(C_i)$	Δ_i	$u(\Delta_i)$
KRISS	3252.4821	0.0141	0.0095	0.0000	0.0170
CENAM	3252.5000	0.0200		0.0179	0.0262

Table 6. Difference between Pilot and CENAM (KRISS artifact 2, Round 1&3, 1625 nm).

Participant	C_i	$u(C_i)$	$u_{ad}(C_i)$	Δ_i	$u(\Delta_i)$
KRISS	13315.6851	0.0550	0.0002	0.0000	0.0170
CENAM	13315.6900	0.0200		0.0049	0.0585